SUBMERGED VANES FOR FLOW CONTROL AND BANK PROTECTION IN STREAMS

by

A. Jacob Odgaard and Hong-Yuan E. Lee

submitted to
the Highway Division of the Iowa Department of Transportation
and
the Iowa Highway Research Board
Project HR-255

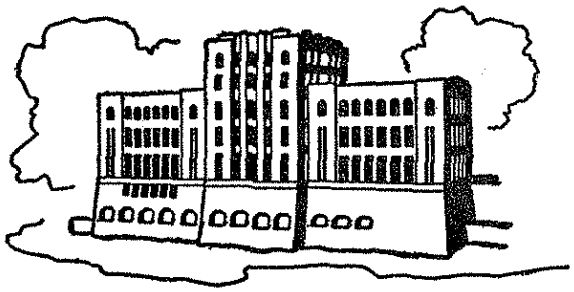

IIHR Report No. 279

Iowa Institute of Hydraulic Research
The University of Iowa
Iowa City, Iowa 52242

July 1984

ACKNOWLEDGEMENTS

This investigation was sponsored by the Iowa Highway Research Board of the Iowa Department of Transportation. The authors are grateful for IDOT's support and they wish to express their special thanks to Messrs. Vernon Marks and Mark Looschen, IDOT, for providing help at various stages of this project. The authors also wish to acknowledge the support provided by IIHR's mechanical and electronic shops, in particular by Messrs. James R. Goss and Michael Kundert, who assisted on the field surveys; Mr. James Cramer who constructed specialized electronic data acquisition equipment for the model tests; and Mr. Dale C. Harris who supervised the laborious mixing of the sediment grades used in the model tests. The data on flow and bed characteristics obtained in the model tests served as basis for the second author's Ph.D. thesis.

Dr. John F. Kennedy's critical review of the manuscript was greatly appreciated.

The opinions, findings, and conclusions of this report are those of the authors and not necessarily those of the Highway Division of the Iowa Department of Transportation.

ABSTRACT

The study has evaluated the effectiveness of Iowa Vanes in reducing depth and velocity near the outer bank in a curved, alluvial channel flow. A procedure for the design of a vane system for a given river curve has been developed and tested in a laboratory model. The procedure has been used for the design of an Iowa-Vane bank-protection structure for a section of East Nishnabotna River along U.S. Highway 34 at Red Oak, Iowa.

TABLE OF CONTENTS

Page

LIST OF SYMBOLS.....v

LIST OF TABLES.....vii

LIST OF FIGURES.....viii

I. INTRODUCTION.....1

II. THEORETICAL ANALYSIS.....8
- A. Vane Function.....10
- B. Effective Bend Radius.....13
- C. Lift Coefficient.....15

III. LABORATORY-MODEL EXPERIMENTS.....18
- A. Verification of Design Relations.....18
  - 1. Uniform Bed Material.....18
  - 2. Nonuniform Bed Material.....36
- B. Vanes in Armored Channel.....39
- C. Rock Vanes.....43
- D. Discussion of Results.....45

IV. VANE DESIGN FOR EAST NISHNABOTNA RIVER BEND.....52
- A. Field Surveys.....52
- B. Design Computations.....63

V. SUMMARY, CONCLUSIONS AND RECOMMENDATIONS.....72

REFERENCES.....76

APPENDIX I: Vane-Design Example.....77

APPENDIX II: Grain-Size Distributions from Field Surveys.....79

LIST OF SYMBOLS

b	width of channel
c_L	lift-force coefficient
D	particle diameter
d	flow depth
F	vane function, Eq. 10
F_D	particle Froude number, Eq. 4
f	Darcy-Weisbach friction factor
g	acceleration due to gravity
H	vane height
L	vane length
N	number of vanes
n	exponent in the power-law velocity profile
r	radius
r_e	effective radius, Eq. 12
S	longitudinal slope of water surface
S_T	transverse bed slope
T	torque
T_c	torque due to centrifugal acceleration
T_v	torque induced by vane
u	local velocity
$u*$	shear velocity ($= \sqrt{\tau_o/\rho}$)
$\overline{u}$	depth-averaged velocity
V	volume

α vane-angle of attack

α_e effective angle of attack

α' vane angle with mean-flow direction

ε downwash angle

δ deviation angle, Eq. 23

κ von Karman's constant

θ Shields' parameter

ρ fluid density

ρ_s density of bed material (sand)

τ shear stress

τ_o bed-shear stress

τ_r radial component of τ_o

ϕ bend angle

Subscripts

a cross-sectional average

c centerline

LIST OF TABLES

Table		Page
1.	Minimum Values of the Vane Function, F	13
2.	Summary of Model Test Conditions at Maximum Rates of Flow	21
3.	Effective-Radius Calculations for Model Tests	26
4.	Vane-Design Calculations for Model Tests	27
5.	Summary of Experimental Results of Vane Tests	33
6.	High-Flow Data from East Nishnabotna River Bend	57
7.	Low-Flow Data from East Nishnabotna River Bend	58
8.	Vane-Design Computations for East Nishnabotna River Bend	65
9.	Proposed Emplacement of Vane System for East Nishnabotna River Bend	71

LIST OF FIGURES

Figure		Page
1.	Aerial Photo of East Nishnabotna River and U.S. Highway 34 at Red Oak, Montgomery County, Iowa, March 13, 1972	2
2.	Aerial Photo of East Nishnabotna River and U.S. Highway 34 at Red Oak, Montgomery County, Iowa, March 7, 1977	3
3.	Aerial Photo of East Nishnabotna River and U.S. Highway 34 at Red Oak, Montgomery County, Iowa, August 11, 1982	4
4.	Sequential Centerlines of East Nishnabotna River at Red Oak, Montgomery County, Iowa	6
5.	Vane Function F as a Function of Vane Height-Water Depth Ratio, H/d, for Four Values of n	12
6.	Lift Coefficients for Flat-Plate Vane	17
7.	IIHR's Curved Sediment Flume; (a) Viewed Upstream Toward the Flume Inlet; and (b) Viewed Upstream Around the Curve	19
8.	Layout of IIHR's Curved, Recirculating Sediment Flume, with Section Numbers and Bend Angles	20
9.	Grain-Size Distribution for Uniform Bed Sediment, Test Series 1 and 2	22
10.	Streamwise Variation of Transverse Bed Slope Development, Test Series No. 1	24
11.	Development of Bed Profile at Section 80, Test Series No. 1	25
12.	Development of Bed Profile at Section 112, Test Series No. 1	25
13.	Test Series 1: Measured Radial Average-Distributions of Depth and Depth-Averaged Mean Velocity Compared with the Predicted Distributions; (a) Before Installation of Vanes; (b) After Installation of Vanes	28
14.	Test Series 1 Vane Emplacement	28

15. Streamwise Variation of Transverse Bed Slope Development after Installation of Vanes; Test Series No. 1.....30

16. Development of Bed Profiles at Section 80 after Installation of Vanes; Test Series No. 1.....31

17. Development of Bed Profile at Section 112 after Installation of Vanes; Test Series No. 1.....31

18. Test Series 2: Measured Radial Average-Distributions of Depth and Depth-Averaged Mean Velocity Compared with the Predicted Distributions; (a) Before Installation of Vanes; (b) After Installation of Vanes.....35

19. Test Series 2 Vane and Vane Emplacements.....35

20. Grain-Size Distribution for Nonuniform Bed Sediment; Test Series No. 3.....37

21. Test Series 3: Measured Radial Average-Distributions of Depth and Depth-Averaged Mean Velocity Compared with the Predicted Distributions; (a) Before Installation of Vanes; (b) After Installation of Vanes.....38

22. Grain-size Distributions for Nonuniform Bed Sediment; Test Series No. 4.....40

23. Test Series No. 4: Radial Average-Distributions of Depth, Depth-Averaged Mean Velocity, and Median-Grain Diameter; (a) Before Installation of Vanes; (b) After Installation of Vanes.....41

24. Test Series No. 4 Run 3 Vane Emplacement.....41

25. Test Series No. 4: Radial Average-Distributions of Depth; (a) Before Installation of Vanes; (b) After Installation of Vanes.....44

26. Test Series No. 5: Radial Average-Distributions of Depth, and Depth-Averaged Mean Velocity between Sections 72 and 112; (a) Before Installation of Vanes; (b) After Installation of Vanes.....44

27. Test Series No. 5: Rock Vanes before Admission of Flow.....46

28. Test Series No. 5: Rock Vanes after Admission of Flow.....46

29. Naturally Formed Bed Topography in Test Series No. 4 (Looking Upstream).....48

30. Bed Topography in Test Series No. 4 (Looking Upstream) after Installation of 14-in. Vanes.....48

31. Depth Distribution at Section 112 in Test Series No. 4 Before Installation of Vanes.....49

32. Depth Distribution at Section 112 in Test Series No. 4 After Installation of 14-in Vanes.....49

33. Close-Up of Bed with 14-in. Vane (one barely visible) at Section 112 in Test Series No. 4.....50

34. Bed Topography Downstream from Section 112 in Test Series No. 4 with 14-in. Vanes.....50

35. Depth Distribution at Section 112 in Test Series No. 4 After Installation of 9-in. Vanes.....51

36. Depth Distribution at Section 112 in Test Series No. 2 After Installation of 9-in. Vanes.....51

37. Plan-View Sketch of IIHR's Sediment Flume Overlaid the East Nishnabotna River Bend at Red Oak, Using a Scale Ratio of 1:10.....53

38. Plan-View Sketch of the East Nishnabotna River Bend at Red Oak, Iowa.....54

39. East Nishnabotna River on May 2, 1984, Looking Upstream from the U.S. Highway 34 Bridge.....56

40. Survey at Section 4, May 2, 1984.....56

41. Sections 1 through 10 of the East Nishnabotna River Bend.....59

42. Rating Curve for the U.S.G.S. Water-Stage Recorder on East Nishnabotna River at Red Oak (at Coolbaugh Street Bridge).....62

43. East Nishnabotna River on May 2, 1984, Looking Downstream toward the Highway 34 Bridge (The rock protection is along the right bank in the upper-center portion of the picture).....64

44. Frequency Distribution for Discharge in East Nishnabotna River at Red Oak.....68

45. Proposed Emplacement of Vane System for the East Nishnabotna River Bend.....70

46. Proposed Combination of Vanes and Rock Rip Rap at the Highway 34 Bridge.....70

47. U.S. Highway 34 Bridge over East Nishnabotna River, Viewed Downstream toward Right Bank of River.....75

48. U.S. Highway 34 Bridge over East Nishnabotna River, Viewed Downstream from Left Bank of River.....75

SUBMERGED VANES FOR FLOW CONTROL AND BANK PROTECTION IN STREAMS

I. INTRODUCTION

The final report on work conducted under the Streambank Erosion Control Evaluation and Demonstration Act of 1974 (Section 32, Public Law 93-251) was submitted recently to Congress by the U.S. Army Corps of Engineers (December 1981). The main conclusion of the work was that streambank erosion continues to be a serious problem along many of the Nation's streams and waterways, resulting in serious economic losses of private and public lands, bridges, etc. According to this report, approximately 148,000 bank-miles of streams and waterways are in need of erosion protection. The cost to arrest or control this erosion, using conventional bank protection methods currently available, was estimated to be in the excess of $1 billion annually.

The problem is difficult because bank erosion is often the result of a complex interaction between water and sediment in the streams. The sediment-transport capacity and erosion potential of a stream flow become greater with increasing boundary shear stress and flow velocity. Along curved reaches and in bends, the interaction between the vertical gradient of streamwise velocity and the curvature of the primary flow generates a so-called secondary or spiralling flow, which produces larger depths and therefore also larger velocities and boundary shear stresses near the outer (concave) bank. The channel deepening undermines this bank, and the larger local velocities attack it, and thus is the stage set for river-bank erosion.

The problem in Iowa is illustrated in Figs. 1, 2, and 3, which show aerial photos of East Nishnabotna River at Red Oak, Montgomery County. The photos were taken at 5-year intervals in 1972, 1977, and 1982. Over the 10-year period, a total of 20 acres of farmland was lost by bank erosion along this 1.6-mile reach of the river. Erosion at a comparable rate is occuring along the entire length of East

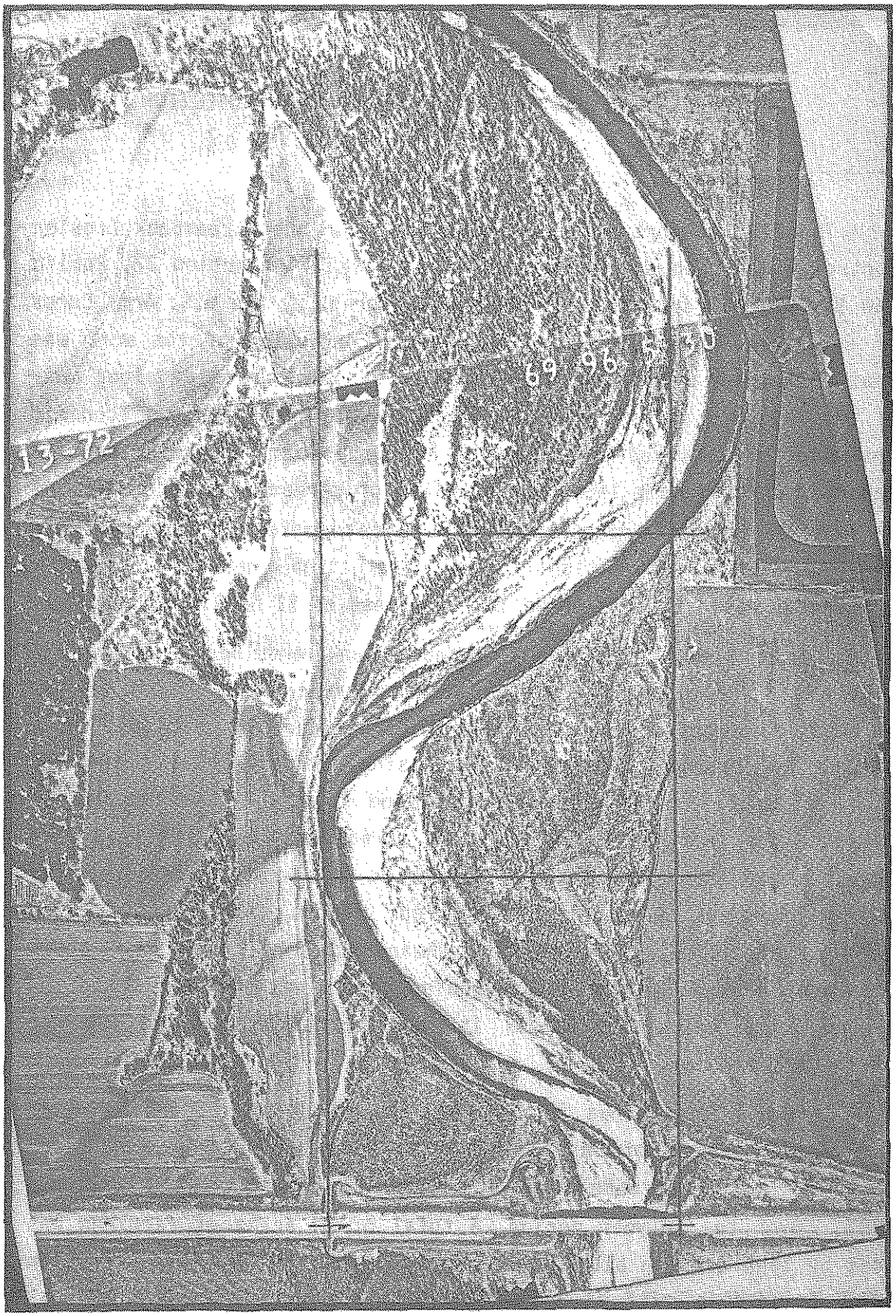

Figure 1. Aerial Photo of East Nishnabotna River and U.S. Highway 34 at Red Oak, Montgomery County, Iowa, March 13, 1972

Figure 2. Aerial Photo of East Nishnabotna River and U.S. Highway 34 at Red Oak, Montgomery County, Iowa, March 7, 1977

Figure 3. Aerial Photo of East Nishnabotna River and U.S. Highway 34 at Red Oak, Montgomery County, Iowa, August 11, 1982

Nishnabotna River, and along a very significant part of all the rivers in Iowa. Many highways and bridges throughout the State are in imminent danger of being damaged by bank erosion. Examples are: Highway (HW) 34's crossings of West and East Nishnabotna River, Walnut Creek, and West Nodaway River; HW 6's crossing of West Nishnabotna River; HW 92's crossing of East Nishnabotna River; HW 2's crossing of West Nodaway River; HW 101's crossing of Cedar River; HW 136's crossing of Maquoketa River; I 35's crossing of Raccoon River; HW 6/I 80's crossing of West Nodaway River; the section of HW 175 that is running along Maple River; in particular at Castana and Battle Creek; and HW 183 along Soldier River.

At some of these locations protective measures have been installed by the Iowa Department of Transportation. The methods in current general use involve either armoring of concave banks by one means or another, ranging from paving with stone or concrete to enhanced vegetative cover; or reduction of the nearbank velocity by dikes or other structures that increase the local channel roughness. Many of these methods are of a temporary nature and do not solve the problem on a long-term basis. For example, HW 34's crossing of East Nishnabotna River (at Red Oak, Montgomery County) is presently being protected by rip-rap structures along certain reaches of the river bank just upstream from the crossing. In a few years time a major section of the rip-rap structure is going to be undermined from behind and washed away unless substantial, additional protection work is undertaken. The problem at this location is seen very clearly on the aerial photos in Figs. 1, 2, and 3; and in Fig. 4 which shows the location of the channel-center line in 1972, 1977, and 1982). The present rip-rap structure along the right bank of the river (between the points A and B in Fig. 2, a total of 600 ft), which was installed in 1977, has so far offered excellent protection of the highway. However, during the 10-year period, shown in the figures 1, 2, 3, and 4, apex of the lower meander curve has moved approximately 500 ft southward and is now only about 500 ft from the

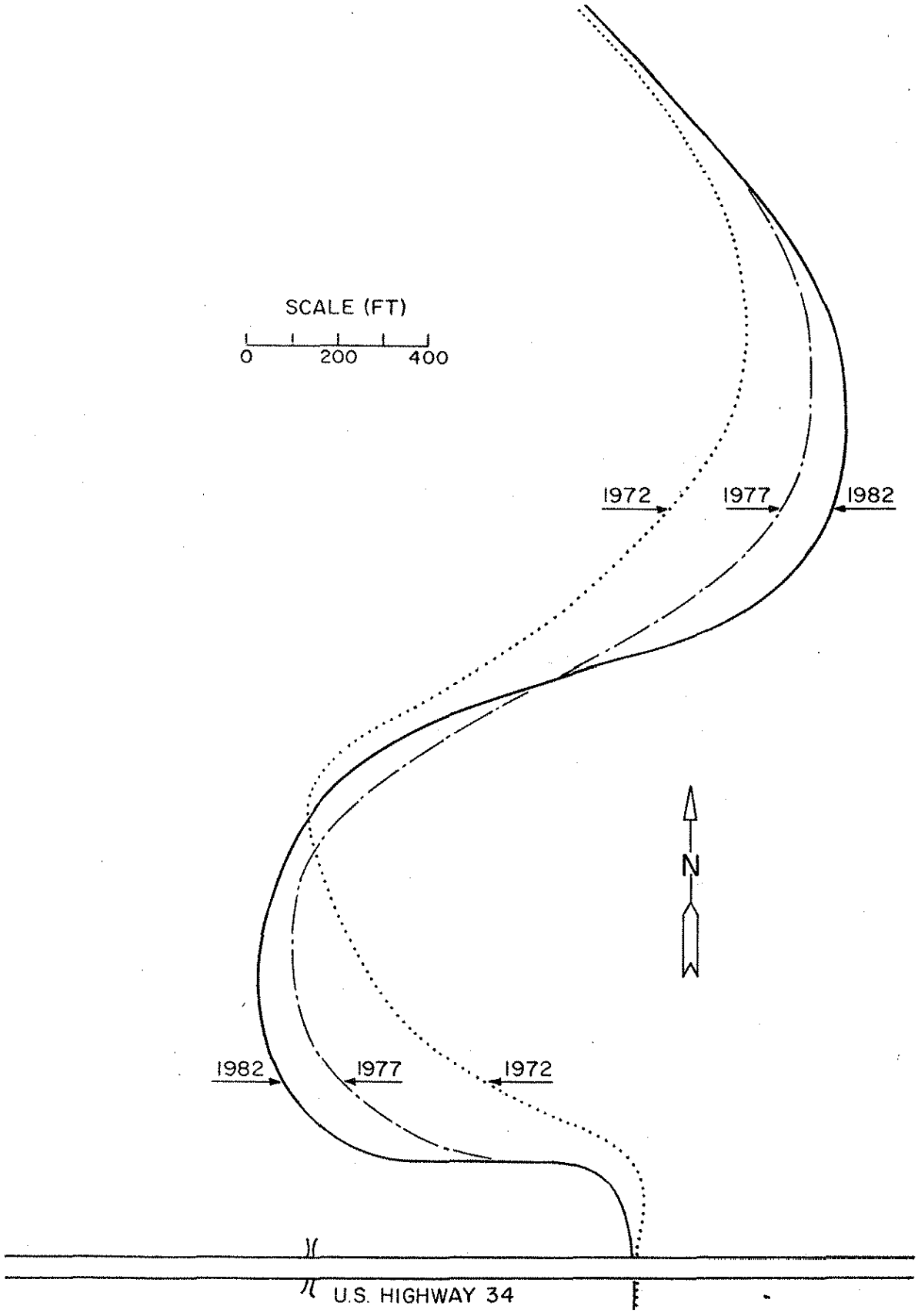

Fig. 4 - Sequential Centerlines of East Nishnabotna River at Red Oak, Montgomery County, Iowa.

highway. It is obvious that the present bank protection will be insufficient for the protection of the highway in the future. At the present rate of bank erosion at this site, the rip-rap structure between A and B will be undercut and 1000 ft of Highway 34, including the highway bridge, will be seriously damaged within the next 5 to 7 years unless additional protection is provided. Problems of similar nature are being faced at several other highway sections and bridge crossings in Iowa, some of which were mentioned in the preceding paragraphs.

Many minor roads in Iowa also face this problem. Examples here are the low-water crossings where dips in the road have been provided to allow flood flows to pass the road. As the courses of most streams tend to change with time, the flood flows are often seen to attack the roads at points (away from these dips) that are not designed to withstand the impact of high velocity flow. In such cases there is a need for a simple inexpensive technique that can insure that the flood flows always cross the roads at the predesignated points.

Considering the risks that are at stake at so many sections of Iowa's highway system, which is one of the State's major investments, and considering the inadequacy of the protection methods that are in current use, there appears to be an urgent need for the development of new ideas or approaches for the safeguarding of these investments against the erosive attack of the streams.

This study was conducted for the purpose of evaluating a new concept for a bank-protection structure: The Iowa Vane (Odgaard and Kennedy, 1983). The underlying idea involves countering the torque exerted on the primary flow by its curvature and vertical velocity gradient, thereby eliminating or significantly reducing the secondary flow and thus reducing the undermining of the outer banks and the high-velocity attack on it. The new structure consists of an array of short, vertical, submerged vanes installed with a certain

orientation on the channel bed. A relatively small number of vanes can produce bend flows which are practically uniform across the channel. The height of the vanes is less than half the water depth, and their angle with the flow direction is of the order of 10°. In this study, design relations have been established (Chapter II). The relations, and the vanes' overall performance, have been tested in a laboratory model under different flow and sediment conditions (Chapter III). The results are used for the design of an Iowa-Vane bank protection structure for a section (Fig. 3) of East Nishnabotna River along U.S. Highway 34 at Red Oak, Iowa (Chapter IV).

II. THEORETICAL ANALYSIS

The objective of the analysis in this chapter is to establish a set of design relations for use in the design of a vane system for the protection of river banks. The vane system is to produce a reduction of near-bank depth and velocity sufficient to prevent the banks from being undermined and eroded. It follows that the design criteria are related to maximum allowable values for near-bank depth and velocity.

Preceding studies have shown (Odgaard, 1984) that the radial distribution of depth-averaged mean velocity in the fully developed part of a constant-radius river curve can be adequately described by an equation based on Darcy-Weisbach's resistance law:

$$\frac{\overline{u}}{\overline{u}_c} = \left(\frac{d}{d_c}\right)^k \left(\frac{r_c}{r}\right)^{1/2} \tag{1}$$

in which $\overline{u}$ = depth-averaged mean velocity at radius r from the center of the curve; d = depth of flow at radius r; and k = factor of the order 2/3. Subscript c denotes the center-line values. Generally, the center-line value of d can be set equal to the cross-sectional average depth, d_a, and the variation of depth can be taken to be linear in the radial direction:

$$d = d_a + S_T (r - r_c) \tag{2}$$

in which S_T = radial or transverse slope of the bed surface. According to Odgaard (1984), S_T is related to primary flow variables by the equation

$$S_T \simeq 4.8 \sqrt{\theta}\, F_D \frac{d_a}{r_c} \tag{3}$$

in which θ = Shields' (1936) parameter; and F_D = densimetric particle Froude number defined as

$$F_D = \frac{u_a}{\sqrt{\frac{\rho_s - \rho}{\rho} gD}} \tag{4}$$

in which D = median-grain size of the bed material; g = acceleration due to gravity; u_a = cross-sectional average velocity; and ρ and ρ_s = density of fluid and bed sediment, respectively. Substituting Eq. 2 into Eq. 1 yields the following relationship between S_T and $\bar{u}$:

$$S_T = \frac{d_a}{r - r_c} \left[\left(\frac{\bar{u}}{\bar{u}_c} \right)^{1/k} \left(\frac{r}{r_c} \right)^{1/2k} - 1 \right] \tag{5}$$

Hence, a criterion for $\bar{u}$ is equivalent to a criterion for S_T, and the design objective for the vane system can be formulated as a maximum allowable value for S_T. To reduce (or eliminate) the transverse bed slope S_T, the vane system must reduce (or eliminate) the secondary flow in the river curve.

The effectiveness of a vane depends on the lift and drag induced by the flow as it passes the vane, and the height of the vane in relation to the water depth. (The lift is the sum of the forces (pressure and viscous) that acts normal to the free-stream direction; the drag is the sum that acts parallel to the free-stream direction). The lift and drag, in turn, depend on the shape of the vane; its aspect ratio (height-length ratio); and angle of incidence

with the free-stream direction, α. To maximize the effectiveness of a vane design, the moment of the lift force about the centroid of the channel-cross section must be maximized and the drag force on the vane must be minimized (large drag would change the overall characteristics of the river flow increasing channel roughness, which should be avoided). In addition, the vane emplacement must be designed such that the effectiveness of the vane array as a whole is maximized. In other words, adverse interference among the vanes must be avoided (cascade effect). The following analysis provides a guide to the design of a vane system.

A. Vane Function

The secondary flow in a river curve is produced by the torque, T_c, due to the centrifugal force being distributed nonuniformly over the depth. For fully developed flow in a rectangular channel with constant radius and a power-law velocity distribution, T_c is given by (Eq. 3 in Ref. 3)

$$T_c = \frac{1}{2} \rho \bar{u}^2 \frac{n+1}{n(n+2)} d^2 b\phi \tag{6}$$

in which ϕ = included bend angle; b = channel width; and n = velocity-profile exponent. n is related to the Darcy-Weisbach friction factor, f, by (Zimmermann and Kennedy, 1978)

$$n^2 = \frac{8\kappa^2}{f} \tag{7}$$

in which κ = von Karman's constant. (Hence, $n = \kappa\bar{u}/\sqrt{gSd}$, S = longitudinal slope of water surface). The Iowa Vanes exert a torque on the flow that is given by (Eq. 6 in Ref. 3, with $2\pi \sin\alpha = c_L$)

$$T_v = \frac{1}{4} c_L \rho \bar{u}^2 L d^2 \left(\frac{H}{d}\right)^{(2+n)/n} \left[\frac{(n+1)^2}{n(n+2)} - \frac{n+1}{n} \frac{H}{d}\right] N \tag{8}$$

in which c_L = lift coefficient; L = vane length; H = vane height; and

N = number of vanes. To eliminate the secondary flow that is generating the transverse bed slope, S_T, the vanes must exert a torque that balances the driving torque, T_c. Equating T_c and T_v yields

$$\frac{1}{2} c_L \left(\frac{r_c}{d}\right) \left(\frac{NLH}{r_c \phi b}\right) = F \tag{9}$$

F is a function (termed the vane function) of n and H/d given by

$$F = \frac{1}{\left(\frac{H}{d}\right)^{2/n} \left[(n+1)-(n+2)\frac{H}{d}\right]} \tag{10}$$

Eq. 9 yields the total vane area (lifting surface) needed per unit surface area of channel bed $[NHL/(r_c \phi b)]$ as a function of the radius-depth ratio of the channel, r_c/d; lift coefficient, c_L; and the vane function, $F = F(n,H/d)$. The vane function is graphed in Fig. 5. It is seen that for given value of H/d the value of F, and therefore the required lifting surface, increases when n decreases (i.e., when the frictional resistance increases). The vane function has its minimum at $H/d = 2(n+1)/(n+2)^2$:

$$F_{min} = \frac{n+2}{n(n+1)} \left[\frac{2(n+1)}{(n+2)^2}\right]^{-2/n} \tag{11}$$

Corresponding values of F_{min}, H/d, and n are listed in Table 1. The vane function is seen to be relatively insensitive to variations of H/d over a fairly large range of H/d-values. For example, for n = 4, F is within 20% of its minimum value (the design value) when H/d is within the range of $0.12 < H/d < 0.48$ (that is, when the water depth is between 2 and 8 times the vane height). A typical river bend

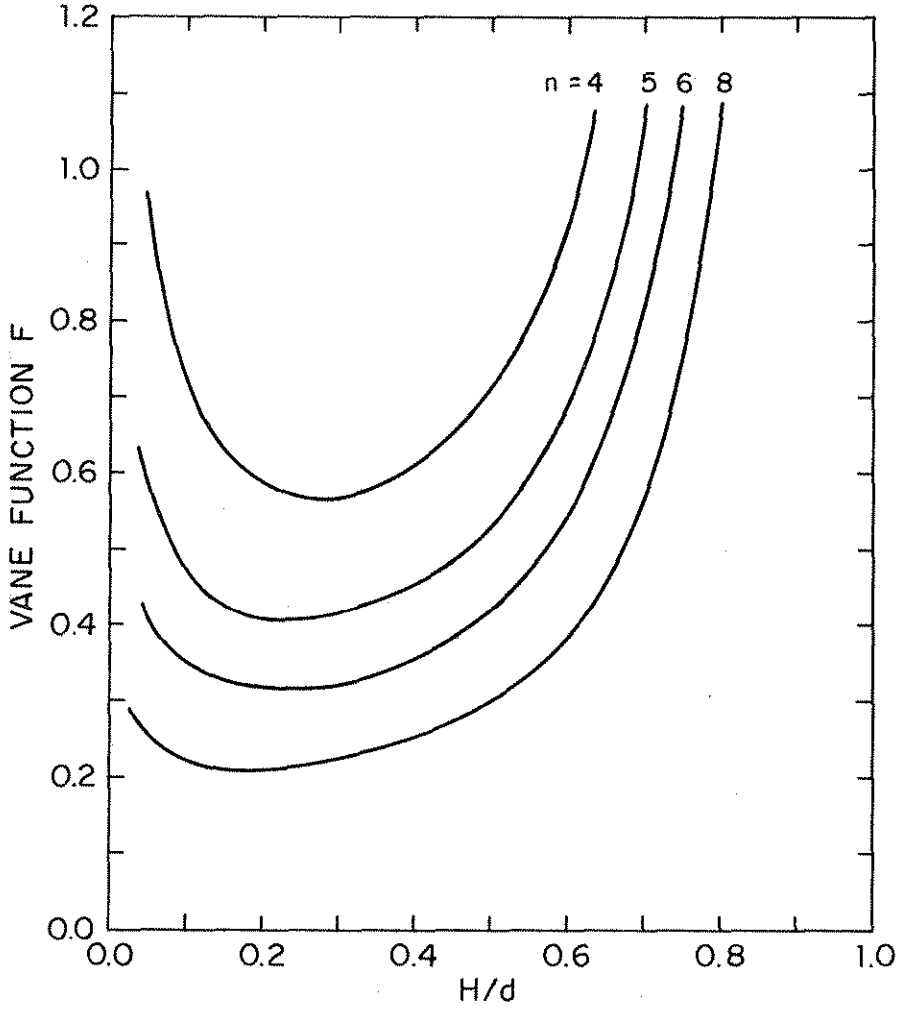

Figure 5. Vane Function F as a Function of Vane Height-Water Depth Ratio, H/d, for Four Values of n

Table 1 - Minimum Values of the Vane Function, F.

Velocity profile exponent, n	Minimum value of F, F_{min}	Value of H/d at which $F = F_{min}$	H/d-range within which $F \leq 1.2\ F_{min}$
4	0.57	0.28	0.12-0.48
5	0.41	0.24	0.09-0.46
6	0.32	0.22	0.07-0.45
7	0.26	0.20	0.06-0.43
8	0.21	0.18	0.05-0.40

would have an r_c/d ratio of about 100 and an n value of about 4. With H/d = 0.28 (yielding F = 0.57), and $c_L = 1$ (the selection of the c_L - value will be discussed in Section C), Eq. 9 shows that the total lifting surface required would then be 1.14% of the surface area of the channel bend. With a width-depth ratio, b/d, of 10, which is typical, the total length of vanes required (NL) is 41% of the length of the channel to be protected ($r_c\phi$). Adding 20% to allow for the aforementioned fluctuation in water depth yields the percentages 1.37 and 49, respectively.

B. Effective Bend Radius

Eq. 9 applies to fully-developed, constant-radius bend flow. Most natural bends are not constant-radius bends, nor is the flow in them fully developed, and Eq. 9 cannot be used. However, if the channel's radial distribution of depth is known (measured) an effective-radius concept can be used for the vane design. The effective radius, r_e, is the radius at which a fully-developed, constant-radius bend flow would form a transverse bed slope of the known or measured magnitude. According to Eq. 3, r_e is then related to the transverse bed slope, S_T, by the equation

$$S_T = 4.8\sqrt{\theta}\, F_D \frac{d_a}{r_e} \tag{12}$$

The vanes must produce a torque that balances the torque, T_c, responsible for this transverse bed slope. The driving torque in this case is given by Eq. 6 with $\phi = \phi_e$, where ϕ_e = effective bend angle (the angle corresponding to the effective radius, r_e). The design relation, obtained by equating T_c and T_v, then reads

$$\frac{1}{2} c_L \left(\frac{r_e}{d}\right) \left(\frac{NLH}{r_e \phi_e b}\right) = F \tag{13}$$

or, since $r_e \phi_e = r_c \phi$,

$$\frac{1}{2} c_L \left(\frac{r_e}{d}\right)\left(\frac{NLH}{r_c \phi b}\right) = F \tag{14}$$

Eqs. 9 and 14 are based on complete elimination of the secondary current and the achievement of zero transverse bed slope. Practical considerations may not justify such an ideal (asymptotic) objective. Also, the vane height or the total number of vanes (or both) may become a practical problem, in which case lower or fewer vanes (or both) may have to be combined with minimal slope protection on the banks. A vane system would be adequate if it can make the bank-shear stress stay below the critical value at all flow rates. If the critical bank-shear stress is relatively high due to slope protection, some transverse slope on the river bed may be acceptable. If the acceptable transverse bed slope is S_{To}, the vanes must produce a torque that can reduce the slope from S_T to S_{To}, or, according to Eq. 12, increase the effective radius from r_e to r_{eo}, where

$$r_{eo} = 4.8\sqrt{\theta}\, F_D \frac{d_a}{S_{To}} \tag{15}$$

The required lifting surface (NLH) would then be obtained as the difference between the lifting surface required for zeroing S_T and that required for zeroing S_{To}:

$$NHL = \frac{2}{c_L} Fr_c \phi bd \left(\frac{1}{r_e} - \frac{1}{r_{eo}}\right) \tag{16}$$

C. Lift Coefficient

If the flow around the vane were ideal and two-dimensional, the Kutta condition (Sabersky and Acosta, 1964) would yield

$$c_L = 2\pi \sin \alpha \tag{17}$$

in which α = the vane's angle of attack with the mean flow. However, the flow around the vane is not ideal nor two-dimensional. As the aspect ratio, H/L, decreases, c_L decreases relative to the value given by Eq. 17. Also, with increasing value of α, flow separation becomes more and more important increasing the drag and decreasing the lift. The decrease of c_L with decreasing aspect ratio is due partly to the tip vortices (the vortices trailing the upper edge of the vane), which induce a downward motion (downwash) in the fluid passing over the vane. The downwash has the effect of turning the undisturbed free-stream velocity, so the effective angle of attack is reduced by a certain angle ε to

$$\alpha_e = \alpha - \varepsilon \tag{18}$$

Nothing is known about the value of ε for small-aspect-ratio foils that are wall- (or bottom-) attched. For a finite-span airfoil in undisturbed freestream air, the downwash angle ε can be calculated by (Bertin and Smith, 1979, pp. 170-174)

$$\varepsilon = \frac{c_L}{\pi (H/L)} \tag{19}$$

This equation is obtained by using an elliptic spanwise circulation distribution in the relationship between circulation and lift coefficient. For a finite-span airfoil, the geometric angle of attack is then given by

$$\alpha = \alpha_e + \frac{c_L}{\pi (H/L)} \tag{20}$$

If two airfoils have the same lift coefficient and effective angle of attack, but different aspect ratios, H_1/L_1, and H_2/L_2, their geometric angles of attack, α_1 and α_2, are thus related by the equation

$$\alpha_2 = \alpha_1 + \frac{c_L}{\pi} \left(\frac{L_2}{H_2} - \frac{L_1}{H_1}\right) \tag{21}$$

The validity of Eqs. 20 and 21 have been verified experimentally (Bertin and Smith, 1979) for airfoils with aspect ratio greater than or equal to one. For a bottom-attached flat plate it is tentatively assumed that Eq. 17 applies at large aspect ratios, and that the downwash angle is half that given by Eq. 19 (as a bottom-attached foil has only one edge with tip vortices). Using Eq. 21, the lift coefficient can then be determined as a function of α and H/L (Fig. 6). Note that although the aforementioned assumptions are reasonable, they have not been verified experimentally.

The angle α to be used for the calculations of c_L is the angle as seen by the fluid approaching the vane. Because of the centrifugal acceleration, the near-bed velocity distribution (the velocity distribution seen by the vane) is skewed toward the inside of the bend. The angle the near-bed velocity forms with the mean-flow direction, δ, is given by (Falcon, 1979)

$$\delta = \arctan \left(\frac{\tau_r}{\tau_o}\right) \tag{22}$$

in which τ_o = bed-shear stress; and τ_r = radial component of τ_o. Substituting $\tau_o = (\kappa^2/n^2)\, \rho \bar{u}^2$ and $\tau_r = \rho\, (n+1)/[n(n+2)]\, (d/r_e)\, \bar{u}^2$ (Falcon, 1979) into Eq. 22 yields

$$\delta = \arctan \left[\frac{1}{\kappa^2} \frac{n(n+1)}{n+2} \frac{d}{r_e}\right] \tag{23}$$

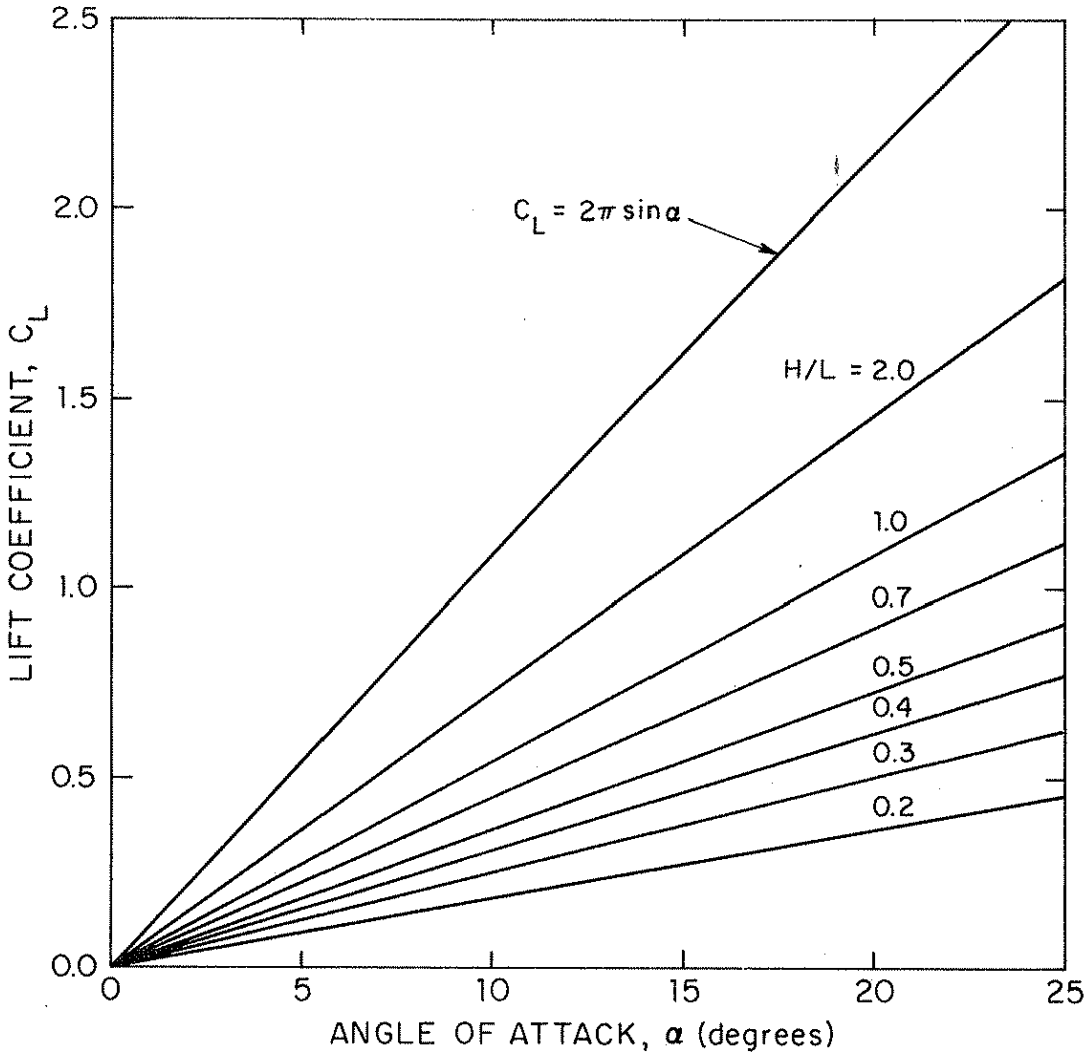

Figure 6. Lift Coefficients for Flat-Plate Vane

Hence, if a vane is placed at an angle with the mean-flow direction of α', the angle α to be used for the calculation of c_L is given by

$$\alpha = \alpha' + \delta \tag{24}$$

III. LABORATORY-MODEL EXPERIMENTS

The validity of the foregoing design relations, and the effectiveness of the vanes in producing more uniform lateral distributions of depth and velocity, were tested in IIHR's 250-ft long, 8-ft wide, and 2-ft deep, curved, recirculating sediment flume (Fig. 7) Fig. 8 shows the layout of the flume with section numbers, which are the distances, in feet, from the inlet, measured along the inner flume wall. The center-line radius of the curved part of the flume is 43 ft. The instrumentation and measurement technique were described by Odgaard and Kennedy (1983). Tests were conducted with both uniform and nonuniform bed material with smooth and rough banks; with different vane lengths and emplacement; and with vanes composed of modeled sheet piling and steep-sided windrows of rock. A summary of test conditions is given in Table 2.

A. Verification of Design Relations

The formula for the transverse bed slope, Eq. 12, and the vane-design relations, Eqs. 9, 14, or 16, were tested in three series of experiments with two different grades of bed sediment.

1. Uniform Bed Sediment - In Test Series No. 1, the sediment was sand with a median diameter of 0.30 mm and a geometric standard deviation of 1.45 (Fig. 9). The sand was placed in the flume in a 9-in. thick layer throughout. After about an hour of gentle wetting, the sand bed was subjected to a flow of 5.2 cfs for a period of 160 hours. The bed topography was measured after periods of 10, 20, 40,

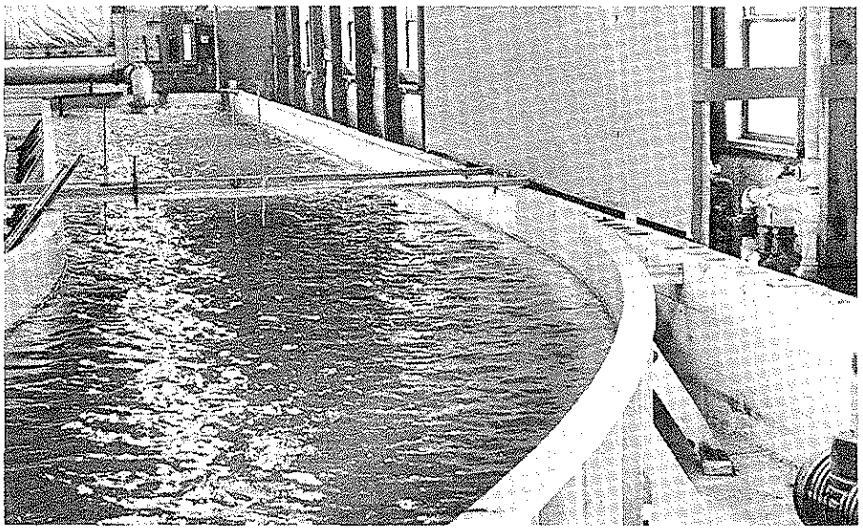

(a)

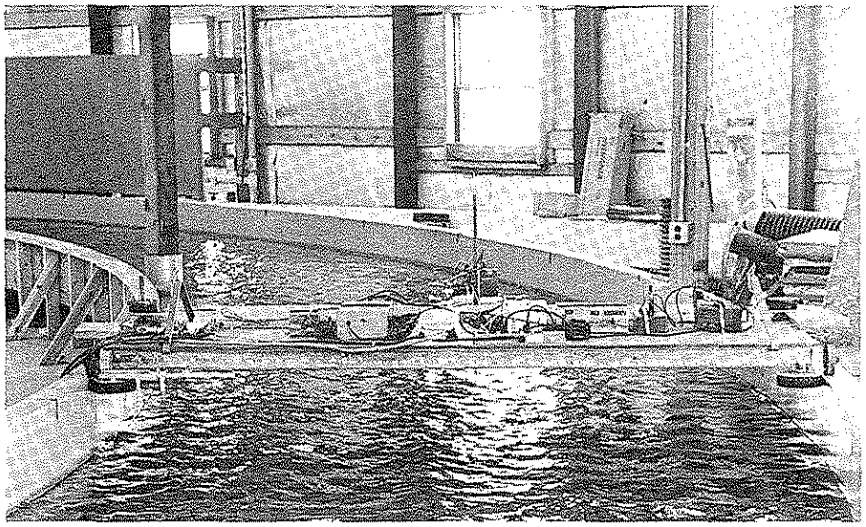

(b)

Figure 7. IIHR's Curved Sediment Flume; (a) Viewed Upstream Toward the Flume Inlet; and (b) Viewed Upstream Around the Curve

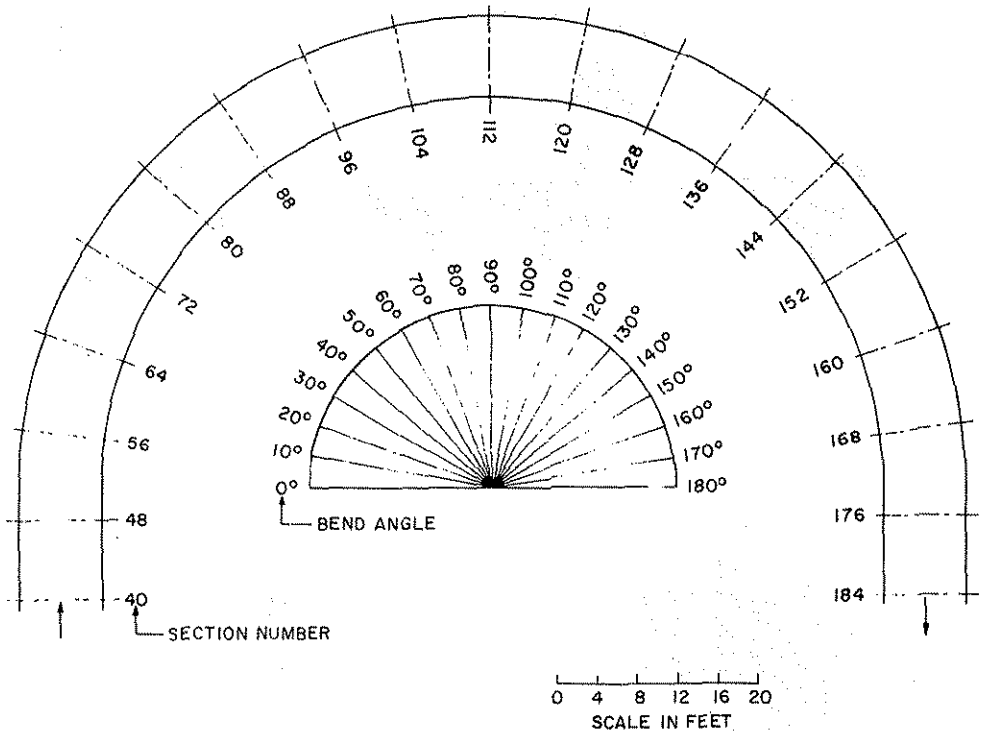

Figure 8. Layout of IIHR's Curved, Recirculating Sediment Flume, with Section Numbers and Bend Angles

Table 2. Summary of Model Test Conditions at Maximum Rates of Flow

Test Series	Flow rate, in cubic feet per second	Cross-sectional average depth, d_a, in feet	Median-grain diameter, D in millimeters	Geometric standard deviation of bed material	Longitudinal slope of water surface	Velocity-profile exponent	Cross-Sectional average velocity, u_a, in feet per second	Condition of channel side wall
1	5.2	0.50	0.30	1.45	0.00104	4.0	1.30	smooth
2	6.0	0.54	0.30	1.45	0.00146	3.5	1.40	rough
3	5.8	0.47	0.90	1.90	0.00063	6.5	1.56	smooth
4,5	5.8	0.50	2.7	2.78	0.00217	3.1	1.45	rough

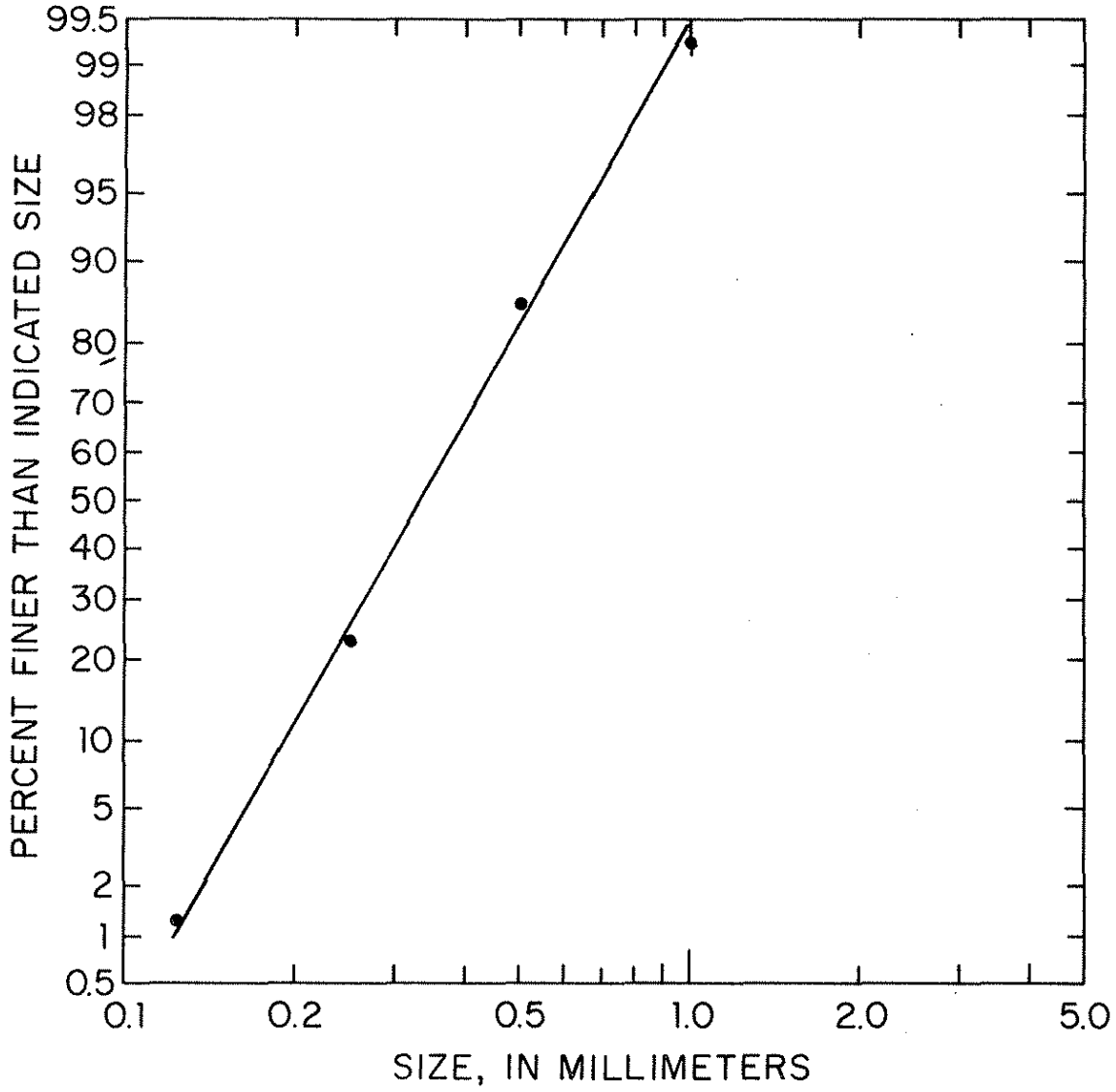

Figure 9. Grain-Size Distribution for Uniform Bed Sediment, Test Series 1 and 2

80, and 160 hours. Each time, the depth was measured at 19 points across each of 25 sections throughout the bend. At each section the topography was characterized by the transverse slope of the bed as determined by linear regression. (The actual slope was not complely constant across the channel especially not at the end of the time period; however, the test objective did not call for any higher degree of mathematical sophistication). The transverse bed slope changed quite rapidly within the first 10 hours after the start of the test (Fig. 10). After 10 hours, the changes were minor. The maximum transverse bed slope (0.092) developed at Sections 80 and 84. Figs. 11 and 12 show the bed profile at Sections 80 and 112 at times 0, 10, and 160 hours. Over the 160-hour period, a total of 30 ft^3 of sand was moved from the outer half of the channel to the inner half generating point bars and scour holes, typical features of an alluvial channel bend. The longitudinal slope of the water surface, and the cross-sectional average depth and velocity were measured to be 0.00104, 0.50 ft, and 1.30 ft/sec, respectively. Thus, $F_D = 5.67$, $n = 4.0$, and $u* = \kappa u_a/n = 0.10$ ft/sec ($u*$ = shear velocity = $\sqrt{\tau_o/\rho}$). The value of the boundary Reynolds number, u_*D/ν (ν = kinematic viscosity), was approximately 12 yielding (from Shields' curve) a Shields parameter of $\theta \approx 0.04$. Based on these flow data, Eq. 12 predicts a transverse bed slope of $S_T = 0.063$. This slope is seen (Figs. 10 and 13a) to compare favorably with those measured, indicating that the theory on which the vane-design formula is based is valid.

The vane-design formula was tested with a system of 42 14-in. long vanes (plane pieces of 28-gage galvanized steel) each placed at an angle of 15 degrees to the mean-flow direction. This system corresponds with the design objective of obtaining a reduction of the transverse bed slope to 0.03 throughout the bend. The design calculations for this objective are summarized in Tables 3 and 4. Because of the significant variation of the transverse bed slope along the channel, the calculations are based on the effective-radius

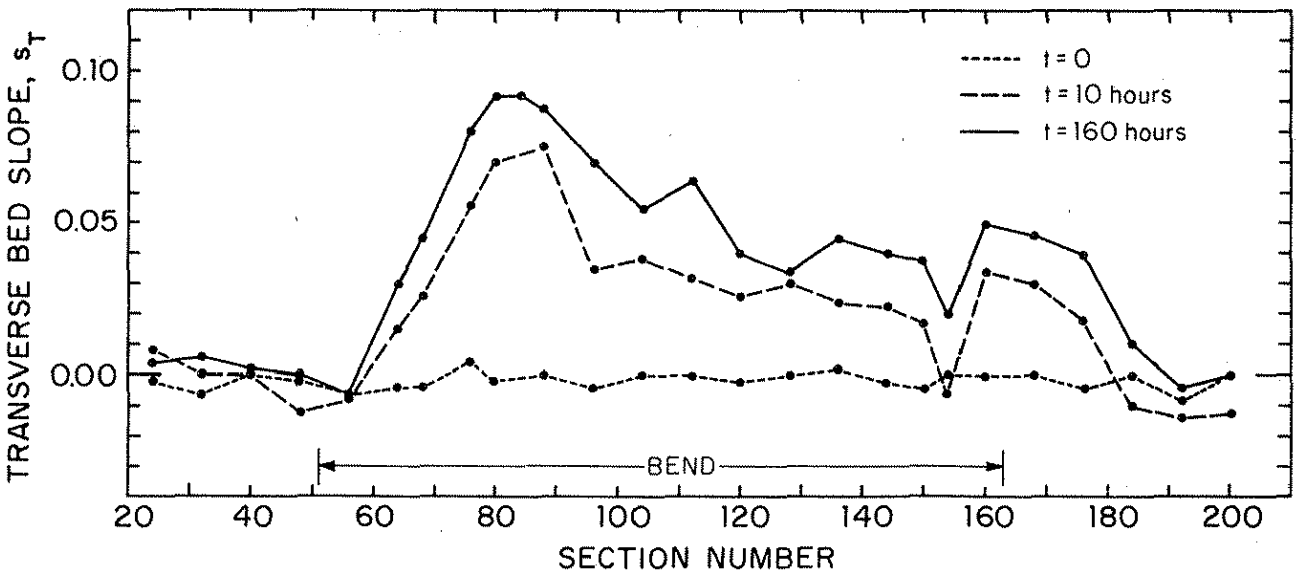

Figure 10. Streamwise Variation of Transverse Bed Slope Development, Test Series No. 1

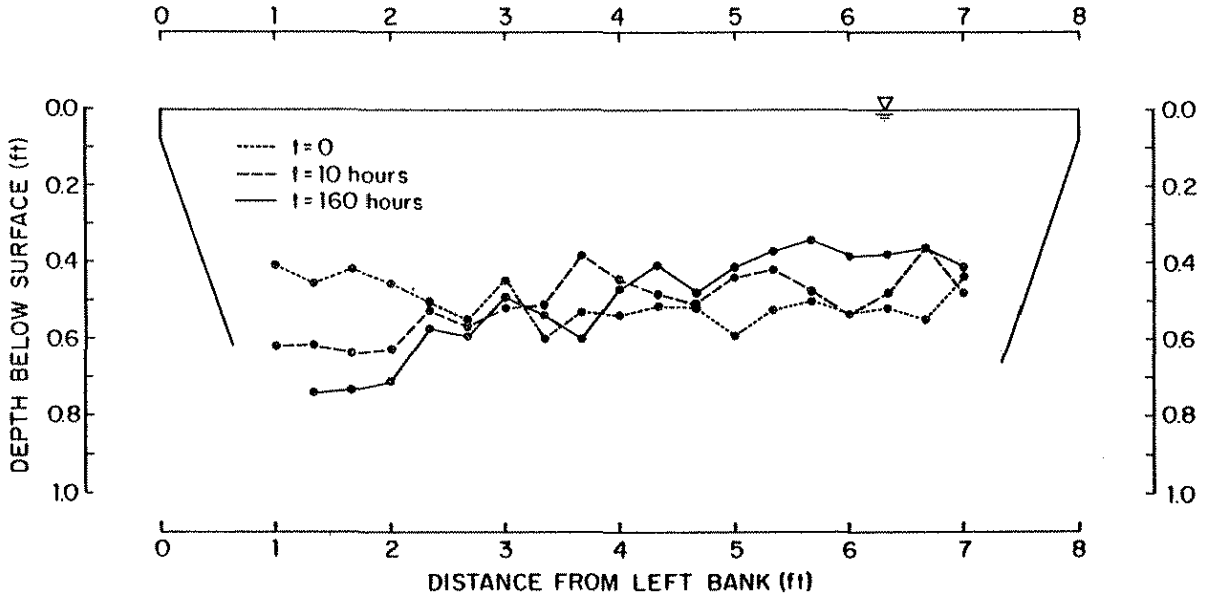

Figure 11. Development of Bed Profile at Section 80, Test Series No. 1

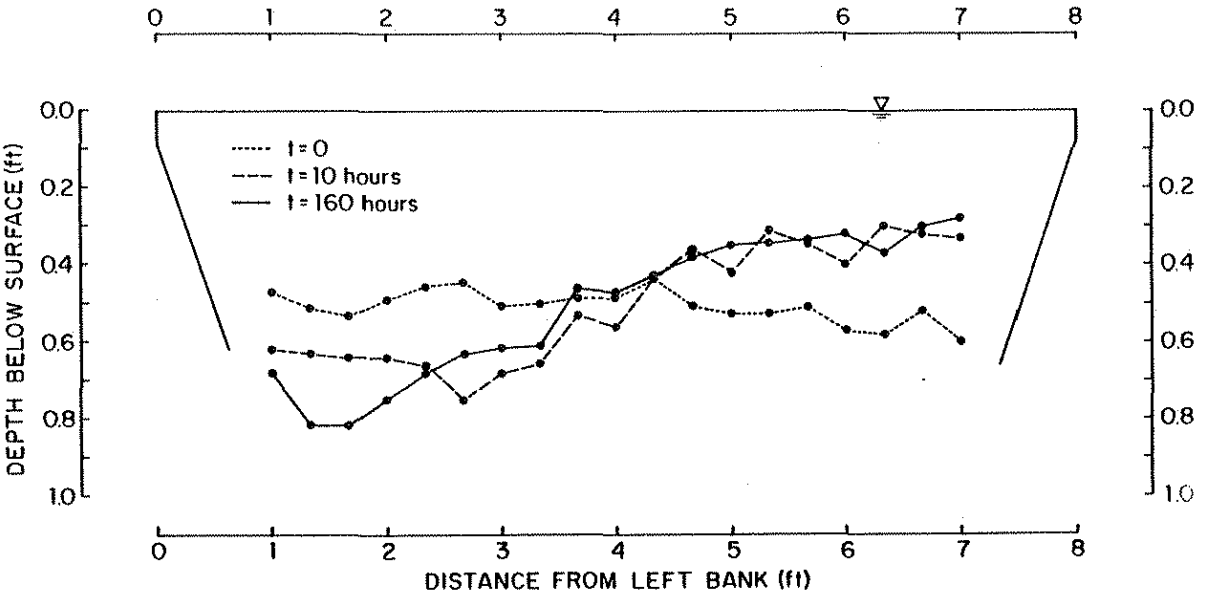

Figure 12. Development of Bed Profile at Section 112, Test Series No. 1

Table 3. Effective-Radius Calculations for Model Tests

Test series -run no.	Length channel reach, $r_c\phi$, in feet	Shields' factor, Θ	Particle Froude number, F_D	Transverse bed slope		Effective radius	
				Measured, S_T	Desired, S_{To}	r_e, in feet (based on S_T)	r_{eo}, in feet (based on S_{To})
1-1	36	0.04	5.67	0.070	0.030	38.9	90.7
	76	0.04	5.67	0.045	0.030	60.5	90.7
2-1	112	0.04	6.11	0.074	0.030	43.0	90.7
3-1	112	0.04	5.27	0.070	0.030	34.0	90.7
4-1	112	0.04	2.11	0.16	0.11	43.0	64.5
4-2	112	0.04	2.11	0.16	0.13	43.0	54.5
4-3	112	0.04	2.11	0.16	0.09	43.0	78.8

Table 4. Vane-Design Calculations for Model Tests

Test series -run no.	Length of channel reach $r_c\phi$, in ft	Vane Length, L, in inches	Vane-aspect ratio, H/L	Vane-angle of attack, α in degrees	Lift coefficient, C_L	Vane function, F	Number of vanes required	Lifting surface required per unit length of channel
1-1	36	14	0.2	22	0.4	0.57	26	0.17
	76	14	0.2	22	0.4	0.57	20	0.06
2-1	112	9	0.3	25	0.6	0.70	90	0.12
3-1	112	14	0.2	25	0.5	0.30	40	0.08
4-1	112	14	0.2	25	0.5	0.85	50	0.10
4-2	112	14	0.2	17	0.3	0.85	50	0.10
4-3	112	9	0.4	25	0.7	0.85	70	0.09

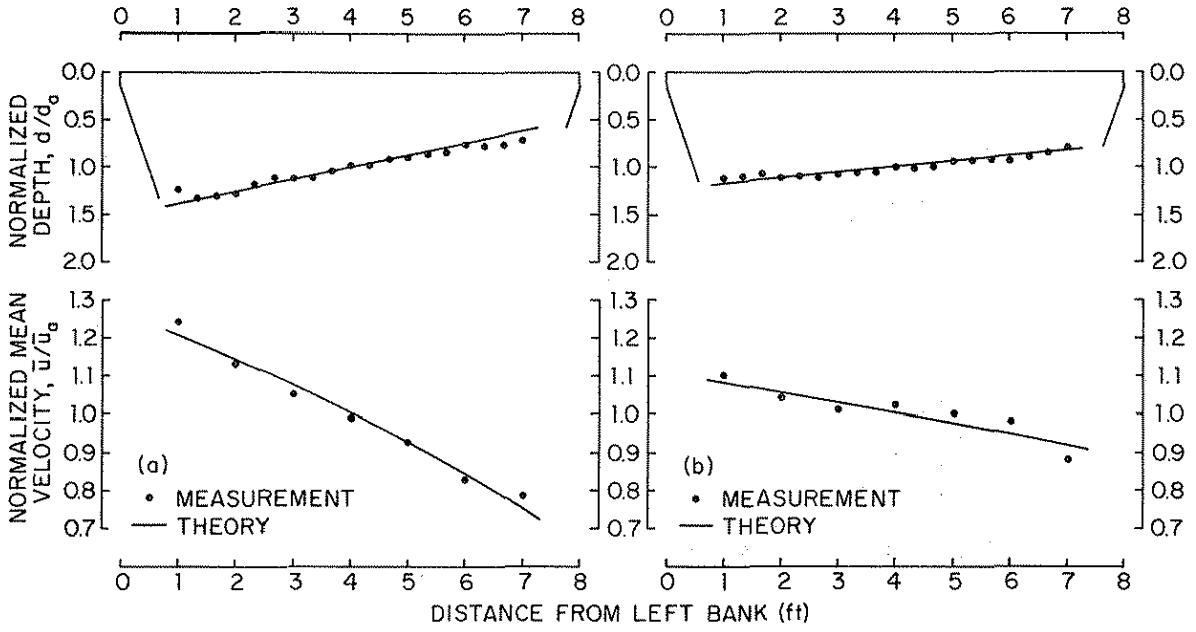

Figure 13. Test Series 1: Measured Radial Average-Distribution of Depth and Depth-Averaged Mean Velocity Compared with the Predicted Distributions; (a) Before Installation of Vanes; (b) After Installation of Vanes

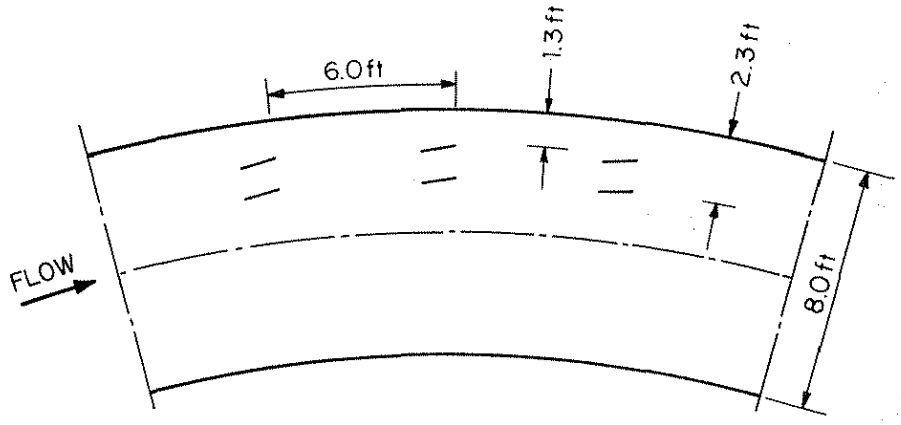

Figure 14. Test Series 1 Vane Emplacement

concept. Between Sections 64 and 100, the average transverse bed slope was measured to be S_T = 0.070, yielding an effective radius of 38.9 ft. Between Sections 100 and 176 (the end of the bend), the transverse bed slope was 0.045, yielding an effective radius of r_e = 60.5 ft. The "desired" effective radius (that corresponding to S_{To} = 0.030) is r_{eo} = 90.7 ft. To meet the objective at minimum lift surface, the vane height H must be about 33% of the water depth at the vanes. (Note that because c_L decreases when H/L decreases, NHL is not minimum when F is minimum). As the vanes are placed at a distance from the channel-center line of 2 to 3 ft, and are to reduce the water depth there to approximately 0.6 ft, their height should be H ≈ 0.2 ft, yielding an aspect ratio of approximately 0.2. The near-bed deviation angle is calculated from Eq. 22 (with n = 4.0, d = 0.6 ft, and r_e = (90.7 + 2.5) ft) to be $\delta \approx 7°$, yielding a total angle of attack of α = 15° + 7° = 22°. According to Fig. 6, the lift coefficient is then $c_L \approx 0.4$. The value of F is obtained from Eq. 10 (or Fig. 5) to be F = 0.577 (using n = 4 and H/d = 1/3). The number of vanes is then readily determined by substitution into Eq. 16: N = 26 between Sections 64 and 100; and N = 20 between Sections 100 and 176. Hence, according to this design procedure, a total of 46 vanes (four more than was actually used) would be required to reduce the transverse bed slope to 0.03 throughout the channel.

The vanes were installed in a two-row array up until Section 104, and a one-row array beyond Section 104. The emplacement of the two-row array is sketched in Fig. 14. The emplacement of the one-row array was the same as that of the outer row in Fig. 14. The vanes were installed on the dry 5.2-cfs channel bed such that their top edge was 0.4 ft under the 5.2-cfs water surface. The flow rate was then gently increased to 5.2 cfs, and maintained at this rate for a period of 160 hours. The bed topography was measured after 10, 20, 40, 80, and 160 hours. The transverse bed slope was observed to change very rapidly within the first 10 hours after the start of the flow, as Figs. 15, 16, and 17 indicate. Over the 160-hour period, a

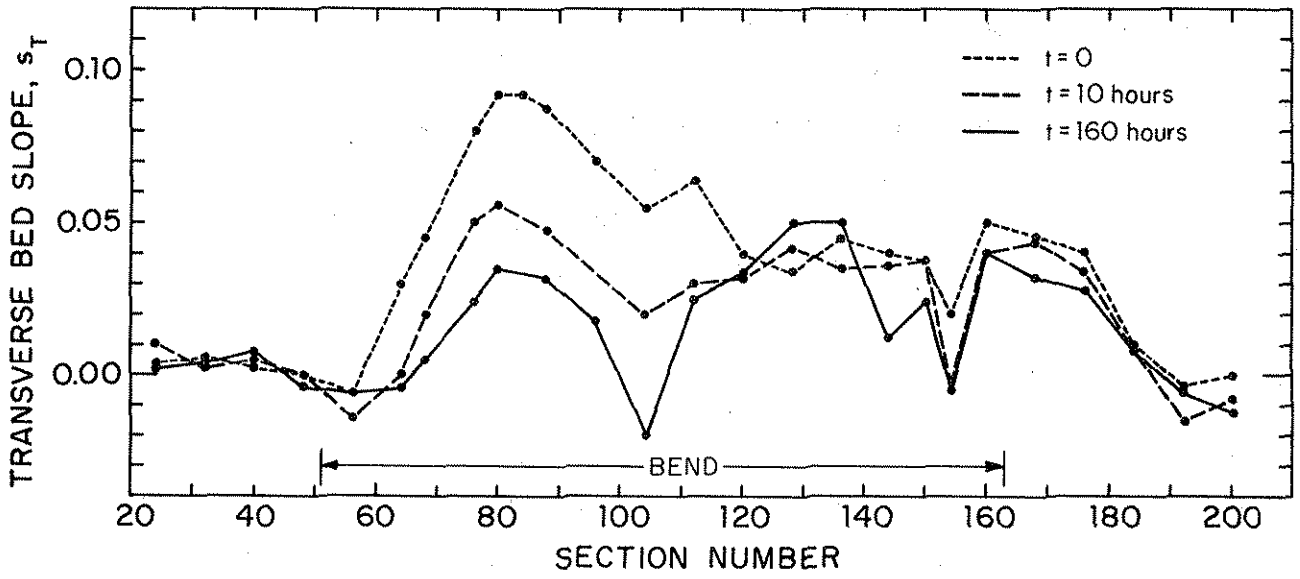

Figure 15. Streamwise Variation of Transverse Bed Slope Development after Installation ofVanes; Test Series No. 1

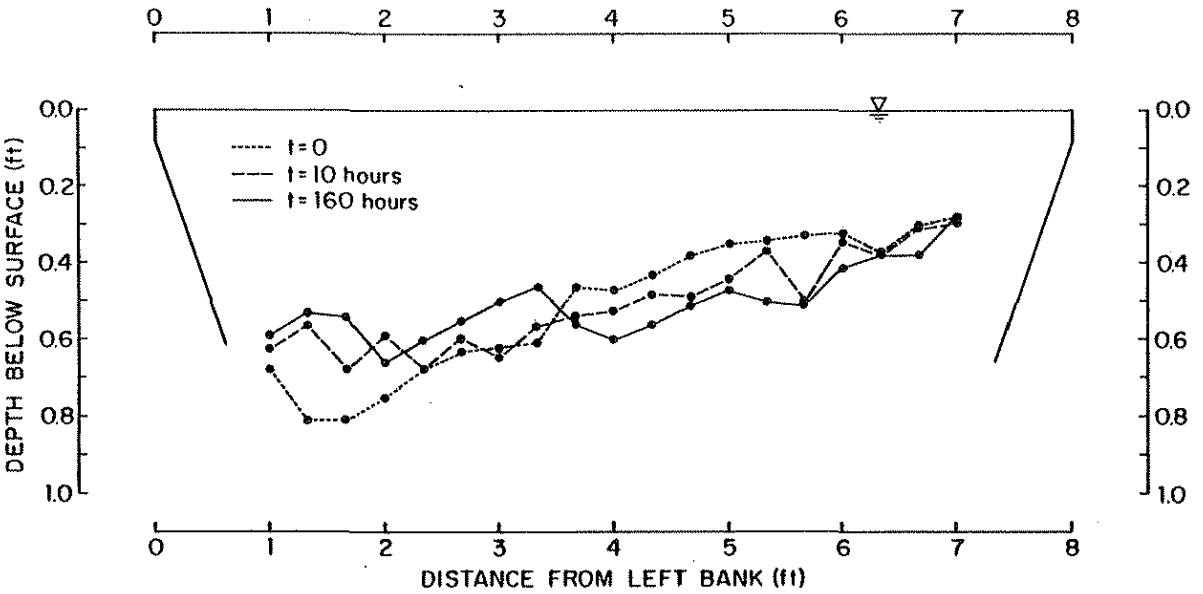

Figure 16. Development of Bed Profiles at Section 80 after Installation of Vanes; Test Series No. 1

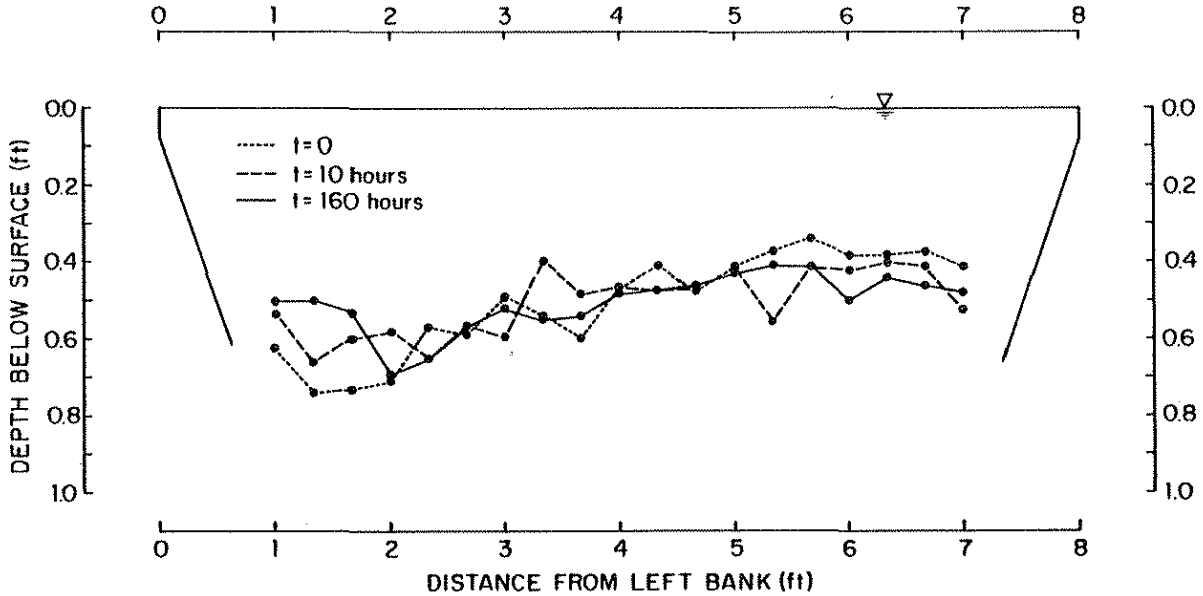

Figure 17. Development of Bed Profiles at Section 112 after Installation of Vanes; Test Series No. 1

total of 15.7 ft^3 of sand was moved from the inner half of the channel to the outer half. In other words, the vane system caused 52% of the sand that was originally moved (during the initial bed-forming process) from the outer half to the inner half to return to the outer half of the channel. As Fig. 13b shows, the average distributions of depth and velocity are in good agreement with those predicted by the design procedure. In Fig. 15 it is seen that the vane system performed better over the first half of the bend than over the second half. This may have been due to the fact that the reach between Sections 64 and 104 was furnished with 28 vanes (in double-array) whereas the remaining part of the bend had only 14 vanes (in single array), or 30 percent fewer vanes than called for by the design calculations (which were done after the completion of the tests).

Table 5 summarizes the overall effectiveness of the vane system tested in terms of recovery of: (1) Sediment volume in outer half of channel (the percentage returned to the outer half of the channel of the sediment volume that was originally moved from the outer half to the inner half); (2) near-bank depth (the reduction of near-bank depth in percent of the reduction required for achieving uniform depth); and (3) near-bank velocity (the reduction in near-bank velocity in percent of the reduction required for the achievement of uniform velocity). The numbers in parentheses are the recovery percentages computed by the theory on the basis of the number of vanes employed. If these numbers equal the actual recovery percentage, the vane system performed exactly as computed. If the numbers in parenthesis are smaller than the actual recovery percentage, the vane system performed better than computed. Table 5 also shows the reduction of the longitudinal slope of the water surface caused by the vane system. In Test Series 1, the slope was reduced by 10 percent. The objective is to design the vane system such that the change in slope is as small as possible (a local reduction of slope will cause an increase of slope and degradation downstream).

Table 5. Summary of Experimental Results of Vane Tests

Test -run no.	Vane type	Vane length, in inches	Vane angle, d', in degrees	Number of vanes	Effectiveness of Vane System				
					Recovery of sediment volume in outer half of channel, in percent	Recovery of near-bank depth, in percent	Recover of near-bank velocity, in percent	Reduction of slope of water surface, in percent	Number of vanes with significant scour, in percent
1-11	sheet metal	14	15	42	52 (52)	63 (53)	58 (61)	10	9
2-1	sheet metal	9	12*)	84	49 (58)	63 (62)	80 (70)	<5	6
3-1	sheet metal	14	15	42	44 (47)	36 (50)	50 (61)	10	7
4-1	sheet metal	14	15	49	50 (29)	74 (29)	93	12	4
4-2	sheet metal	14	8	49	44 (19)	62 (17)	100	5	0
4-3	sheet metal	9	15	70	47 (41)	66 (44)	Not measured	<5	6
5-1	rock**)	28	15	12***)	30 (58#)	22 (50#)	100 (80#)	21	25

*) slightly curved vanes
**) several unsuccessful, exploratory tests with rock vanes preceded Run 5-1
***) the "rock" vanes were installed between Sections 72 and 112; remaining part of bend was furnished with curved sheet metal vanes in the Run 2-1 configuration
Recovery by sheet metal vanes between Sections 72 and 112 in Run 2-1 configuration

In the test series described above, Test Series 1, the side walls of the flume were of smooth plywood with a roughness much lower than that of the sand bed. The roughness of real river banks is often higher than that of the streambed (due to vegetation, fallen trees, rip-rap, etc.). In view of that, two test series (Nos. 2 and 4) were also conducted with roughened side walls. The roughness elements were 20-in. long, 1/2-in. wide, 1/4-in. thick pieces of wood which were nailed onto the side walls 1.5 in. center to center.

Test Series No. 2 was conducted with the same grade of sediment in the flume as Test Series No. 1. The maximum flow rate was 6.0 cfs. At fully developed flow and bed topography, the longitudinal slope of the water surface and the cross-sectional average values of depth and velocity were 0.00146, 0.54 ft, and 1.40 ft/sec, respectively. Thus, F_D = 6.11, n = 3.5, u_* = 0.16 ft/sec, and $\theta \simeq 0.04$. Based on these flow data, Eq. 12 predicts a transverse bed slope of S_T = 0.074, which is in good agreement with those measured (Fig. 18a).

In Test Series No. 2, the vane-design formula was tested with a system of 84 9-in. long, slightly curved vanes (Fig. 19). These tests were conducted specifically to verify that the lift force, and therefore the torque T_V, produced by a given lift-surface area increases when the aspect ratio increases. As the design calculations, summarized in Tables 3 and 4, show, the number N = 84 corresponds with the design objective of obtaining a reduction of the transverse bed slope to approximately 0.03, the same objective as in Test Series No. 1. By reducing the vane length from 14 in. to 9 in., the aspect ratio goes up from 0.2 to 0.3, and, according to Fig. 6, the lift coefficient becomes 0.6 as opposed to 0.4 with 14-in. vanes. Hence, with 9-in. vanes, the required lifting surface is 33% lower than if 14-in. vanes were used. The calculations summarized in Table 5 show that the effectiveness of the 9-in. vane system is as good as that of the 14-in. system as far as recovery of sediment volume, near-bank depth and near-bank velocity are concerned. The 9-

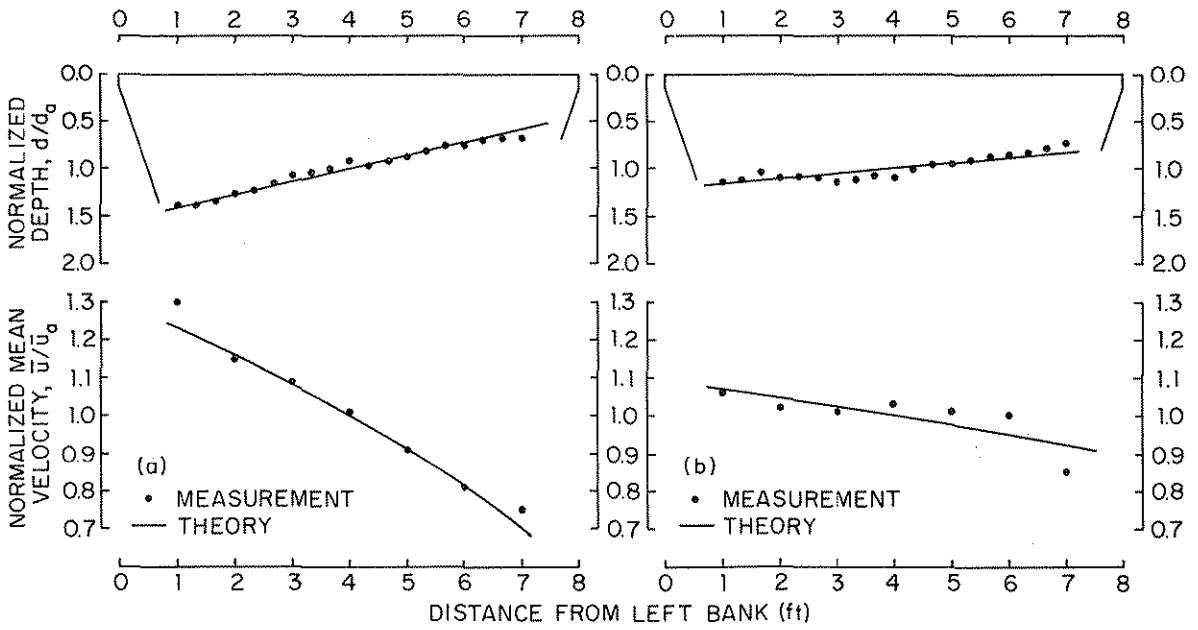

Figure 18. Test Series 2: Measured Radial Average-Distributions of Depth and Depth-Averaged Mean Velocity Compared with the Predicted Distributions; (a) Before Installation of Vanes; (b) After Installation of Vanes

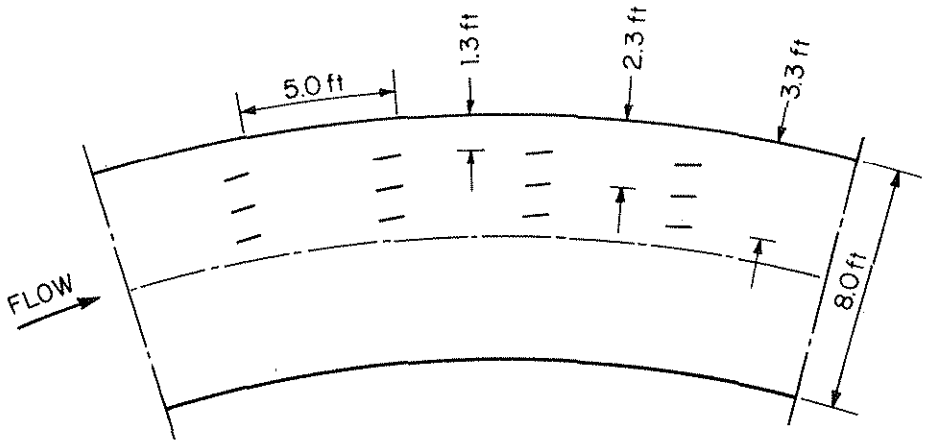

Figure 19. Test Series 2 Vane and Vane Emplacements

in. vane system is seen to have caused less change in water-surface slope than the 14-in. system. Therefore, overall the 9-in. vane system is judged to be more efficient than the 14-in. vane system.

2. Nonuniform Bed Sediment - In Test Series No. 3, the sediment was sand with a log normal grain-size distribution with a median diameter of 0.90 mm and a geometric standard deviation of 1.90 (Fig. 20). The discharge was 5.8 cfs. Initially, the sand was distributed uniformly throughout the flume. As the water-sediment mixture was then propelled through the flume, grain sorting took place. The smaller fractions tended to accumulate near the inside of the bend leaving the larger fractions along the outside. When steady-state conditions were obtained, water-surface elevations, and distributions of depth, velocity, and grain size, were measured. Notable features of the bed topography were a point bar along the inner bank between Sections 88 and 104; and an attendant relatively deep scour hole at Section 80. Deep scour holes occurred also at the outer bend at Sections 136 and 170. It is noteworthy also that the sediment in the surface layer of the bed was generally finer than that below the surface. The coarser fractions only surfaced within a distance of about 2 ft from the outer flume wall. Bed-material samples taken below the surface of the bed throughout the bend showed that the original sand mixture was found at a depth of three to five inches below the bed surface, indicating that grain sorting was limited to the upper three to five inches of the sediment layer. Bed armoring did not occur. The overall median diameter of the sediment in the surface layer of the bed was determined to be D_a = 0.50 mm. The longitudinal slope of the water surface, and cross-sectional average values of depth and mean velocity were measured to be 0.00063, 0.47 ft, and 1.56 ft/sec, respectively, yielding F_D = 5.27, n = 6.5, u_* = 0.10 ft/sec, and $\theta \simeq$ = 0.04. Based on these flow data, Eq. 12 predicts a transverse bed slope of S_T = 0.055, which is in reasonable agreement with those measured (Fig. 21). The overall average transverse bed slope was measured to be 0.07.

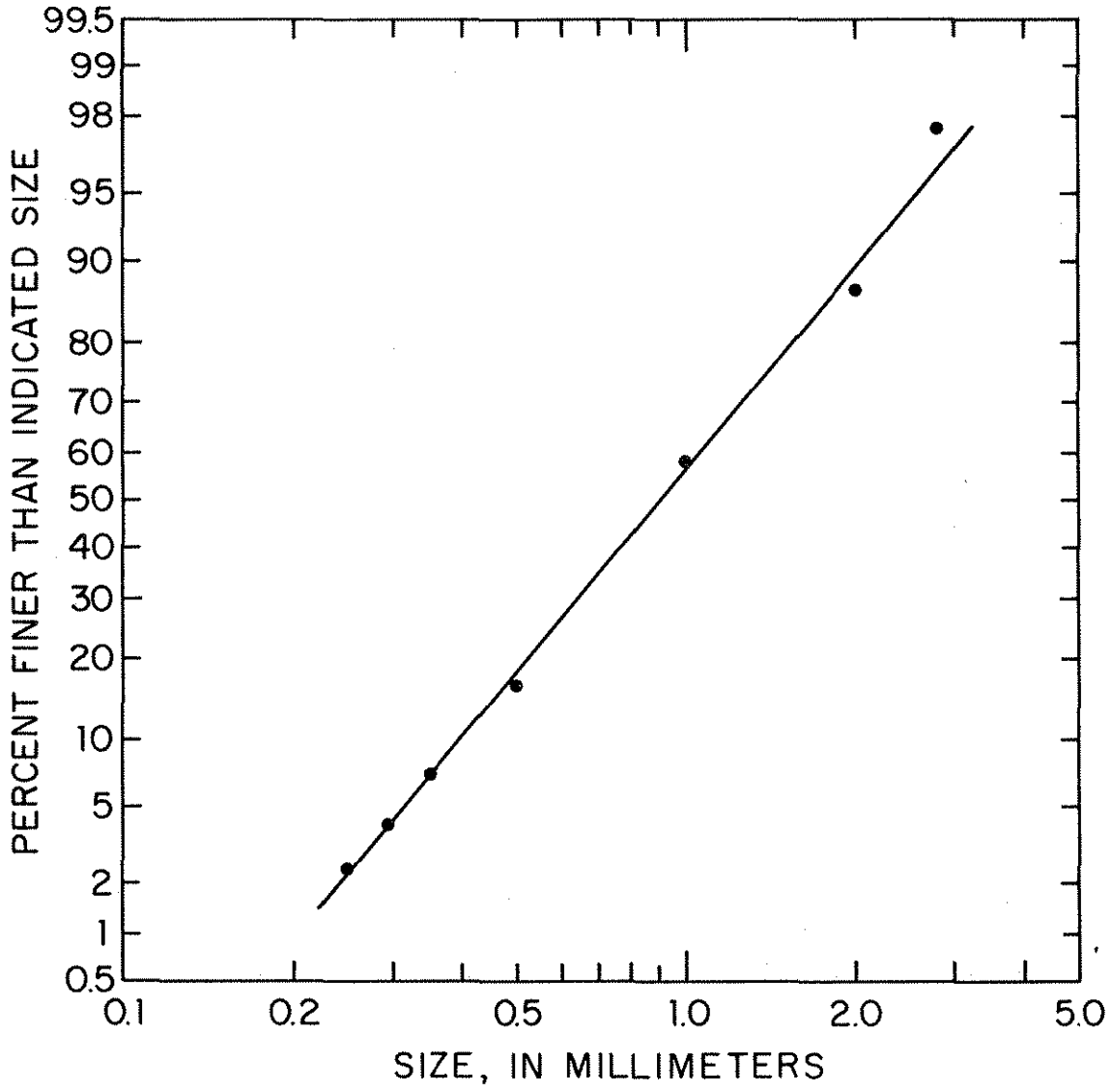

Figure 20. Grain-Size Distribution for Nonuniform Bed Sediment; Test Series No. 3

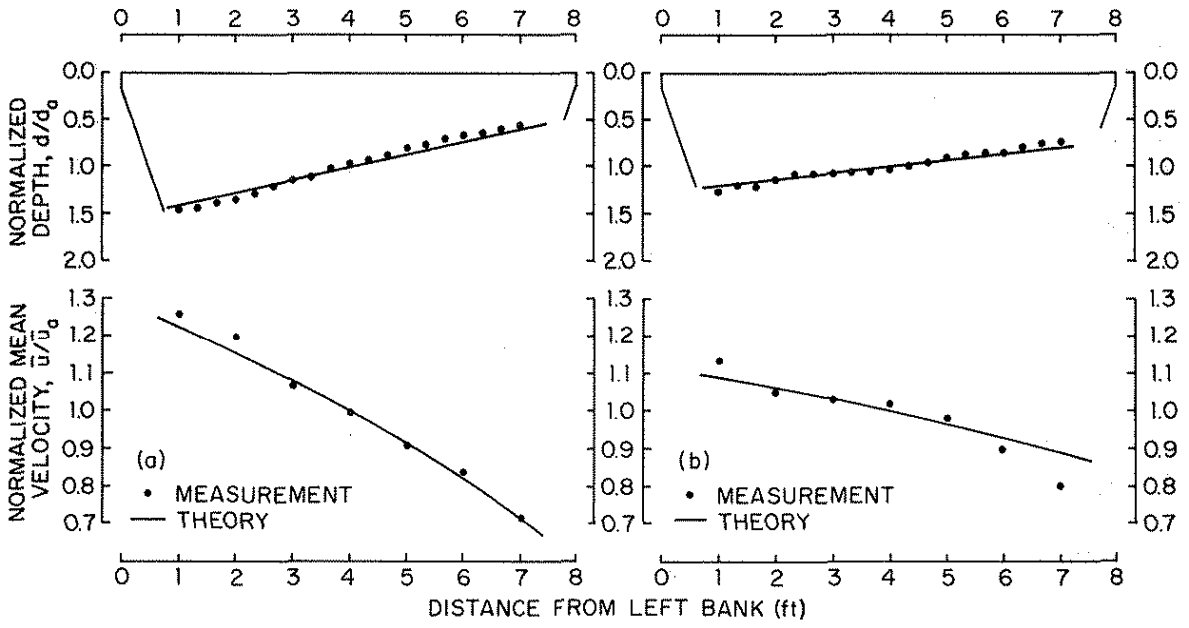

Figure 21. Test Series 3: Measured Radial Average-Distributions of Depth and Depth-Averaged Mean Velocity Compared with the Predicted Distributions: (a) Before Installation of Vanes; (b) After Installation of Vanes

The vane-design formula was tested with a system of 42 14-in. vanes in the Fig. 14 configuration. The design calculations (Tables 3 and 4) show that this system corresponds with the design objective of obtaining a reduction of the transverse bed slope from 0.07 to 0.03, which is seen to be in very good agreement with that measured. The vane system is seen to have performed with about the same efficiency as in the case of uniform sand (Table 5).

B. Vanes in Armored Channel

A series of tests was designed specifically to investigate the vanes' performance in a channel bend with bed armoring. Data from many river bends in the United States, including Iowa, show that some areas of the bends are often heavily armored along some reaches, and raise the question of whether the submerged vanes can achieve reworking of the armored portions of the beds that is required to achieve a flow that is uniform laterally.

The bed material in this test series was that of Test Series No. 3 supplemented with coarse sand to give the grain-size distribution shown in Fig. 22 (several different mixtures were tested before one was found that armored over a significant part of the bend). During the process of bed armoring, the bed level was observed to increase in the straight approach section causing the overall longitudinal bed slope to be somewhat larger than the slope of the water surface. Grain sorting took place both laterally and longitudinally. The bed became fully armored in the entire approach section and in the beginning of the bend up till Section 88. Between Sections 88 and 172 the bed material near the outer bank was coarse sand with a median diameter of about 3.2 mm and a geometric standard deviation of less than 1.4. Armoring occurred over most of the point bar within a distance of 4 to 5 ft from the inner flume wall. At full development, the overall average distributions of depth, velocity, and median-grain size were as shown in Fig. 23a. As was expected, Eq. 12 could not predict the transverse bed slope in this case. So

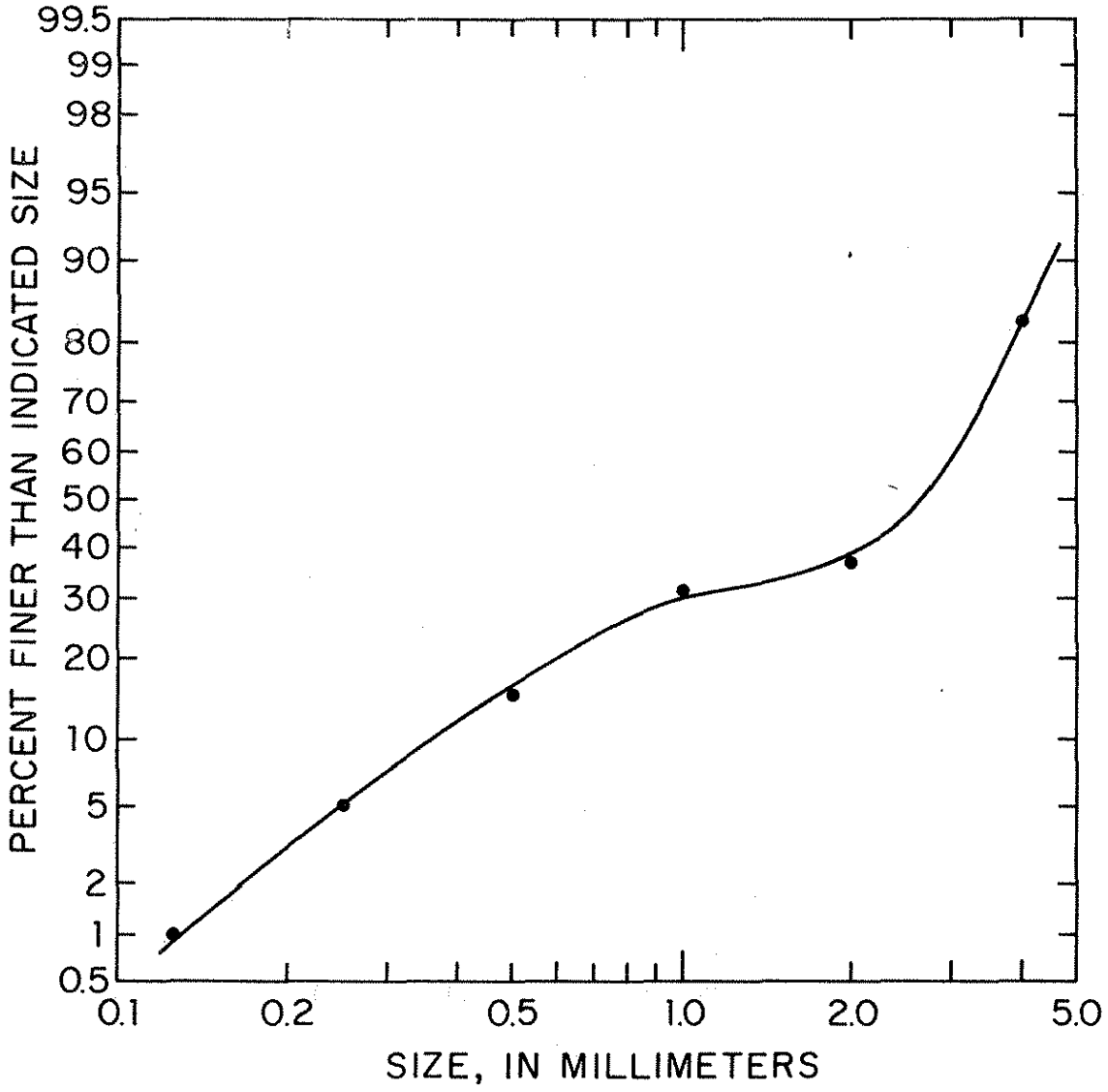

Figure 22. Grain-Size Distributions for Nonuniform Bed Sediment; Test Series No. 4

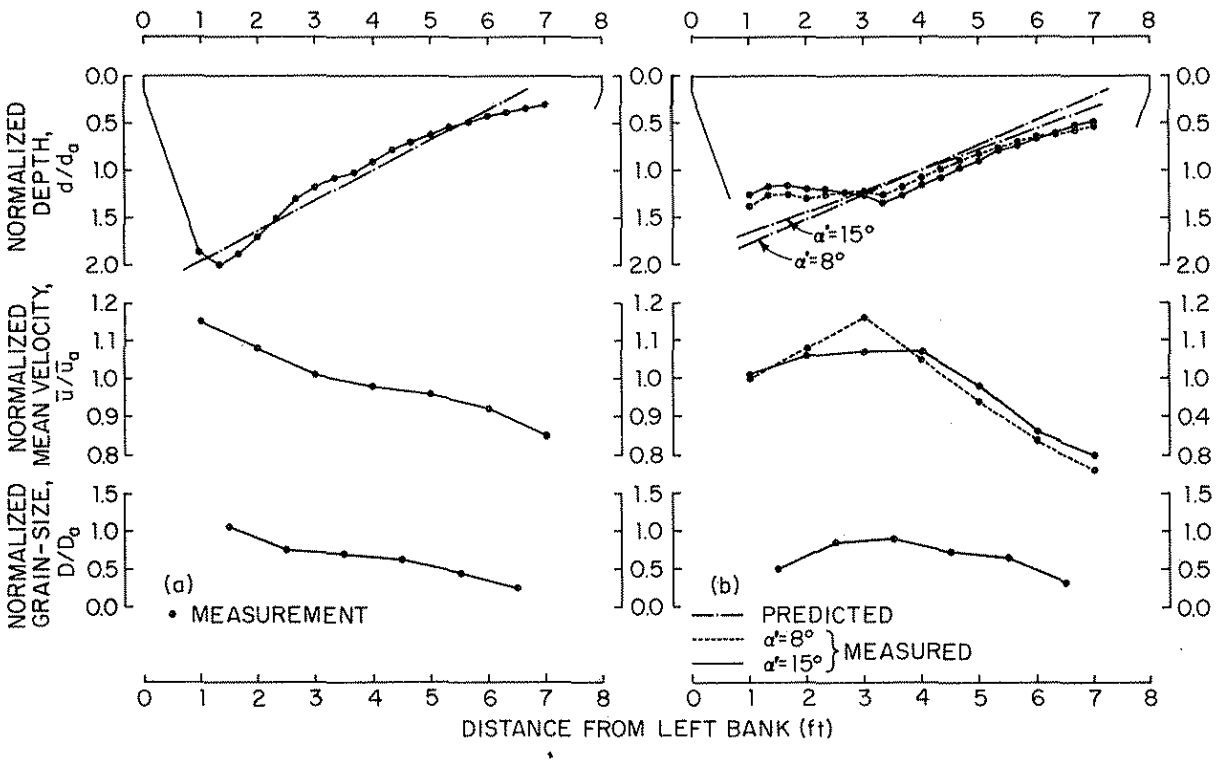

Figure 23. Test Series No. 4: Radial Average-Distributions of Depth, Depth-Averaged Mean Velocity, and Median-Grain Diameter; (a) Before Installation of Vanes; (b) After Installation of Vanes

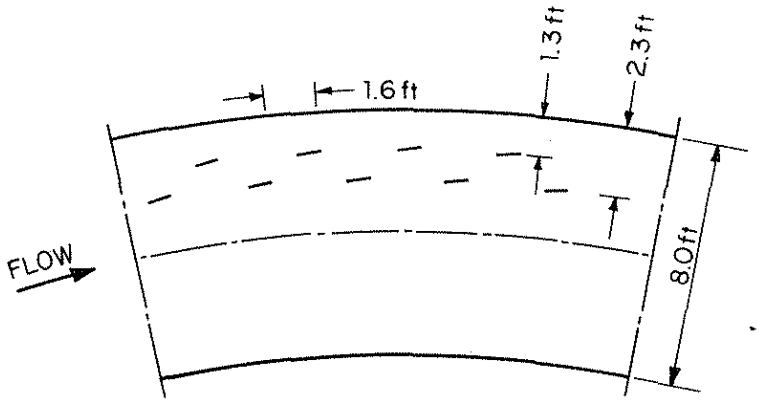

Figure 24. Test Series No. 4 Run 3 Vane Emplacement

far, no mathematical model has been developed that can predict the bed topography in a partially armored river bend. However, the bed profile is formed by the secondary-flow component so the transverse bed slope must correlate with the balance between the radial components of the bed-shear stress and weight of some representative bed particle, or group of bed particles. Therefore, it is reasonable to expect that the parameter constellation of Eq. 12 still applies, and that an acceptable design relation can be obtained by using Eq. 12 with a calibration factor, which obviously must be site specific. With a particle Froude number based on D = 2.7 mm, and θ = 0.04, the calibration factor becomes 7.0.

The test series included experiments with two different vane lengths (L) and two different vanes angles (α'). In Run 4-1, the performance of 49 14-in. vanes, installed at angle $\alpha' = 15°$, were tested; in Run 4-2, the same 49 14-in. vanes were tested with $\alpha' = 8°$. The vane emplacement was as shown in Fig. 14. The system of 49 14-in. vanes at $\alpha' = 15°$ corresponds with the design objective of obtaining a reduction of the transverse bed slope from 0.16 to 0.11; the system of 49 14-in. vanes at $\alpha' = 8°$ corresponds with the design objective to reduce the transverse bed slope from 0.16 to 0.13. A major objective of these two experiments was to verify that the performance of the vane system is sensitive to α', in agreement with the theory. As Fig. 23b shows, the 15-degree system performed slightly better than the 8-degree system, as predicted. In both cases, the vane system performed better than the design calculations predicted in terms of recovery of near-bank depth and velocity. This may have been due to the fact that the calculations (and the analysis) relates to the entire channel cross section, whereas the vanes, by their positioning, affected the flow in mainly the outer half of the channel. Because of armoring, the vanes were not able to move any major amounts of sand away from the inner half of the channel. It is important to note that the 7-degree difference in vane angle had only little effect on the overall performance.

In Run 4-3, the performance of 70 9-in. long vanes, installed at an angle of $\alpha' = 15°$ in the Fig. 24 configuration, were tested. The objective was the same as that of Run 2-1 with uniform sand; i.e., to verify that the efficiency of a system with given lift-surface area increases when the aspect ratio of each individual vane increases. As the design calculations, summarized in Tables 3 and 4, show, the system of 70 9-in. long vanes at $\alpha' = 15°$ corresponds with the design objective of obtaining a reduction of the transverse bed slope from 0.16 to 0.09. The predicted improvement over the 14-in. vane system is not apparent from the test results (Fig. 25); in fact, the performance is seen to have been slightly lower than that of the 14-in. system as far as near-bank depth recovery is concerned. However, it is noteworthy that the lift surface of the 9-in. system was about 10% smaller than that of the 14-in. system, and that the 9-in. system did not produce any measureable change of the slope of the water surface.

At the conclusion of each of the aforementioned runs, the vane system, and the bed topography developed by the vane system, were subjected to a lower flow rate of the order of 3.5 to 4.0 cfs. In no case did the lower flow rate cause any significant change in the bed topography developed at the higher flow rate.

C. Rock Vanes

A number of experiments were carried out with "vanes" composed of windrows of gravel and marbles (scaled-size rock) in an attempt to develop an economical alternative to sheet-pile vanes. The experiments, which are still ongoing, have not produced any encouraging results so far. One of the major problems is the embedment of the vanes. As the flow passes over the windrows, near-bed turbulence generates scour holes in the bed at the bottom of the windrows. As a result, the windrows tend to settle, usually in an uneven manner, and collapse.

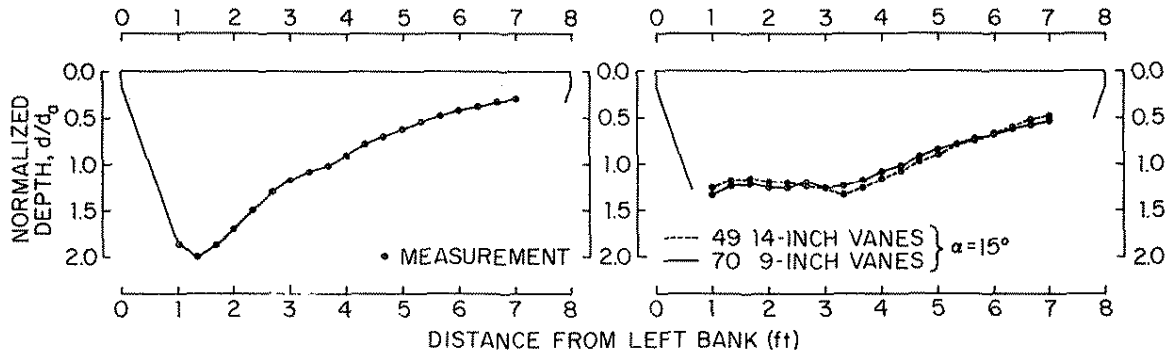

Figure 25. Test Series No. 4: Radial Average-Distributions of Depth; (a) Before Installation of Vanes; (b) After Installation of Vanes

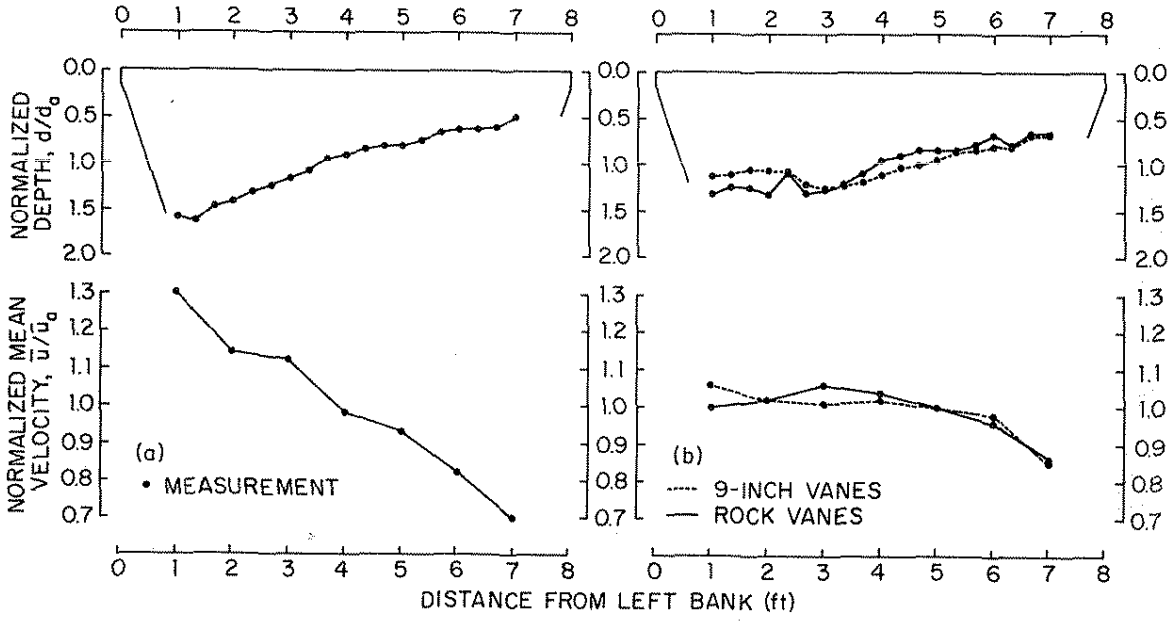

Figure 26. Test Series No. 5: Radial Average-Distributions of Depth, and Depth-Averaged Mean Velocity between Sections 72 and 112; (a) Before Installation of Vanes; (b) After Installation of Vanes

The most encouraging result was obtained in an experiment in which 12 24-in. long windrows of marble-filled baskets were installed between Sections 72 and 112 at 15° with the mean-flow direction (Fig. 27), with the remaining part of the bend furnished with 40 9-in. sheet-metal vanes in the Fig. 19 configuration. The bed sediment was that used in Test Series No. 2. The marble vanes were installed on the Run 2-1 channel bed, as developed by the 84 9-in. vanes, by replacing the 9-in. vanes between Sections 72 and 112 with marble vanes. Fig. 26 shows the average distributions of depth and velocity between Sections 72 and 112 before any vanes were installed (Fig. 26a); after the 9-in. vanes were installed (dotted curves in Fig. 26b); and after the 9-in. vanes were replaced by the marble vanes (solid curves in Fig. 26b). Approximately 50% of the sand that the 9-in. vanes recovered in the outer half of this channel portion was lost again when the 9-in vanes were replaced by the marble vanes. The marble vanes reduced the near-bank velocity to the cross-sectional average value for this portion of the bend, as indicated in Fig. 26b; however, this reduction was accompanied (and explained) by a very significant decrease of the slope of the water surface over this reach. Despite that this experiment was by far the most successful of the rock-vane experiments, Fig. 28 clearly show that more development work is needed before "rock vanes" can be considered to be an efficient alternative to sheet-pile vanes.

D. Discussion of Results

All tests were conducted with a vane angle of $\alpha' = 15$ degrees with the exception of Runs 2-1 and 4-2 in which the angle was 12 and 8 degrees, respectively. It was very clear from the tests that $\alpha' = 15$ degrees was at the upper limit of the workable α'-range. Objectionable scour always occured at a few of the vanes, even at $\alpha' = 12$ degrees, although this was not reflected in the "recovery" efficiencies. However, no scour occurred when α' was 8 degrees. As δ was always of the same order of magnitude (approximately 10

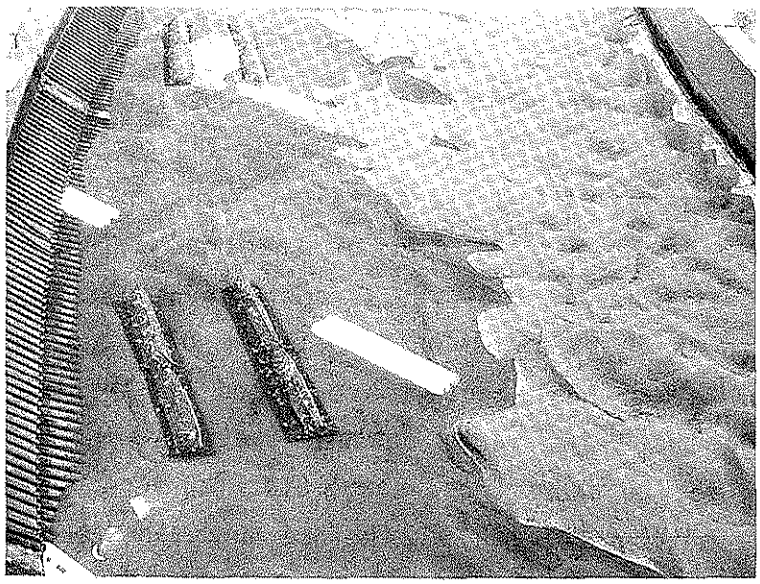

Figure 27. Test Series No. 5: Rock Vanes before Admission of Flow

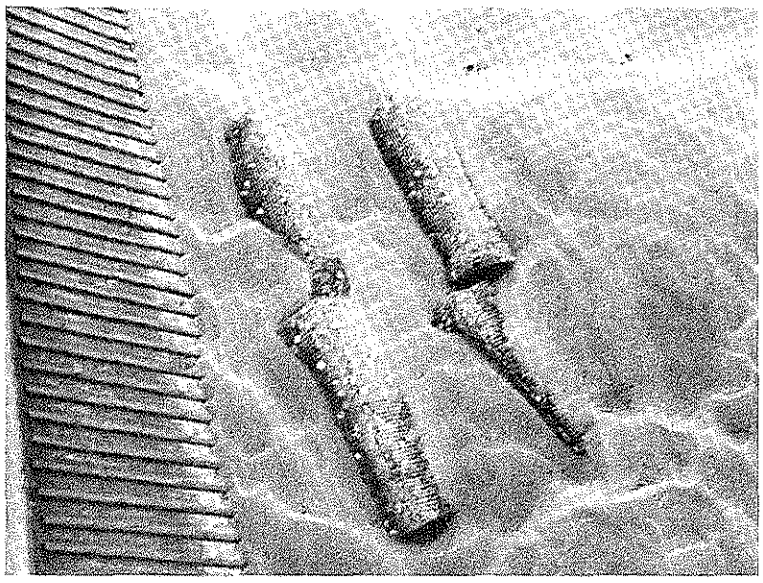

Figure 28. Test Series No. 5: Rock Vanes after Admission of Flow

degrees) it would appear that the optimum angle of attack, α, is of the order of 20 degrees. (α = the angle at which the bottom current approaches the vane).

The curving of the vanes in Run 2-1 was done in the belief that the lift and drag characteristics would be improved. Separate tests with straight and curved vanes in one of IIHR's straight, rigid-bed flumes showed that flow separation was less severe when the vanes were curved. As Table 5 shows, the efficiency of the curved-vane system was very good, in particular considereing that there was no measurable reduction of the longitudinal slope of the water surface. However, objectionable scour was observed at a few of the vanes. This might not have happened if the vanes had been slightly less curved.

Throughout the study the performance of the various vane systems was checked also by observations of the behavior of surface floats. Floats released at the center line of the channel should be carried sidewards toward the outside at a rate that can be calculated from the transverse bed slope that the vane system is designed to achieve (Odgaard, 1984). The float technique was used also, together with dye injections, to study the flow behavior around each individual vane. These tests led to the conclusion that the length of the vanes and their lateral spacing should not be more than about twice the water depth. If the length of the vanes or their lateral spacing, or both, exceeded twice the water depth the vanes tended to generate two (or more) secondary flow cells downstream rather than one, which obviously would reduce the overall performance of the vane system.

The performance of the various sheet metal vanes is illustrated on the photographs in Figs. 29 through 36. Fig. 29 shows a naturally formed bed topography with partial armoring (from Test Series No. 4). Notable features are the flat point bar and the steep slope at the edge of it. Fig. 29 also shows the 14-in vanes installed in a two-row array up to Section 98 (at the top of the picture) and a one-

Figure 29. Naturally Formed Bed Topography in Test Series No. 4 (Looking Upstream)

Figure 30. Bed Topography in Test Series No. 4 (Looking Upstream) after Installation of 14-in. Vanes

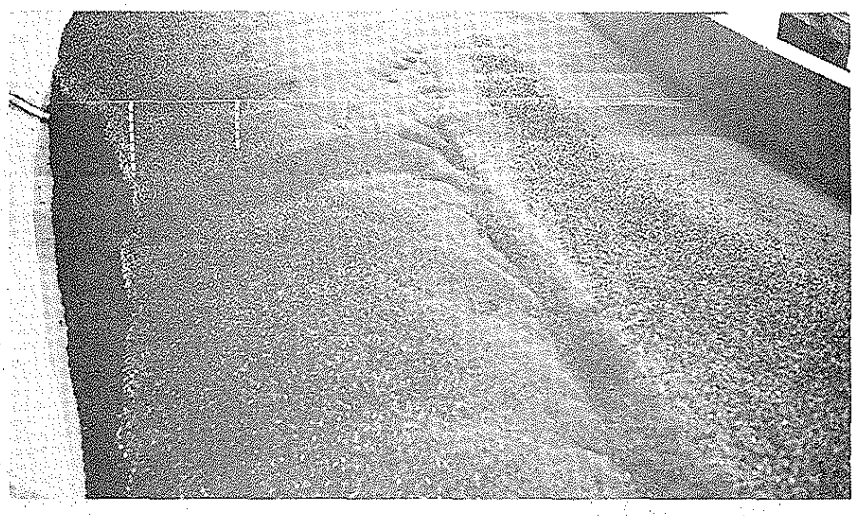

Figure 31. Depth Distribution at Section 112 in Test Series No. 4 Before Installation of Vanes

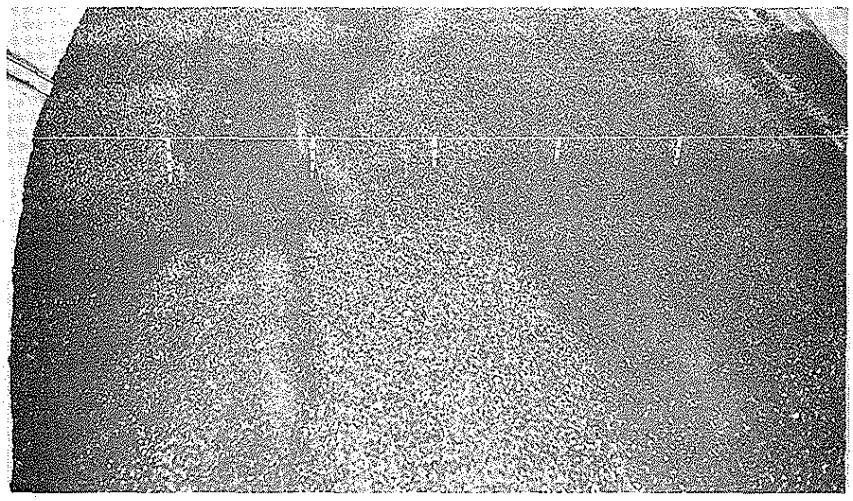

Figure 32. Depth Distribution at Section 112 in Test Series No. 4 After Installation of 14-in Vanes

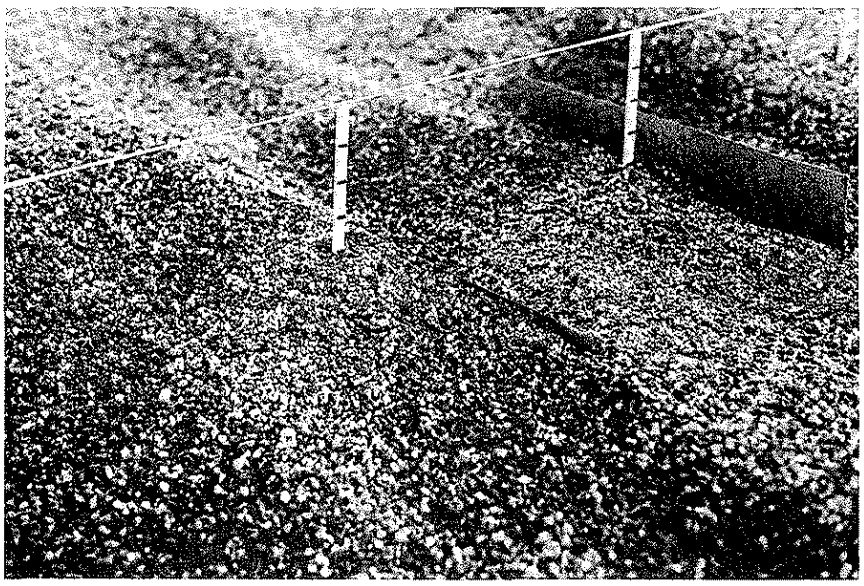

Figure 33. Close-up of Bed with 14-in. Vanes (one barely visible) at Section 112 in Test Series No. 4

Figure 34. Bed Topography Downstream from Section 112 in Test Series No. 4 with 14-in Vanes

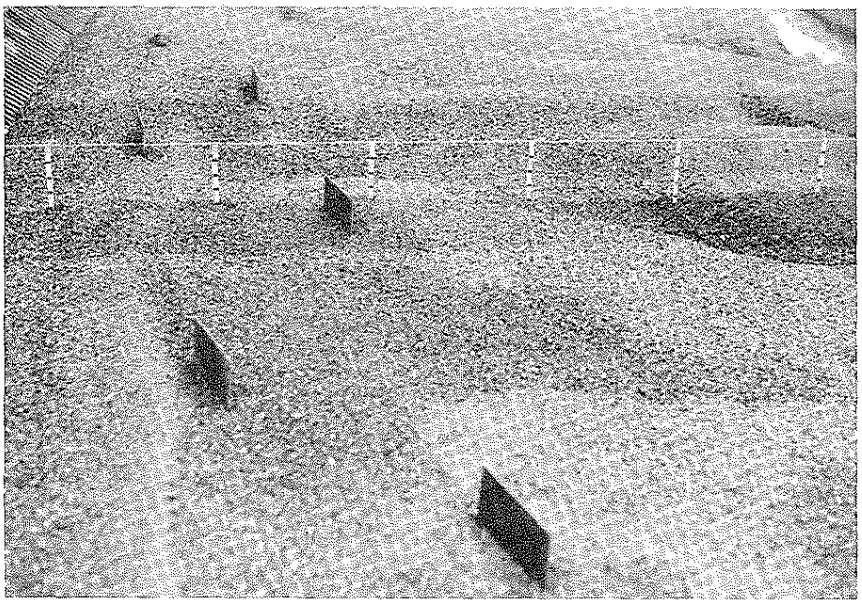

Fgiure 35. Depth Distribution at Section 112 in Test Series No. 4 After Installation of 9-in. Vanes

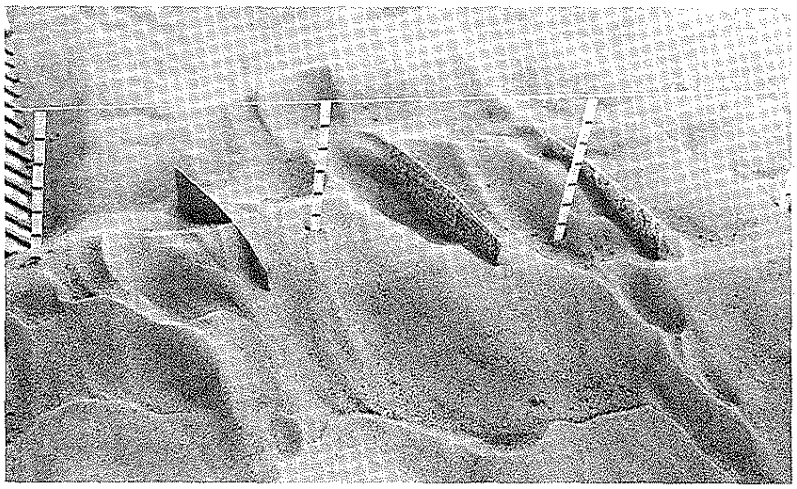

Figure 36. Depth Distribution at Section 112 in Test Series No. 2 After Installation of 9-in. Vanes

row array over the rest of the bend. The two-row array was later extended up to Section 112 (at the lower edge of Fig. 29). After 160 hours with a discharge of 5.8 cfs through the flume, most of the point bar had disappeared (Fig. 30). Note in Fig. 30 that some of the vanes in the outer row had become completely covered with sand. The depth distribution at Section 112 is indicated in Figs. 31 (before installation of vanes) and 32 (after installation of vanes). For visualization, a string was extended horizontally at the water level, and 5 thin staffs with 1/10-ft marks were driven into the sand bed (after draining of the flume) at 1 ft intervals. The outer staff was 2 ft from the outer flume wall. The depth at this staff is seen to have been 0.8 ft before vanes were installed. After the vanes were installed the depth here was reduced to 0.4 ft (Figs. 32 and 33). Downstream from 112, where only one row of vanes were installed, the result was also very satisfactory, as Fig. 34 clearly shows. The bed recovery at Section 112 with 9-in. vanes is shown in Figs. 35 (Test Series No. 4-3) and 36 (Test Series No. 2-1).

IV. VANE DESIGN FOR EAST NISHNABOTNA RIVER BEND

The results of the theoretical analysis and the laboratory-model experiments were used for the design of a vane structure for the meander bend in Fig. 3 for the protection of U.S. Highway 34 and its bridge over East Nishnabotna River. The flume in which the aforementioned experiments were conducted, models, with some idealization, this meander bend at an undistorted scale of approximately 1:10. Fig. 37 shows the IIHR flume overlaid the prototype bend, using the scale ratio 1:10.

A. Field Surveys

Cross sections of the river bend (of which a plan view is shown in Fig. 38) were surveyed October 6-7, 1983 (eight cross sections), and April 30 through May 2, 1984 (ten cross sections) to define the channel geometry at two different times for two different flow rates

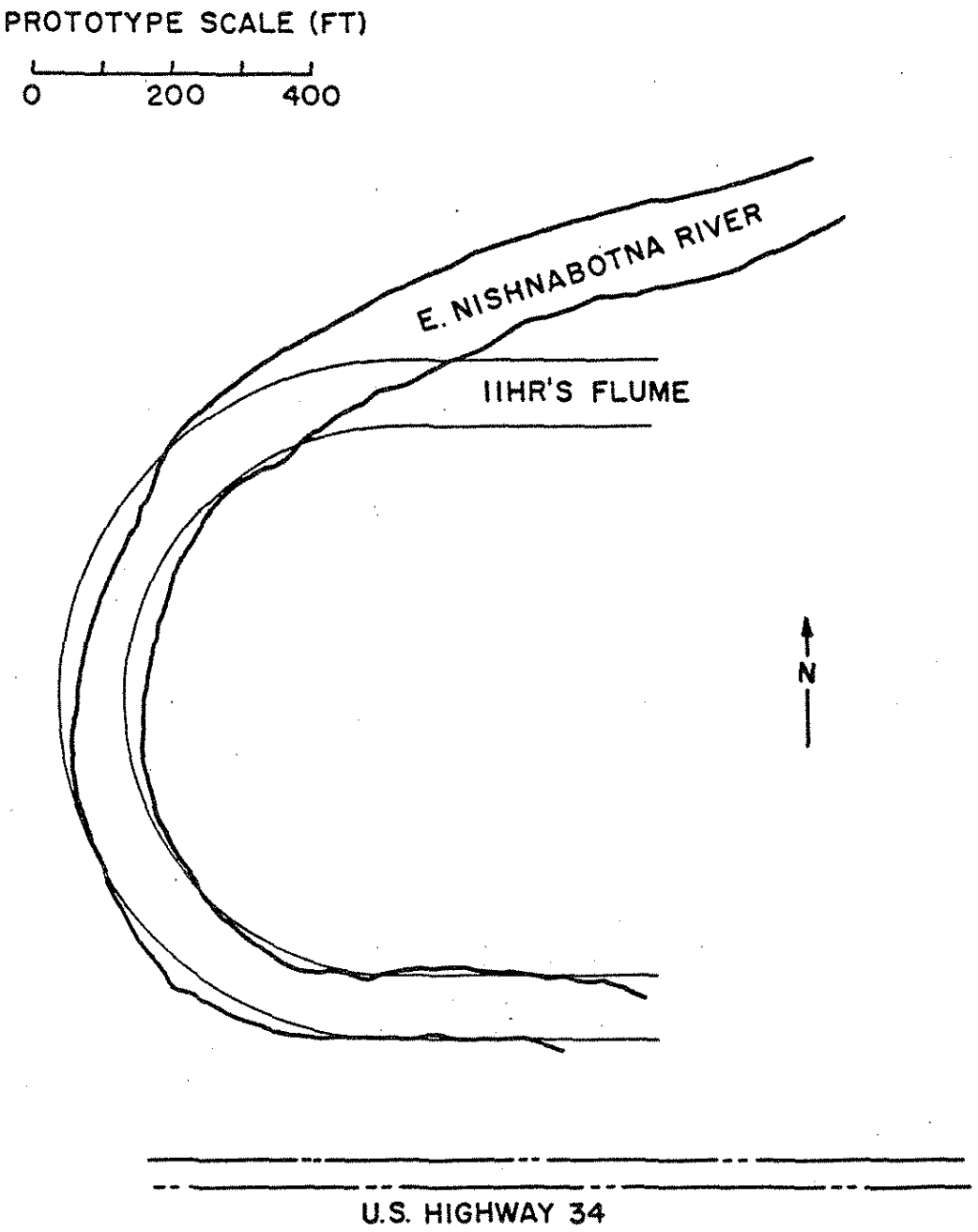

Figure 37. Plan-View of IIHR's Sediment Flume Overlaid the East Nishnabotna River Bend at Red Oak, Using a Scale Ratio of 1:10

COORDINATES OF REFERENCE POINTS (APPROXIMATE)		
POINT	WEST (FT)	NORTH (FT)
R	0	0
A	-90	85
B	45	160
C	245	165
D	430	175
E	610	250
F	740	510
G	690	870
H	320	1,080
I	-125	1,240
J	-360	1,300

NOTE:
REFERENCE POINT R IS AT NORTH WEST WING OF BRIDGE, DOT STATION 421, 18 FT NORTH OF HIGHWAY CENTER LINE.

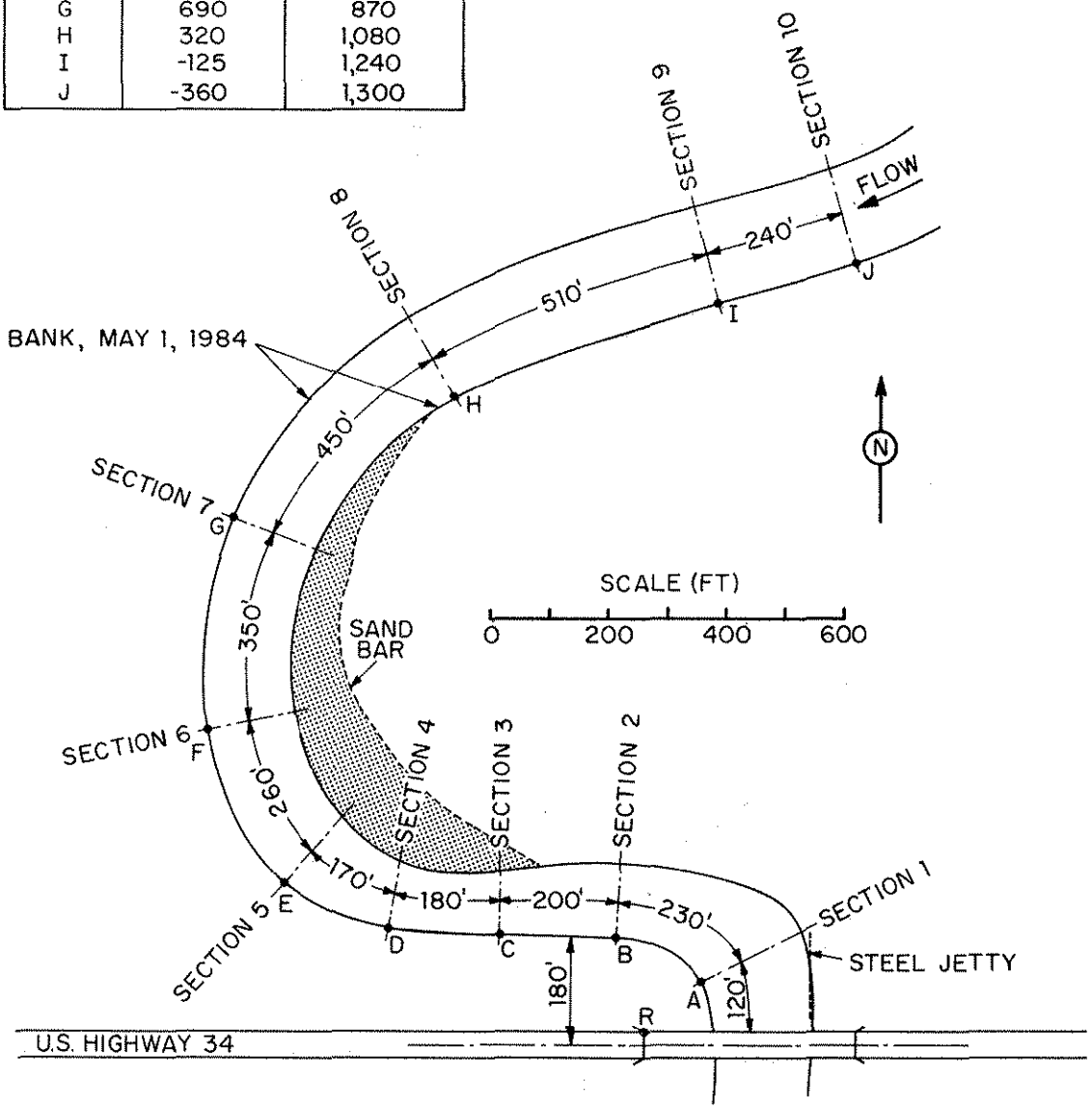

Figure 38. Plan-View Sketch of the East Nishnabotna River Bend at Red Oak, Iowa

(Figs. 39 and 40). Also, detailed velocity measurements and bed-material samples were taken at each cross section to determine the variations in the velocity profiles and the size of the bed sediment. The velocity was measured over 5-6 verticals across each section using a 5-in. Ott current meter. In each vertical, the velocity, u, was measured in five points; the recording time was 30-40 seconds at each point. Based on these measurements, a depth-averaged velocity, $\bar{u}$, was determined for each vertical. The cross-sectional average velocity, u_a, was determined by dividing the flow rate (obtained by integrating the velocity distribution) by the measured cross-sectional area. The bed samples were taken by a grab-bucket sampler which samples to a depth of 5-6 in. below the bed surface. The samples were dried, weighed, and sieved for size-distribution analysis.

The data are summarized in Tables 6 and 7 and in Fig. 41. The sections are indentified by their distance from the northern guardrail of the bridge. The distances are along the May 1, 1984, channel-center line. The elevations are listed in relation to mean sea level using the stage-discharge relation for the U.S.G.S. gage at Coolbaugh Street bridge in Red Oak (Fig. 42), which is 6,000 ft downstream from the Highway 34 bridge. The datum of this gage is 1005.45 ft above mean sea level. The longitudinal slope of the water surface was measured to be 0.00064 and 0.00066, respectively, in the two surveys. [Note: The Iowa State Highway Commission Bench Mark on the south east wing of the bridge (Station 425+42, 19 ft south of the highway center line) is not tied in with the U.S.G.S. gage at Coolbaugh Street bridge. This was verified by the Office of Bridge Design, Iowa Department of Transportation. Based on the U.S.G.S. gage at Coolbaugh Street, the bench mark is at elevation 1043.58 ft (or 2.97 ft above that indicated on the bench mark)]. The n-values (characterizing the channel resistance) are calculated by the Darcy-Weisbach relation, using measured values of u_a, S and d_a: $n = n_a = \kappa u_a / \sqrt{gSd_a}$. All grain-size distributions for the bed and bank

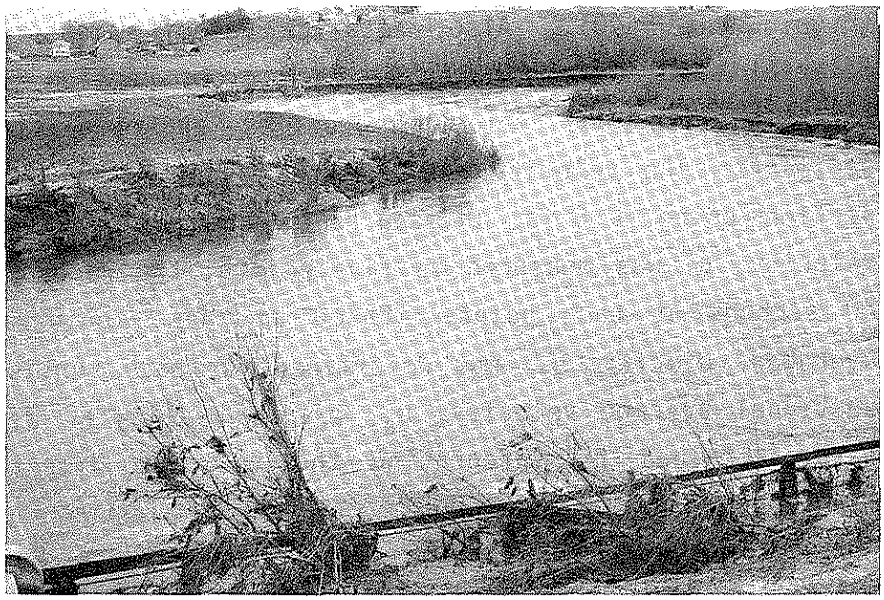

Figure 39. East Nishnabotna River on May 2, 1984, Looking Upstream from the U.S. Highway 34 Bridge

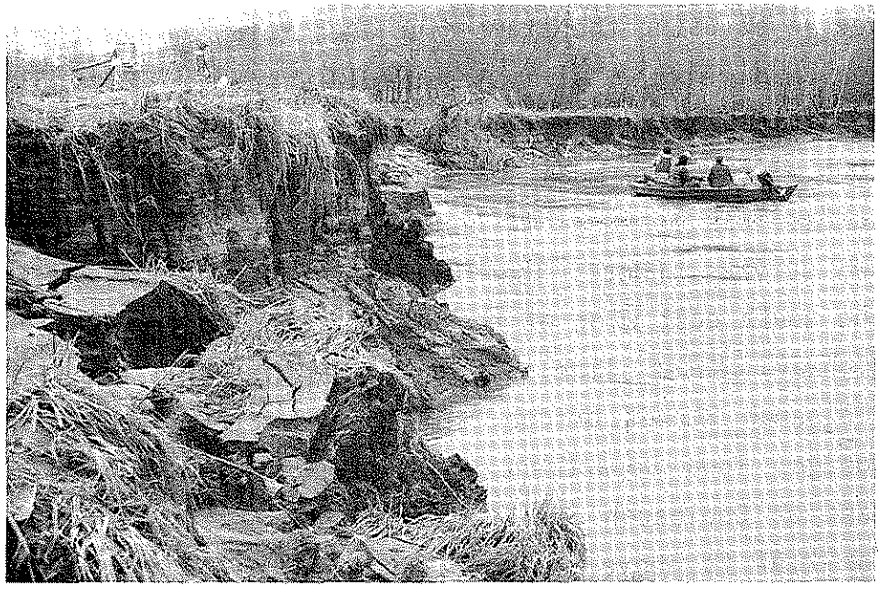

Figure 40. Survey at Section 4, May 2, 1984

Table 6. High-Flow Data from East Nishnabotna River Bend

Section number	Distance from bridge, in feet*)	Flow rate, in cubic feet per second	Cross-sectional area, in square feet	Surface width of channel, b, in feet	Elevation of water surface, in feet above mean sea level	Cross-sectional average velocity, u_a, in feet per second	Cross-sectional average depth d_a, in feet	Cross-sectional average velocity profile exponent n_a
1	120	5,390	1,960	193	1022.4	2.75	10.2	2.4
2	350	4,740	1,360	130	1021.9	3.49	10.5	3.0
3	550	4,370	1,030	135	1021.5	4.24	7.6	4.3
4	730	4,110	990	120	1021.3	4.15	8.3	4.0
5	900	4,430	1,130	170	1021.8	3.92	6.6	4.3
6	1,160	4,620	1,030	170	1022.1	4.49	6.1	5.1
7	1,510	3,810	910	162	1021.5	4.18	5.6	4.9
8	1,960	3,490	900	178	1021.3	3.88	5.1	4.8
9	2,470	3,470	760	185	1021.6	4.57	4.1	6.3
10	2,710	3,600	850	188	1021.9	4.24	4.5	5.6

*) Distance from northern guardrail of bridge, measured along the May 1, 1984, channel-center line

Table 7. Low-Flow Data from East Nishnabotna River Bend

Section number	Distance from bridge, in feet*)	Flow rate, in cubic feet per second	Cross-sectional area, in square feet	Surface width of channel, b, in feet	Elevation of water surface in feet above mean sea level	Cross-sectional average velocity, u_a, in feet per second	Cross-sectional average depth d_a, in feet	Cross-sectional average velocity profile exponent n_a
2	350	118	83	108	1014.3	1.42	0.77	4.5
3	550	118	81	100	1014.4	1.46	0.81	4.5
4	730	118	78	90	1014.5	1.51	0.87	4.5
5	900	118	92	120	1014.6	1.28	0.77	4.1
6	1,160	118	73	116	1014.8	1.62	0.63	5.7
7	1,510	118	83	93	1015.0	1.42	0.89	4.2
8	1,960	109	85	93	1015.3	1.28	0.91	3.7
10	2,710	109	60	64	1015.8	1.82	0.94	5.2

*) Distance from northern guardrail of bridge, measured along the May 1, 1984, channel-center line

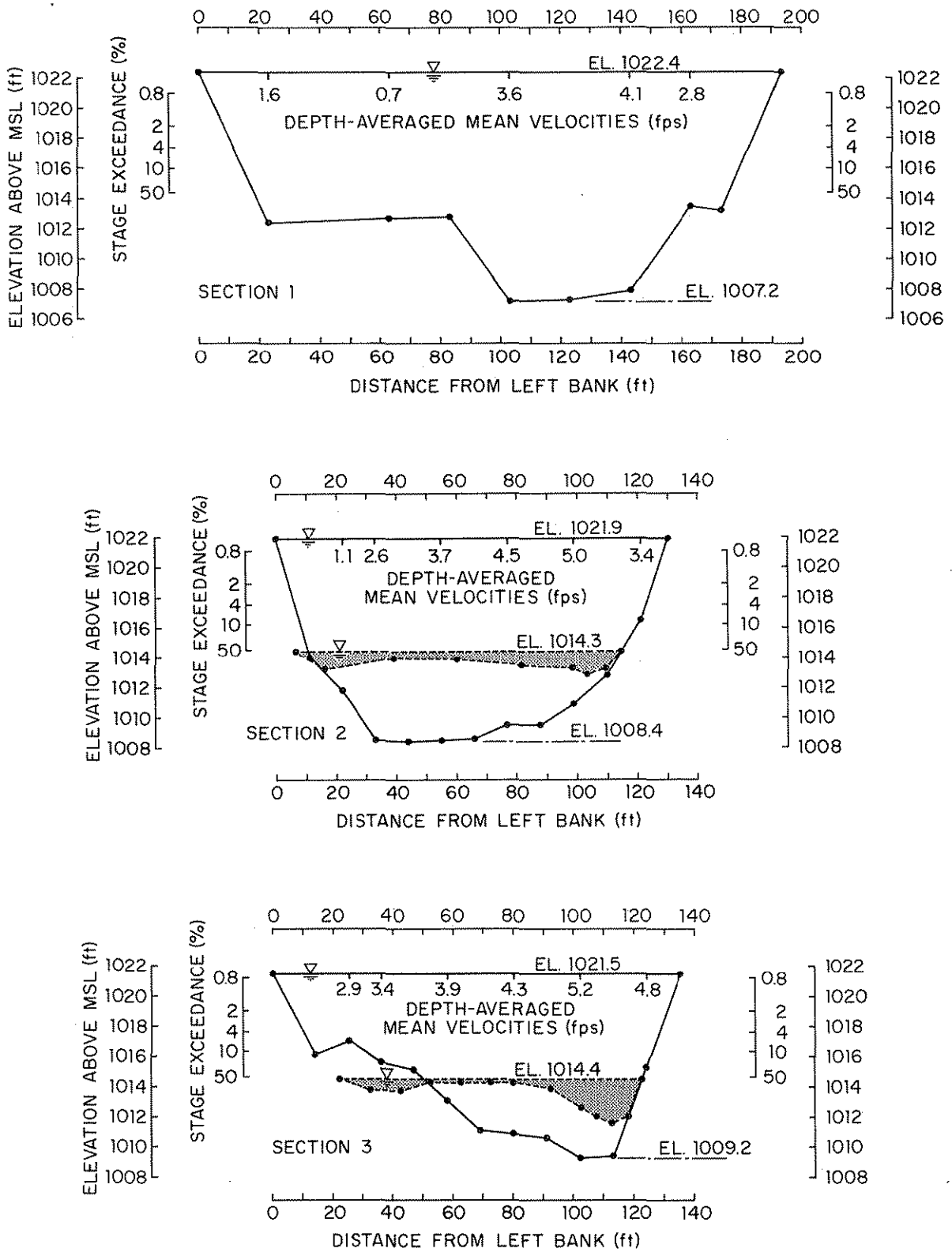

Figure 41. Sections 1 thorugh 10 of the East Nishnabotna River Bend

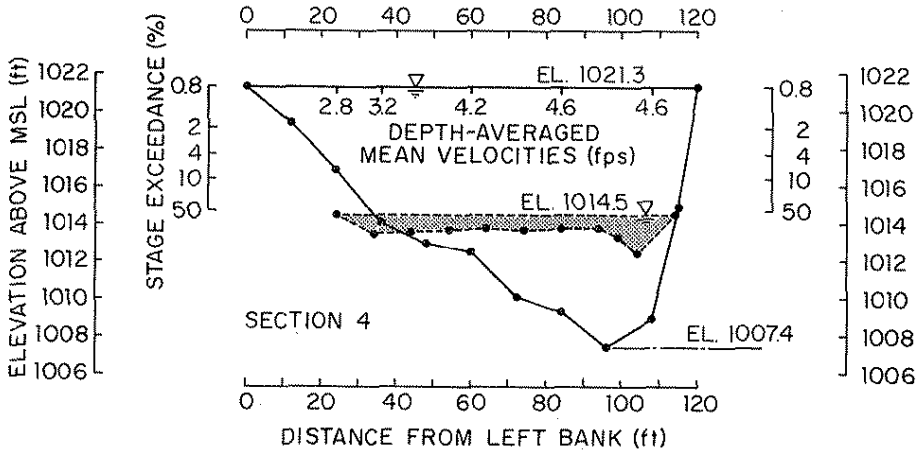

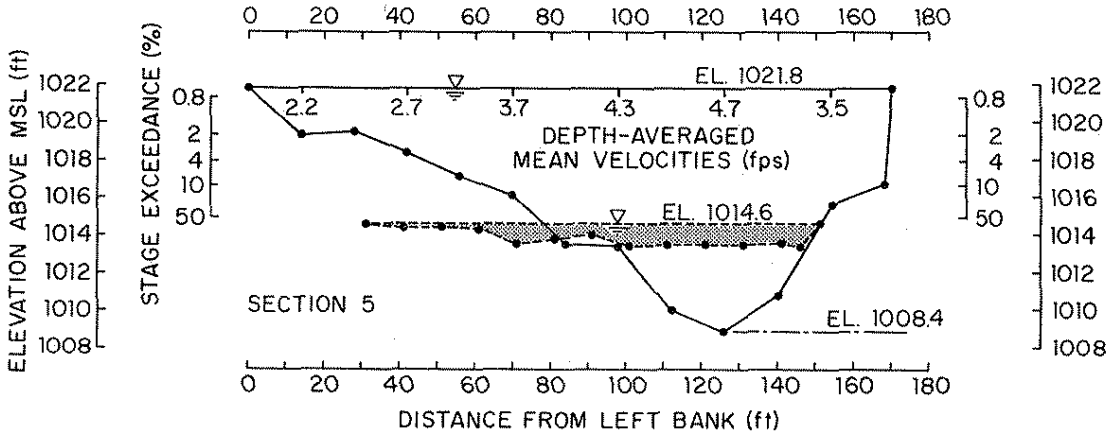

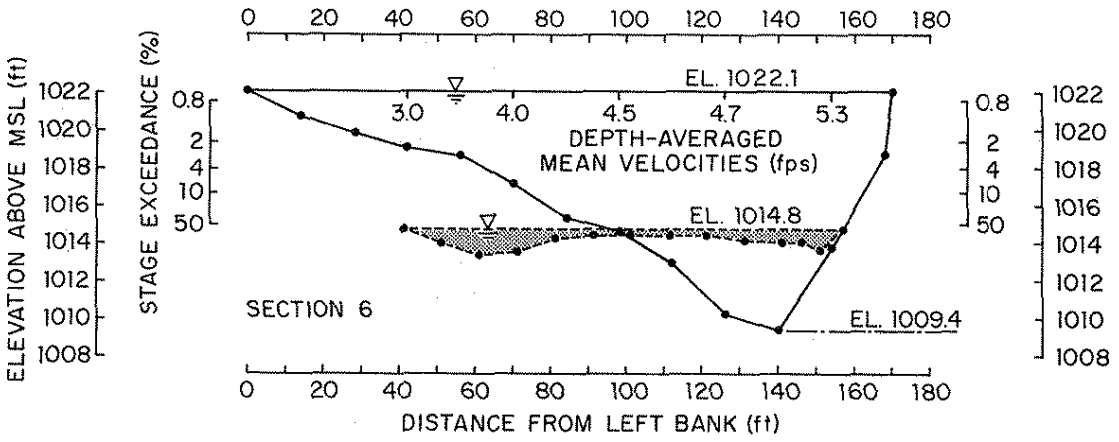

Figure 41. Continued

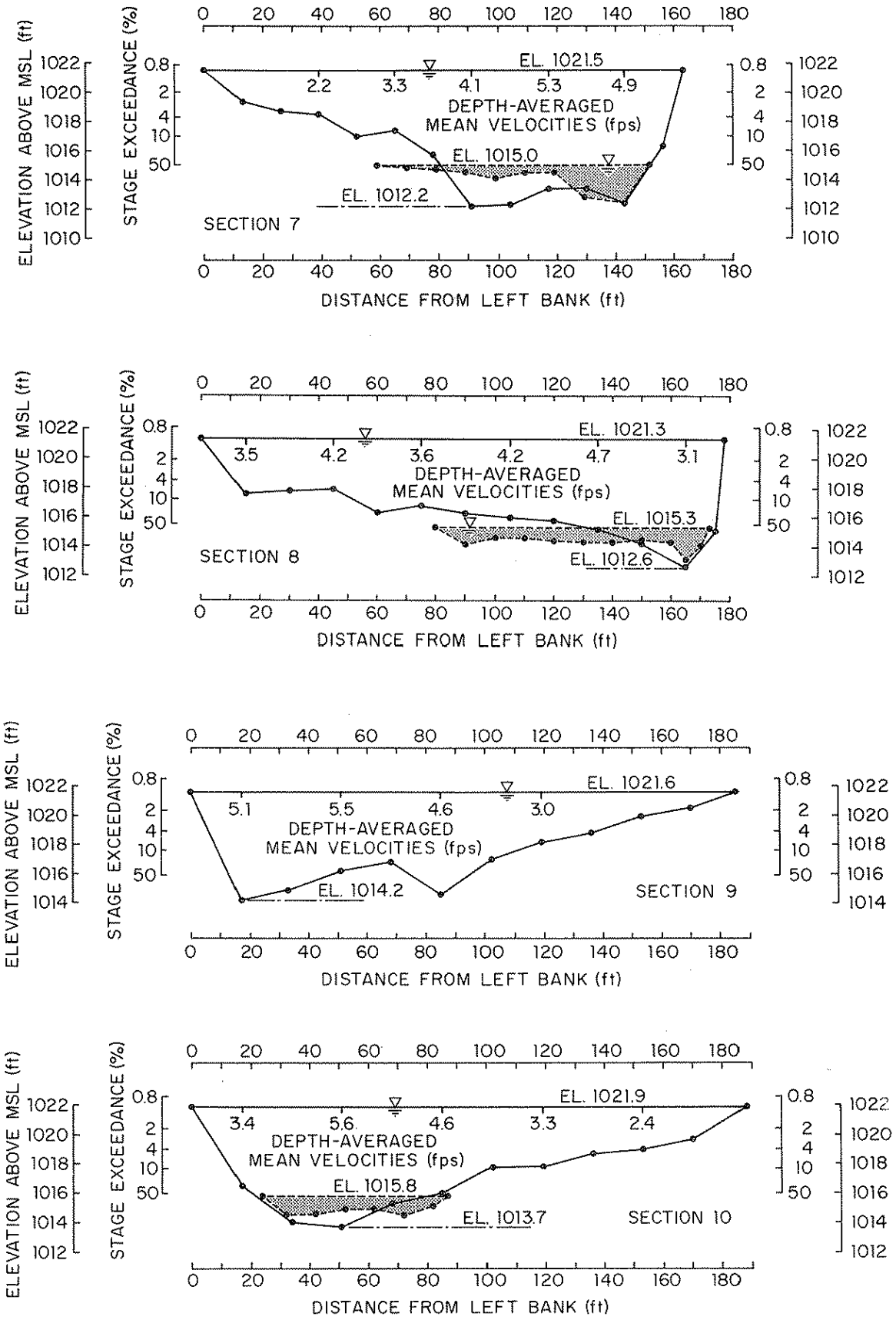

Figure 41. Continued

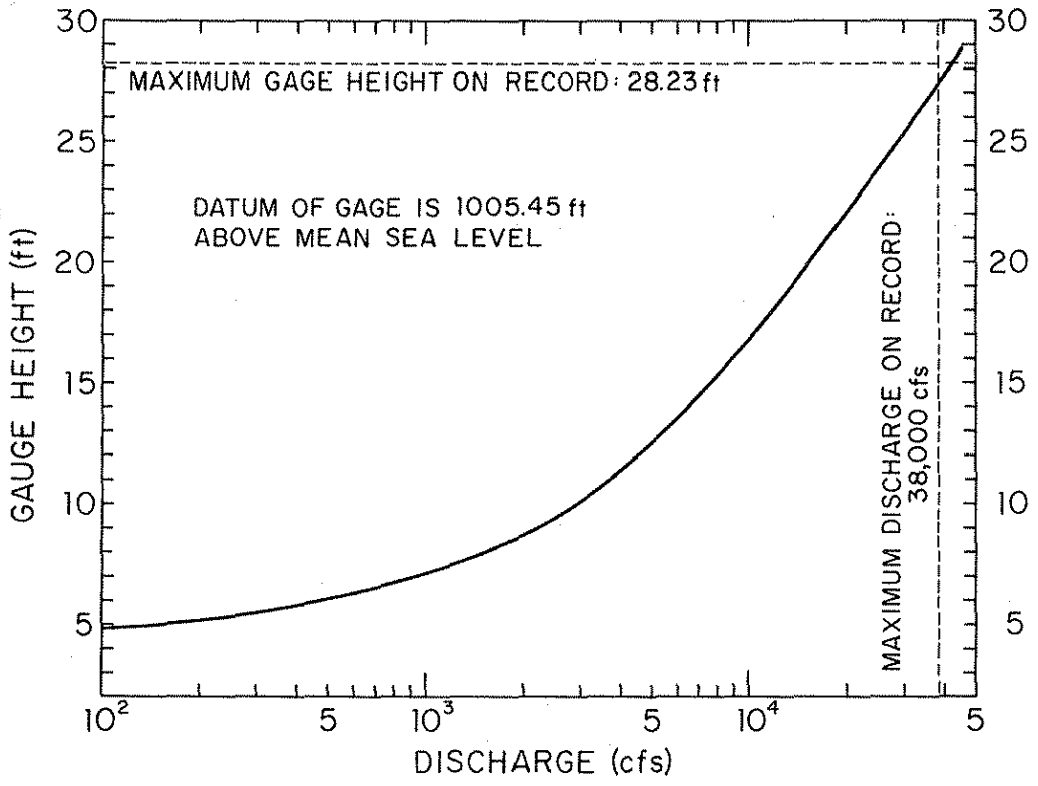

Figure 42. Rating Curve for the U.S.G.S. Water-Stage Recorder on East Nishnabotna River at Red Oak (at Coolbaugh Street Bridge)

sediments are shown in Appendix II. Due to high flow velocities, no samples were taken from the bed of the main channel in the May 1984 survey. Median-grain diameter and geometric standard deviation of the composite grain-size distribution for the bed material of the October 1983 main channel are determined to be 0.45 mm and 2.0, respectively. There is no indication that bed armoring occurred in the channel bend.

Figs. 41 show the ten cross sections measured in the April-May survey with the eight October cross sections superimposed (dotted) for comparison. (The lateral position of the October cross sections relative to the April-May sections is only approximate). It is seen that for most sections the elevation of the bed in the October channel is very close to that of the average depth in the April-May channel. This indicates that the increase in transverse bed slope due to increase of flow rate is accomplished basically by a tilting of the October bed about the April-May channel centerline. At Section 2, the April-May high flow is seen to have caused an overall lowering of the October low flow channel bed by 5-6 ft. Note also that the deepest point in Section 1 (130 ft upstream from the bridge) is at elevation 1007.2 ft, which is about 5 ft lower than the stream-bed elevation for which the bridge foundation was designed (Iowa State Highway Commission, Design No. 262, Montgomery County, File No. 21400, July, 1963). The cause of this overall lowering of the stream bed may be related to the presence of the 600-ft rock protection on the right bank near the bridge (Fig. 43). According to Jansen et al. (1979), fixation of an outer bank which is being eroded induces a steeper slope in the cross section and a greater depth at the toe of the fixation structure.

B. Design Computations

The design computations are summarized in Table 8. The transverse bed slopes listed in Table 8 are determined as the slopes of best-fit lines through the depth points within the central portion

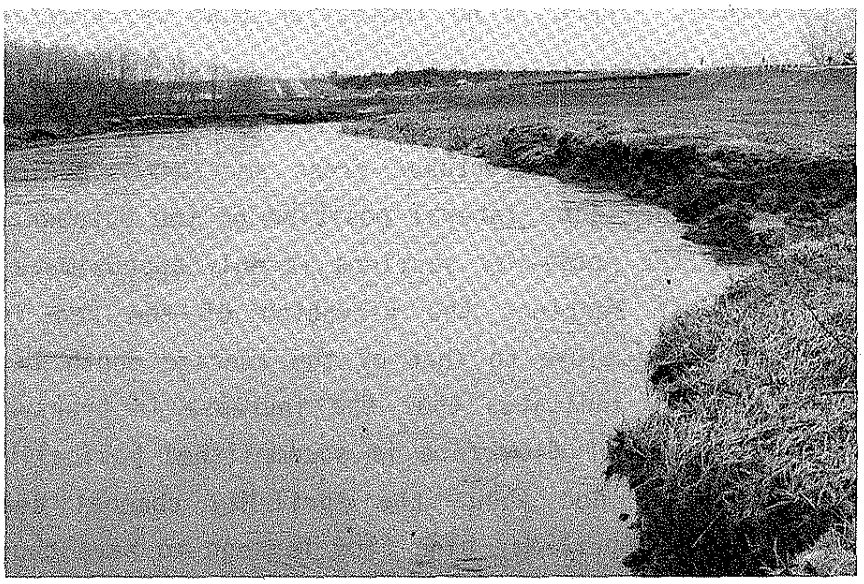

Figure 43. East Nishnabotna River on May 2, 1984, Looking Downstream toward the Highway 34 Bridge (The rock protection is along the right bank in the upper-center portion of the picture)

Table 8. Vane Design Computations for East Nishnabotna River Bend

Section number	Distance from bridge in feet*)	Transverse bed slope S_T	Particle Froude number, F_D	Effective radius of curvature, r_e, in feet	Deviation angle, δ in degrees	Vane angle with mean flow direction, α'	Vane function, F	Rquired lifting surface per unit surface area of channel	Sectional surface area of channel, $r_c \phi b$, in square feet	Required lifting surface, NHL, in square feet	Required number of vanes (3-ft high, 12-ft long)
3	550	0.09	15.1	1,370	7.1	12.9	0.52	0.0115	25,650	295	8
4	730	0.13	14.8	1,010	9.7	10.3	0.41	0.0135	21,000	284	8
5	900	0.11	14.0	900	9.4	10.6	0.52	0.0153	36,550	559	15
6	1,160	0.11	16.0	950	10.0	10.0	0.40	0.0103	51,850	534	15
7	1,510	0.08	14.9	1,120	7.5	12.5	0.43	0.0086	64,800	557	15
8	1,960	0.04	13.8	1,890	3.9	16.1	0.44	0.0047	40,000	188	5

*) Distance from northern guardrail of bridge, measured along the May 1, 1984, channel-center line

of the cross sections. These slopes are seen to be of the same order of magnitude as those measured in the laboratory model. However, the laboratory model is a constant-radius bend following a straight channel (with radius = infinity). The radius of the river curve decreases gradually from infinity at the inflection point near Section 8 to less than 400 ft at Section 5. Between Sections 5 and 3, the radius increases again to infinity. Considering the short distance over which these changes occur, it is quite obvious that the bend flow cannot at any point be considered to be fully developed with depth and velocity distributions as in the downstream reach of a long, constant-radius bend (for which most bend-flow theories are developed). However, the effective-radius concept can be used for the vane design. Table 8 lists the effective radii, r_e, as calculated by Eq. 12, using $\theta = 0.05$; $d = d_a$; $F_D = F_{Da} = u_a/\sqrt{gD(\rho_s-\rho)/\rho}$; and the measured values of S_T.

The laboratory-model tests indicated that the vane-angle of attack should be of the order of 20 degrees. With $\alpha = 20$ degrees, and the near-bed deviation angles, δ, calculated by Eq. 23, the vanes' angle with the mean-flow direction is obtained from Eq. 24: $\alpha' = \alpha - \delta$. The α' values are seen to range from 10 to 16 degrees. Considering the uncertainty involved in the determination of the optimum value of α, there does not appear to be justification for a greater accuracy on α' than about two to three degrees. In view of the greater risk of scour at the larger values of α, it would be advisable to let α' be closer to 10° than 16°.

According to the basic theory the required area of lifting surface decreases with increasing aspect ratio. However, there is a practical upper limit to the aspect ratio. For the vanes to be erosion preventive their height H should be less than half the water depth at the flow rates at which bank erosion occurs; i.e., whenever the flow rate in this river bend is greater than about 1500 cfs. (At 1500 cfs, the near-bank velocity at Section 3 through 6 exceeds 3.5 ft/sec, which is the limiting velocity recommended by the U.S. Bureau

of Reclamation for the design of a stable, firm-loam channel carrying water with colloidal silts.) According to the U.S. Geological Survey, this flow rate is exceeded on the average (based on 60 years of records) 4% of the time, or approximately 15 days per year (Fig. 44). The 1500-cfs river stages are obtained from the U.S.G.S stage-discharge relation for the gage in Red Oak using a longitudinal water-surface slope of 0.00064. The 1500-cfs average water depth is estimated to be approximately 5 ft. Therefore, the top of the vanes should be more than 2.5 ft under the 1500-cfs stage to be erosion preventive at this and higher stages. From Fig. 41 follows that if the vanes are installed at low flow with their top edge 2.5 ft below the 1500-cfs stage and can maintain the present low-flow bed profile, the H/d-value will be optimum (of the order of 0.2-0.3) at the extreme high flow when most erosion losses would occur. For this situation to occur, the vane height must be of the order of 3 ft. In the model, the best performing vane was four times as long as it was high. A 3-ft high prototype vane should then be 12 ft long. If the vane is much longer than that it may generate two (or more) secondary flow cells downstream rather than one, which reduces the overall performance. Using H/L = 0.3, and $\alpha = 20°$; the lift coefficient as given by Fig. 6 is $c_L = 0.5$. The value of F selected for the design was the minimum value, F_{min}, corresponding to the n-value for the section. The lifting surface per unit surface area of the channel, $NHL/(r_c \phi b)$, required to maintain a horizontal "low flow" bed is then readily calculated, and so is the required number of vanes.

Each vane would be acted upon by a maximum lift force of the order of $F_V = 1/2 c_L \rho u^2 HL \simeq 300$ lbf which, when uniformly distributed over the 36 ft^2 lifting surface would yield a bending moment 3 ft from the top of the vane of about 450 ft-lb. If the vanes are made of sheet piles, wood planks, or thin concrete slabs, the drag force on the vanes would not be a design factor. Although the forces on the vanes from the flow are thus very small it is recommended that

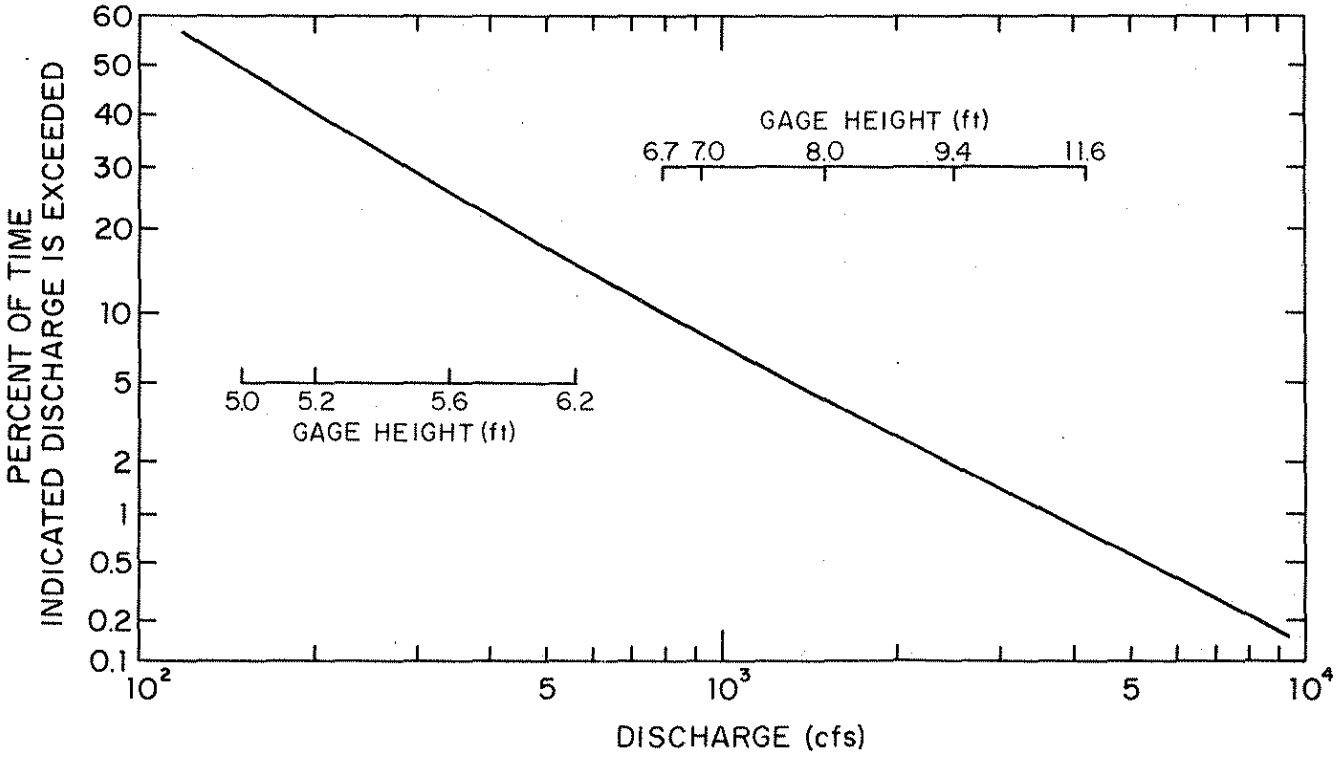

Figure 44. Frequency Distribution for Discharge in East Nishnabotna River at Red Oak

each vane has at least two of its piles extending down below the top of the firm shale layer, which, according to the Iowa State Highway Commission Design No. 262 (File No. 21400, July 1963) is at elevation 1004 ft (sounding dated July 31, 1962). The support piles should thus be at least 15 ft long, and preferably 18 to 20 ft.

The positioning of the vanes on the stream-bed requires careful planning. In order that the vane system as a whole function at optimum efficiency, the longitudinal and lateral spacing of the vanes must be such that a single-cell circulation is induced in the flow section. If the vanes are spaced too far apart laterally, two or more secondary flow cells are induced. Dye and float studies in the laboratory model indicated that the lateral distance between two vanes should be less than or equal to two times the water depth. The optimum distance, which undoubtedly is a function of L and α, was not identified in the model studies. Satisfactory results were obtained in the model with a lateral vane distance of two times the water depth. Based on a 4,000 cfs river flow, the prototype vanes should then be spaced about 12 ft apart in the lateral direction. The proposed emplacement of the vanes is detailed in Fig. 45, and Table 9.

The above emplacement applies to the reach between Sections 2 and 9. However, it is equally important that measures be taken to guide the flow through the bridge section. The effective width of the channel at the bridge section is presently less than half the width for which the bridge was designed. There is obviously a need for measures that can: (1) Turn the river flow southward (90°) over a short distance (less than 300 ft) without endangering the left bridge abutment; and (2) generate a widening of the effective channel width at the bridge section. It is uncertain to what extent Iowa Vanes can accomplish such a task. The most logical solution would be to use a combination of bank rip rap and vanes as sketched in Fig. 46. Note that bank rip rap alone would not produce a widening of the river channel.

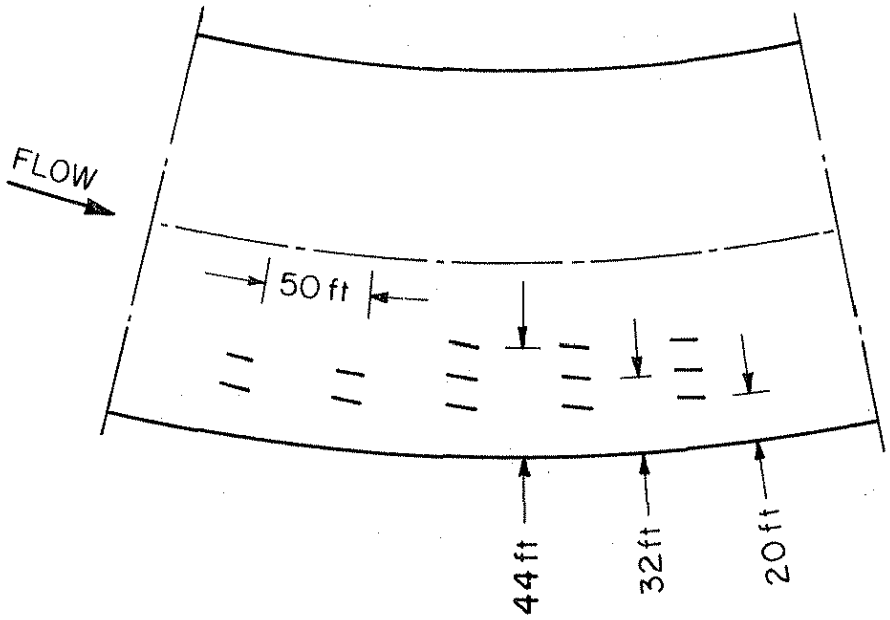

Figure 45. Proposed Emplcaement of Vane System for the East Nishnabotna River Bend

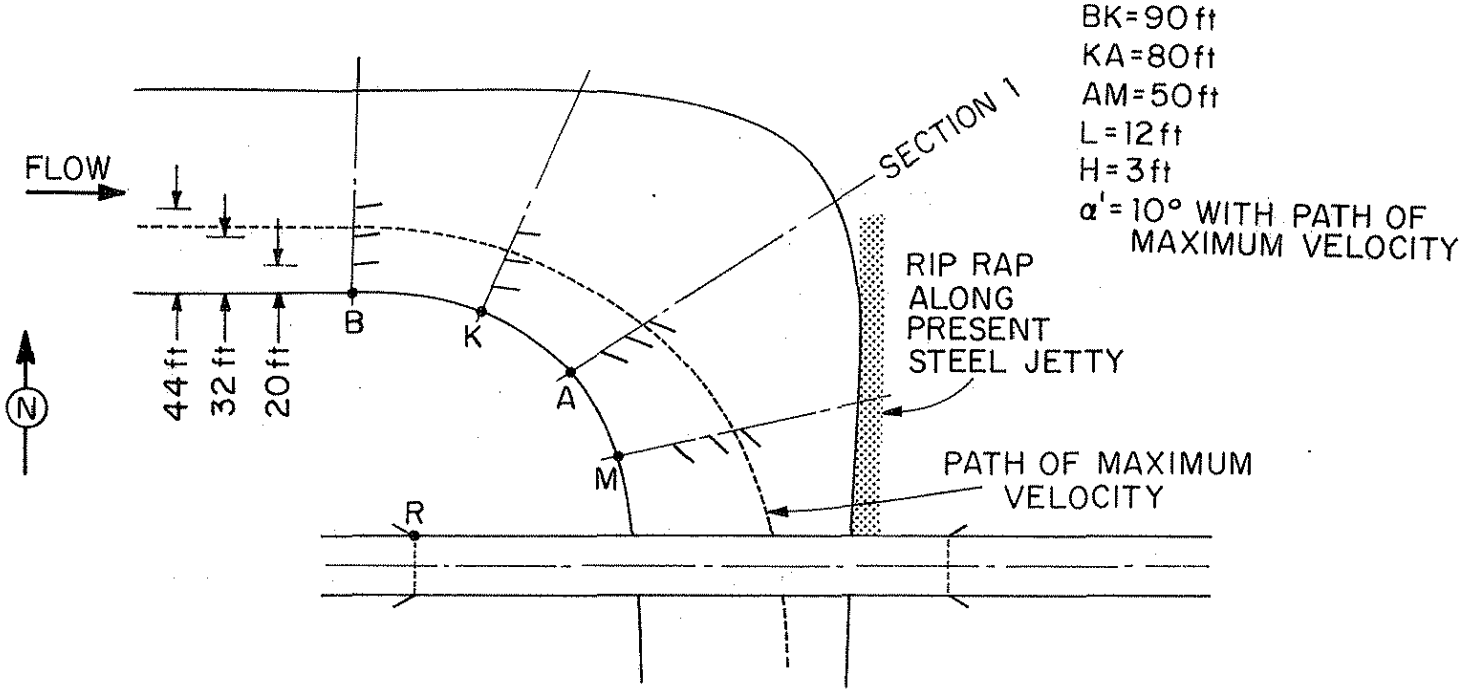

Figure 46. Proposed Combination of Vanes and Rock Rip Rap at the Highway 34 Bridge.

Table 9. Proposed Emplacement of Vane System for East Nishnabotna River Bend

Section number	Distance from bridge, in feet *)	Number of vanes	Elevation of top edge of vanes, in feet above mean sea level
	450	2	1015.1
	500	2	1015.1
3	550	2	1015.2
	600	2	1015.2
	650	2	1015.2
	700	2	1015.3
4	750	2	1015.3
	800	2	1015.4
	850	3	1015.4
5	900	3	1015.5
	950	3	1015.6
	1000	3	1015.8
	1050	3	1015.9
	1100	2	1016.0
6	1150	2	1016.0
	1200	2	1016.0
	1250	2	1016.0
	1300	2	1016.0
	1350	2	1016.0
	1400	2	1016.1
	1450	2	1016.1
7	1500	2	1016.1
	1550	2	1016.1
	1600	2	1016.1
	1650	2	1016.1
	1700	2	1016.1
	1800	2	1016.3
8	1900	2	1016.3
	2100	2	1016.3
	2300	2	1016.3

*) Distance from northern guardrail of bridge, measured along the May 1, 1984, channel-center line

V. SUMMARY, CONCLUSIONS AND RECOMMENDATIONS

The study has evaluated the effectiveness of Iowa Vanes in reducing depth and velocity near the outer bank in a curved, alluvial channel flow. A procedure for the design of a vane system for a given river curve has been developed and tested in a laboratory model. The procedure has been summarized in Appendix I by way of a numerical example, and it has been used for the design of an Iowa-Vane bank protection structure for a section of East Nishnabotna River along U.S. Highway 34 at Red Oak, Iowa (Chapter IV).

The study has verified that Eqs. 9, 14, and 16 can provide a reasonably accurate estimate of the vane-lift surface required to obtain a specified reduction in near-bank velocity or corresponding transverse bed slope. The lift coefficients, c_L, used in the experiments (0.4 to 0.6) were obtained from Fig. 6 which was developed by extrapolation using a procedure that has been verified for aspect ratios (H/L) greater than or equal to one. The dependence of c_L on angle of attack (α) and aspect ratio (H/L) depicted in Fig. 6 has not been verified experimentally for aspect ratios less than one. The results of the theoretical analysis and the model tests suggest that:

1. The vane system should be designed with data for bankful flow in the river;

2. The vane height, H, should be chosen such that the ratio H/d remains within the range $0.2 < H/d < 0.5$ at all erosion-causing flow rates;

3. The vane length, L, should be of the order of four times the vane height;

4. The vanes should form an angle of 10 to 15 degrees with the mean-flow direction at bankful flow; and

5. The lateral spacing of the individual vanes should be less than or equal to twice the water depth at bankful flow.

The laboratory model experiments did not suggest that vanes composed of steep-sided windrows of rock could be a feasible alternative to sheet-pile vanes (or to other types of vanes with vertical, impervious lifting surface). However, more experimentation is needed before any firm conclusions about the feasibility of rock vanes can be made.

It appears that the developmental work is at a point where field experiments are now needed. The laboratory experiments have clearly demonstrated that a system of submerged vanes designed according to the principles developed during this study can fully eliminate the secondary flow, and its consequence (bank scour) in a laboratory model of an alluvial channel bend. A vane system has been designed for the bend of East Nishnabotna River shown in Fig. 3 (for the protection of 1000 ft of U.S. Highway 34 and its bridge over East Nishnabotna River) using the same design principles. A total of 66 12-ft long 3-ft high vanes, positioned as shown in Fig. 45, would be needed for the elimination of the secondary-flow component at high flow (the flow that generated the bed topography that was measured in the May 1984 survey of the river bend). It is recommended that the Iowa Department of Transportation consider installing this system in the river bend.

Because of idealized flow conditions and scale effects in the laboratory model it is uncertain to what extent the vane system can prevent bank erosion in the prototype. Banks may cave in for a number of reasons, some of which may not be related directly to bank shear. However, by eliminating the secondary-flow component, the vane system will make the water and sediment move through the river curve as if the channel had been straight, and the banks of the river bend will be subjected to only the same kind of erosive forces that

the banks along the straight reaches of the river are subjected to. In other words, the vanes will stop the process of meandering and make the river maintain its present alignment.

Another important consideration is that the vanes do not change the overall characteristics of the river. The vane system does not increase the local channel roughness as do other presently used means for reduction of the near-bank velocity (rock rip rap, jetties, dikes, etc.). By increasing the channel roughness locally, the presently used techniques often generate enhanced erosion and channel degradation further downstream (U.S. Army Corps of Engineers, 1981). Extended use of rock rip rap along the bend of East Nishnabotna River upstream from U.S. Highway 34 may have such effects on the river channel at the bridge crossing and could eventually cause a weakening of the foundation of the bridge piers. The bridge was originally designed for a high-water channel width of over 300 ft. During the May 1, 1984, survey the high-water channel width at the bridge section was measured to be only approximately 150 ft (Figs. 47 and 48), which indicates that a very significant degradation of the channel at the bridge has already taken place. Whether the proposed vane system can ameliorate the present situation at the bridge is uncertain. However, the results of this study suggest that the vane system can reduce the risk of further degradation of the channel and erosion of the banks.

The work at IIHR on the submerged-vane concept has generated a significant amount of publicity. If the proposed vane system is installed it will be the first of its kind. (A system is presently being designed also for the Alaska Department of Transportation for bank protection along a reach of the Yukon River at Galena Airfield.) There is no doubt that the performance of the vane system, if installed, will be followed closely by many parties.

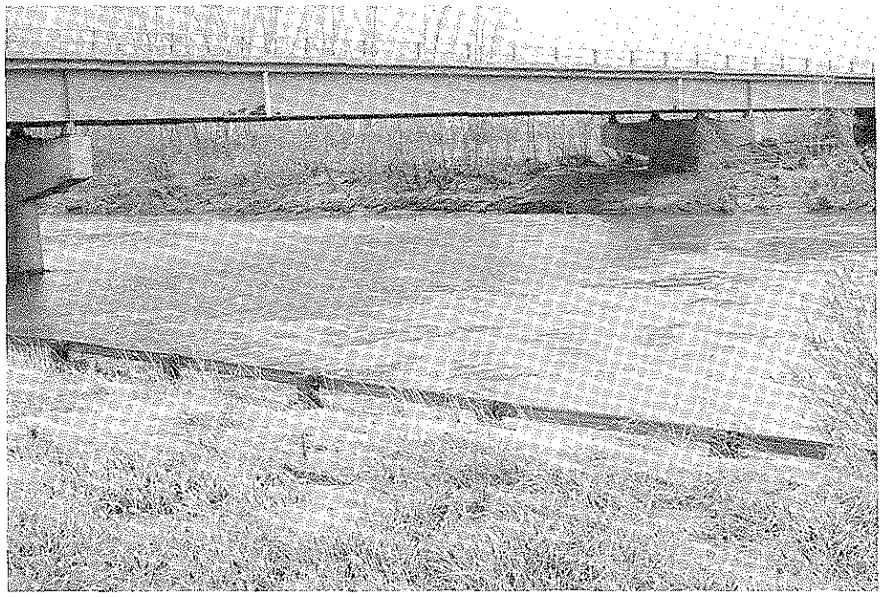

Figure 47. U.S. Highway 34 Bridge over East Nishnabotna River, Viewed Downstream toward Right Bank of River

Figure 48. U.S. Highway 34 Bridge over East Nishnabotna River, Viewed Downstream from Left Bank of River

REFERENCES

1. Bertin, J.J., and Smith, M.L., Aerodynamics for Engineers, Prentice-Hall, Inc., Englewood Cliffs, N.J., 1979.

2. Falcon, M.A., "Analysis of Flow in Alluvial Channel Bends", Thesis presented to The University of Iowa, Iowa City, Iowa, in 1979, in partial fulfillment of the requirements for the degree of Doctor of Philosophy.

3. Jansen, P. Ph., et al., Principles of River Engineering, Pitman Publishing Ltd., London, United Kingdom, 1979.

4. Odgaard, A.J., and Kennedy, J.F., "River-Bend Bank Protection by Submerged Vanes", Journal of Hydraulic Engineering, ASCE, Vol. 109, No. 8, Aug., 1983, pp. 1161-1173.

5. Odgaard, A.J., "Flow and Bed Topography in Alluvial Channel Bends", Journal of Hydraulic Engineering, ASCE, Vol. 110, No. 4, April, 1984, pp. 521-536.

6. Sabersky, R.H., and Acosta, A.J., Fluid Flow, MacMillan Publishing Co., Inc., New York, 1964.

7. Shields, A., "Anvendung der Aenlichkeitsmechanik und der Turbulenzforschung auf die Geshiebebewegung", Mitteilungen der Preussischen Versuchsanstalt fur Wasserbau and Schiffbau, Berlin, Germany, Translated to English by W.P. Ott and J.C. van Uchelen, California Institute of Technology, Pasadena, California, 1936.

8. U.S. Army Corps of Engineers, The Streambank Erosion Control Evaluation and Demonstration Act of 1974 Section 32, Public Law 93-251, Final Report to Congress (Published at the Waterways Experimental Station, Vicksburg, Miss.), December 1981.

APPENDIX I - VANE-DESIGN EXAMPLE

The following numerical example summarizes the procedure for the design of an Iowa-Vane bank protection structure.

A river flow curving at a radius of r_c = 2,000 ft has been observed to cause bank erosion when the discharge exceeds 3,000 cfs. The bed material in the channel is sand with a median-grain diameter of 0.4 mm and a geometric standard deviation of less than 2. The longitudinal slope of the water surface remains constant at a value of S = 0.0006 at all flow rates. At 3,000 cfs, the average width and depth of the river channel are 100 ft and 10 ft, respectively. A vane system is to be designed that prevents the near-bank velocity from exceeding its 3,000-cfs value. Maximum velocity in the channel occurs at bankful stage when the flow is 8,000 cfs and depth and width are 15 ft and 120 ft, respectively.

For the vane system to be erosion preventive at all flow rates, H must be less than half the water depth when the flow is 3,000 cfs; i.e., $H \leq 5$ ft. With H = 5 ft, the H/d ratio is 0.5 at 3,000 cfs and 0.33 at 8,000 cfs. The performance of the vanes is closer to optimum if their height is chosen to be H = 4 ft. The H/d values then range from 0.25 to 0.4 at erosion causing flow rates. The length is selected on the basis of model-test experience to be four time the height: L = 4H = 16 ft.

At bankful flow, the average velocity in the channel is u_a = 8,000/[(120)(15)] = 4.44 ft/sec yielding $n = \kappa u_a/\sqrt{gSd_a} = 3.3$, and δ = arc tan $[\kappa^{-2}(d_a/r_e)\, n(n+1)/(n+2)] = 7°$. Entering Fig. 6 with H/L = 0.25 and α = 10 + 7 = 17° yields c_L = 0.4; substituting n = 3.3 and H/d = 0.25 into Eq. 10 yields F = 0.78. Eq. 4 yields F_D = 16.78.

At 3,000 cfs, u_a = 3,000/[(100)(10)] = 3.0 fps, yielding F_D = 11.34.

The vanes are to reduce the 8,000 cfs transverse bed slope, S_T = (4.8)(0.05)(16.68)(15)/(2,000) = 0.135 to the 3,000 cfs transverse bed slope, S_{To} = (4.8)(0.05)(11.34)(10)/(2,000) = 0.0609. This is equivalent to increasing the effective radius from r_e = 2,000 ft to r_{eo} = (4.8)(0.05)(16.78(15)/(0.0609) = 4,440 ft substituting into Eq. 16 then yields

N = 30 per 1000 ft of channel

APPENDIX II

Grain-Size Distribution from Field Surveys

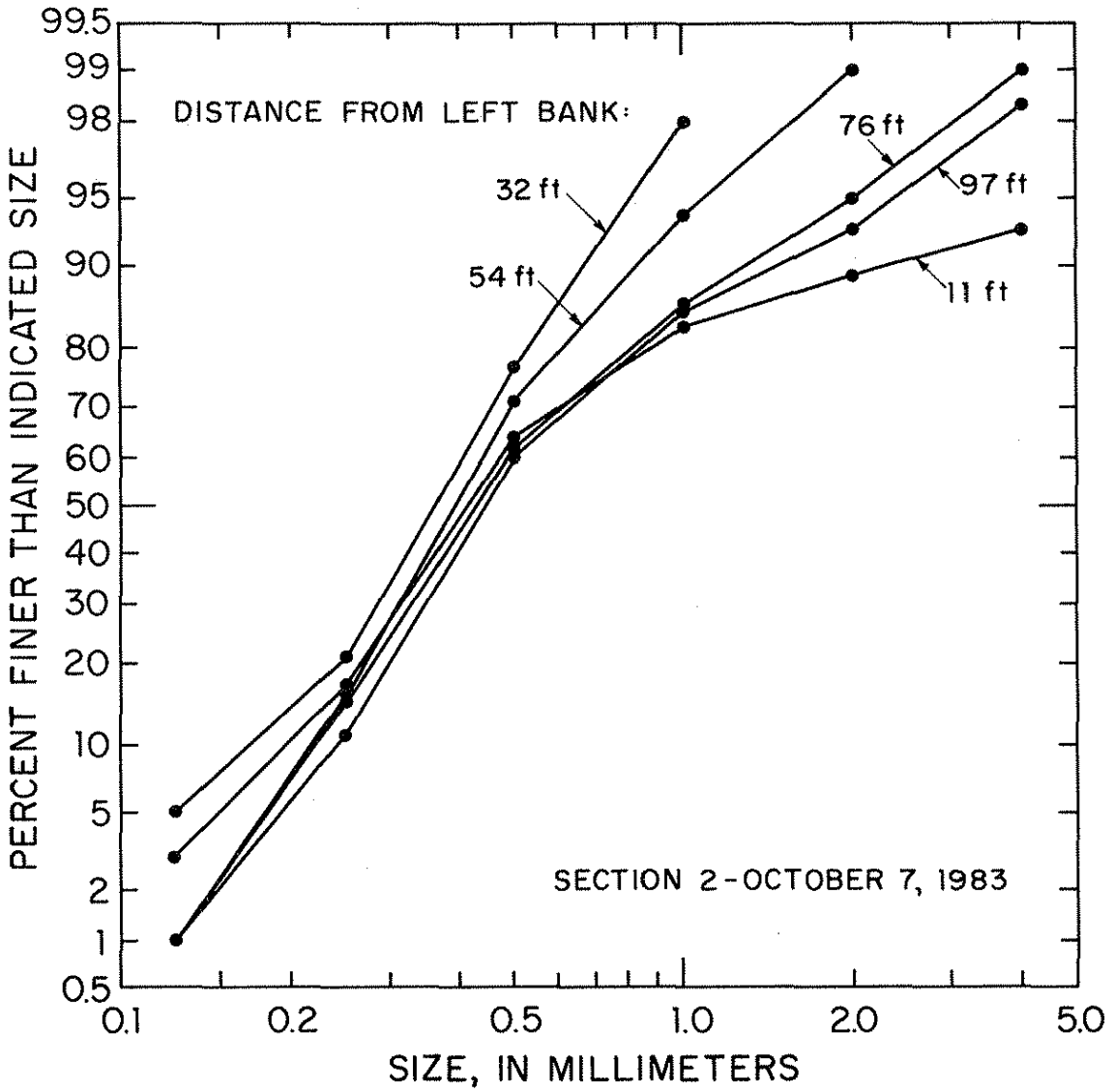
99.5
99
98
95
90
80
70
60
50
40
30
20
10
5
2
1
0.5
PERCENT FINER THAN INDICATED SIZE
DISTANCE FROM LEFT BANK:
32 ft
54 ft
76 ft
97 ft
11 ft
SECTION 2 - OCTOBER 7, 1983
0.1
0.2
0.5
1.0
2.0
5.0
SIZE, IN MILLIMETERS

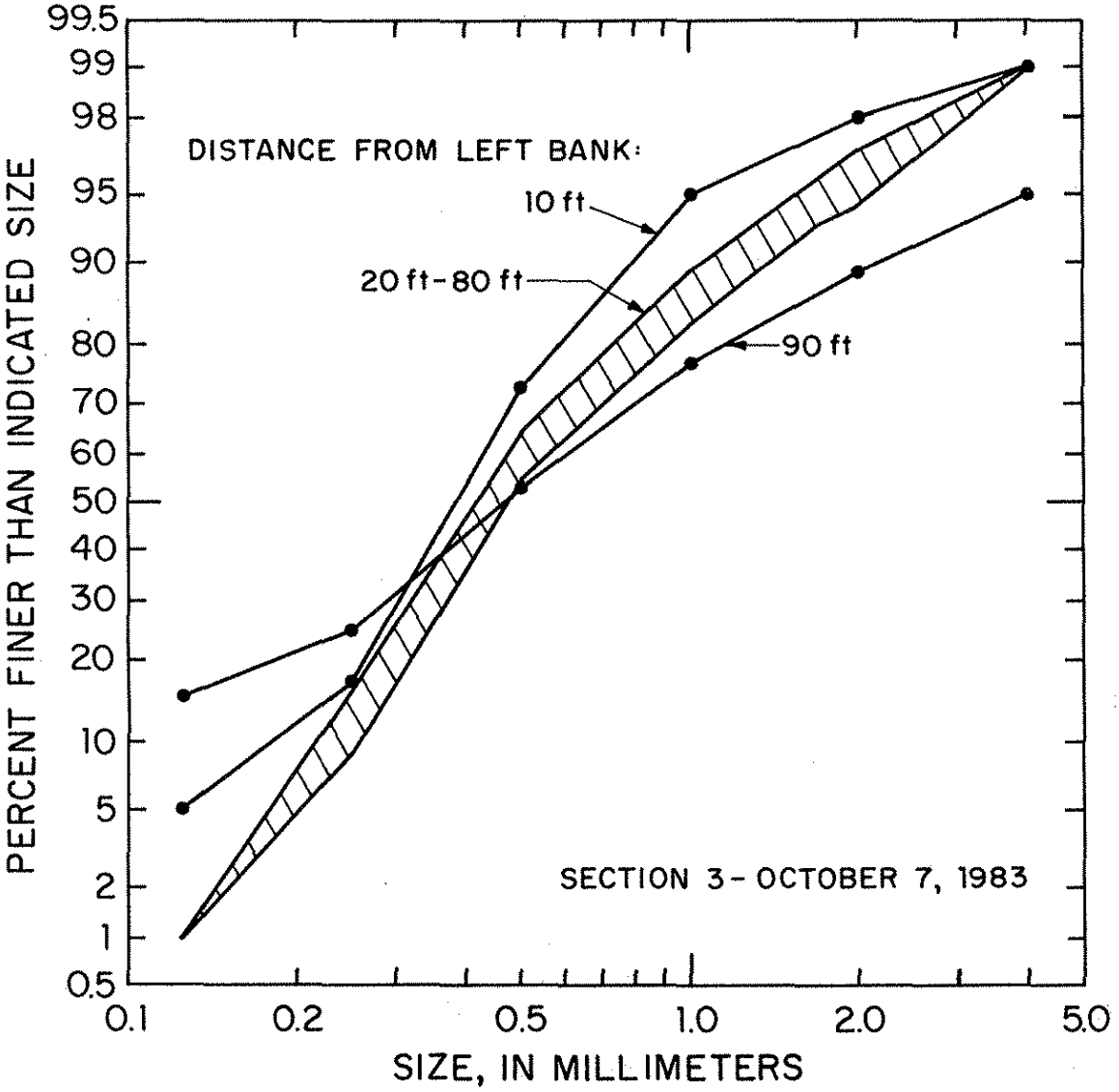
99.5
99
98
95
90
80
70
60
50
40
30
20
10
5
2
1
0.5
PERCENT FINER THAN INDICATED SIZE
DISTANCE FROM LEFT BANK:
10 ft
20 ft-80 ft
90 ft
SECTION 3- OCTOBER 7, 1983
0.1
0.2
0.5
1.0
2.0
5.0
SIZE, IN MILLIMETERS

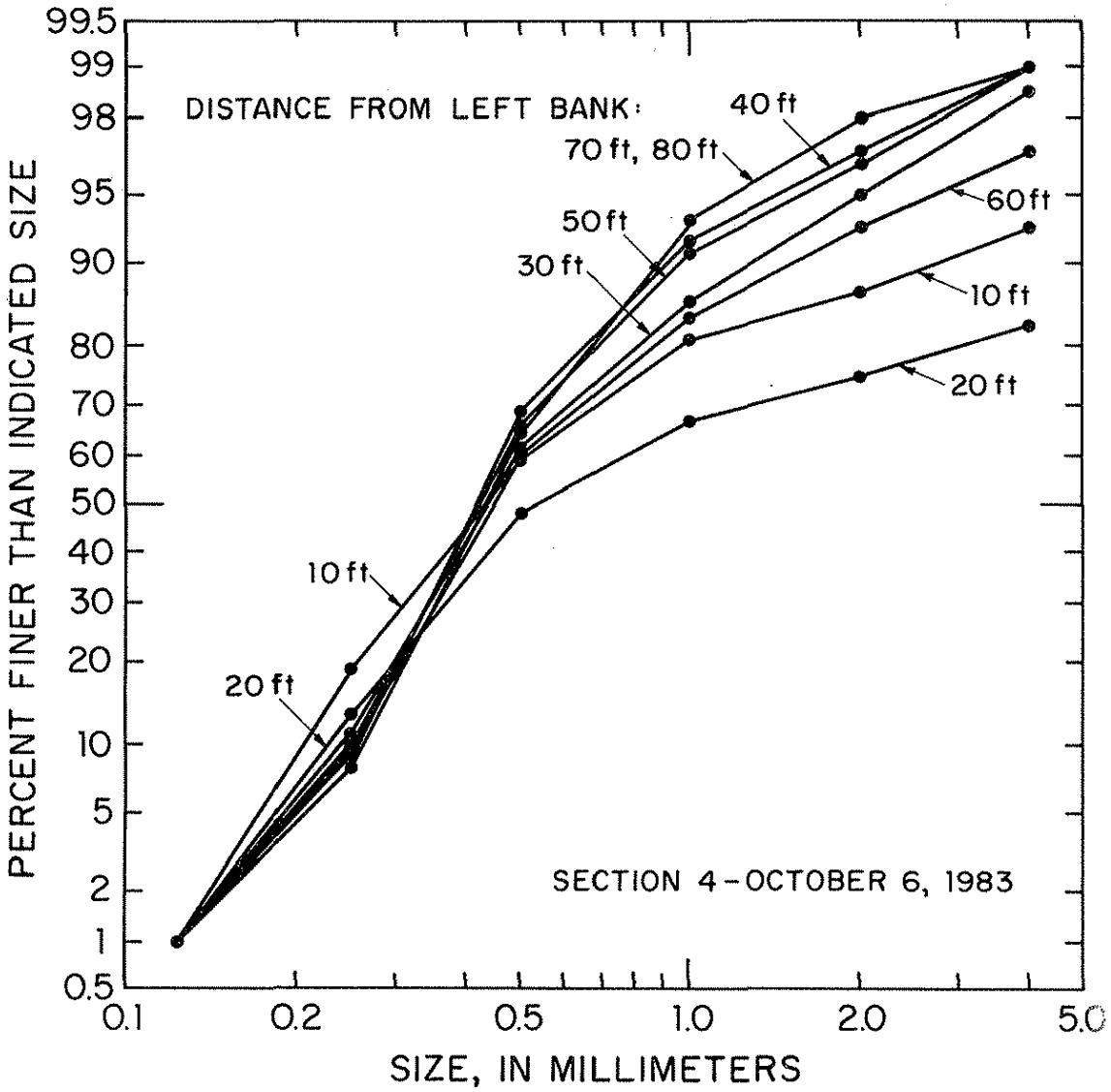
99.5
99
98
95
90
80
70
60
50
40
30
20
10
5
2
1
0.5
PERCENT FINER THAN INDICATED SIZE
DISTANCE FROM LEFT BANK:
40 ft
70 ft, 80 ft
60 ft
50 ft
30 ft
10 ft
20 ft
10 ft
20 ft
SECTION 4 - OCTOBER 6, 1983
0.1
0.2
0.5
1.0
2.0
5.0
SIZE, IN MILLIMETERS

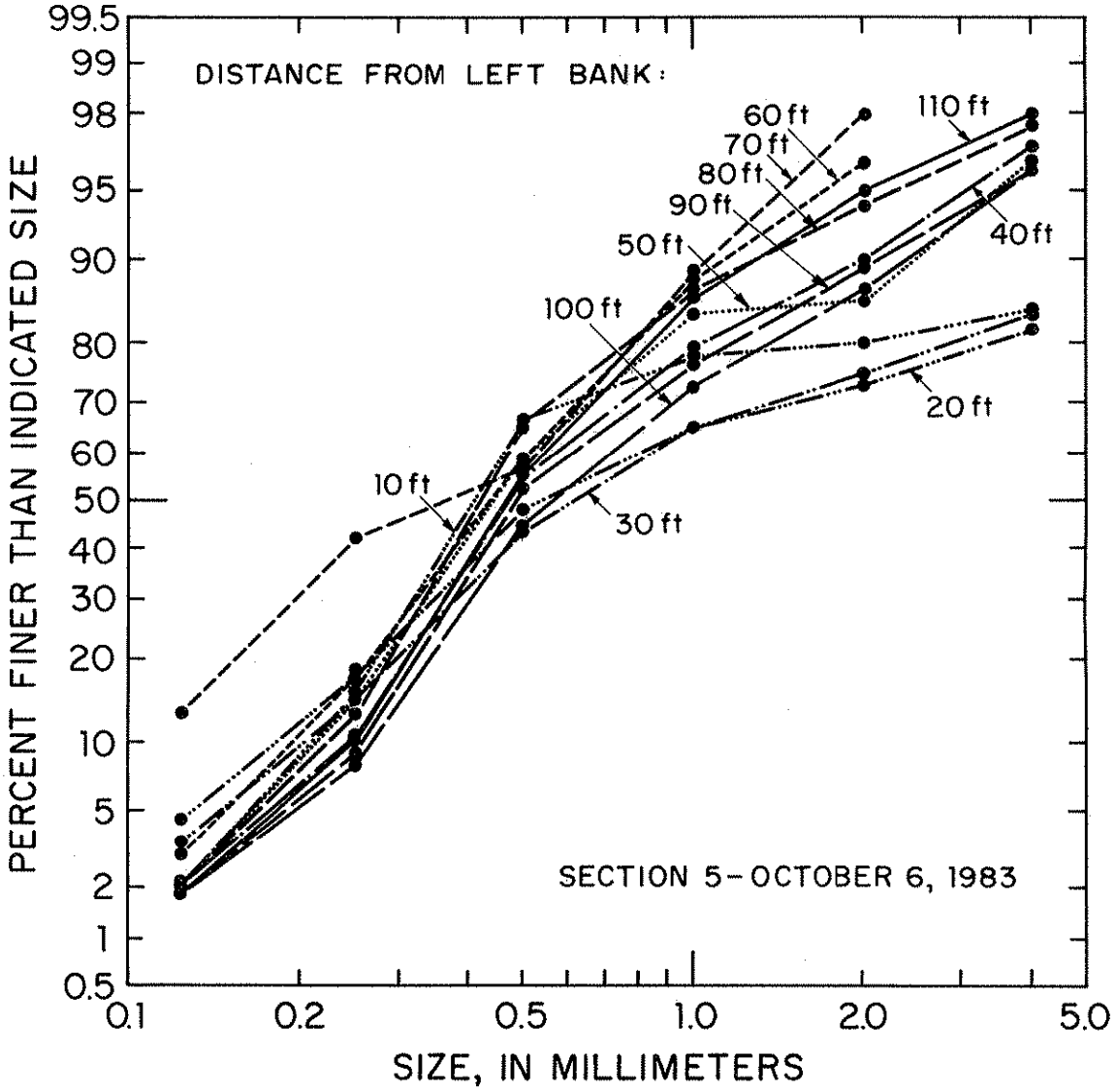
DISTANCE FROM LEFT BANK:
60 ft
70 ft
80 ft
90 ft
50 ft
100 ft
110 ft
40 ft
20 ft
10 ft
30 ft
SECTION 5 - OCTOBER 6, 1983
PERCENT FINER THAN INDICATED SIZE
99.5
99
98
95
90
80
70
60
50
40
30
20
10
5
2
1
0.5
0.1
0.2
0.5
1.0
2.0
5.0
SIZE, IN MILLIMETERS

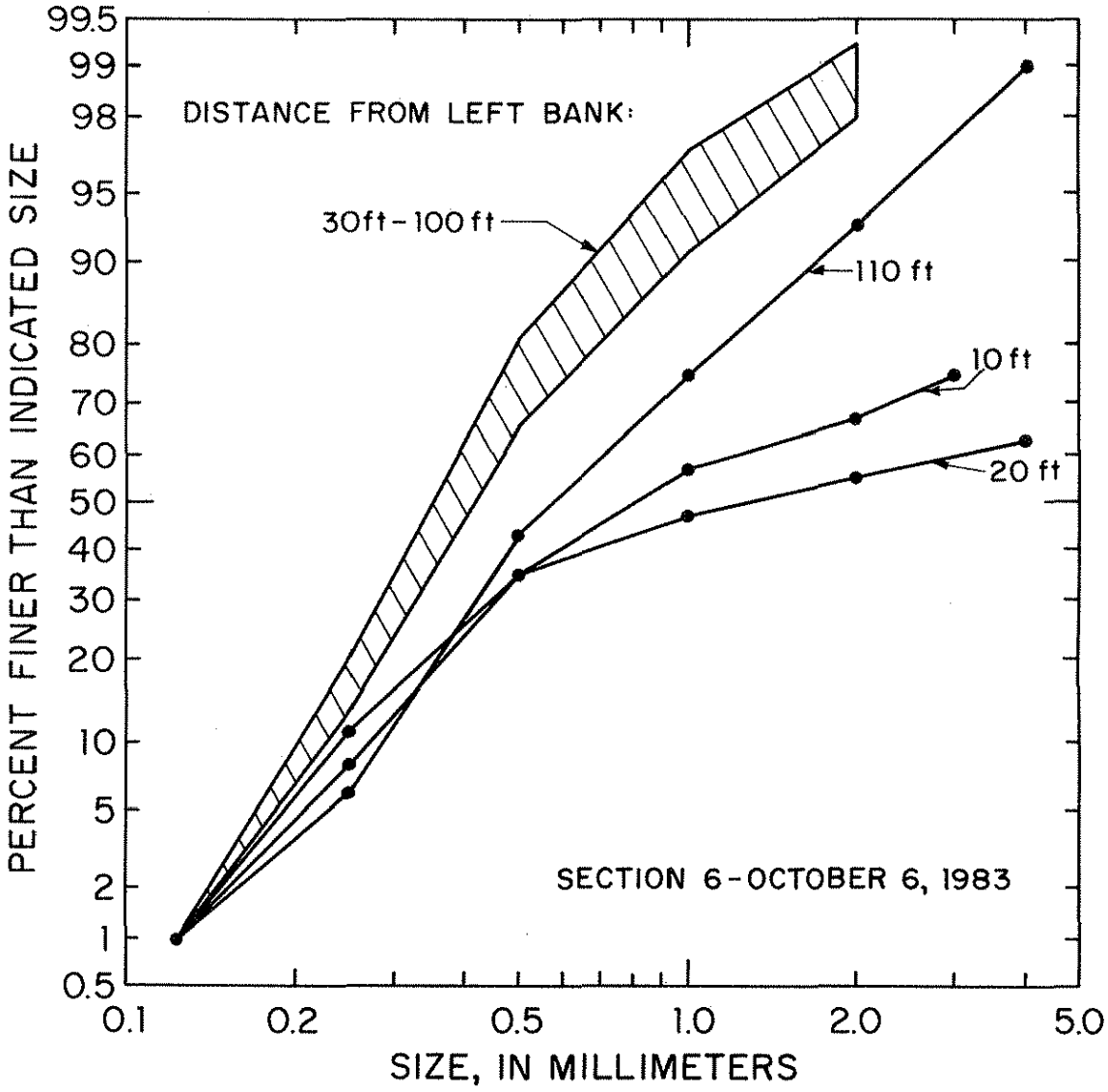
99.5
99
98
95
90
80
70
60
50
40
30
20
10
5
2
1
0.5
PERCENT FINER THAN INDICATED SIZE
DISTANCE FROM LEFT BANK:
30ft-100ft
110 ft
10 ft
20 ft
SECTION 6-OCTOBER 6, 1983
0.1
0.2
0.5
1.0
2.0
5.0
SIZE, IN MILLIMETERS

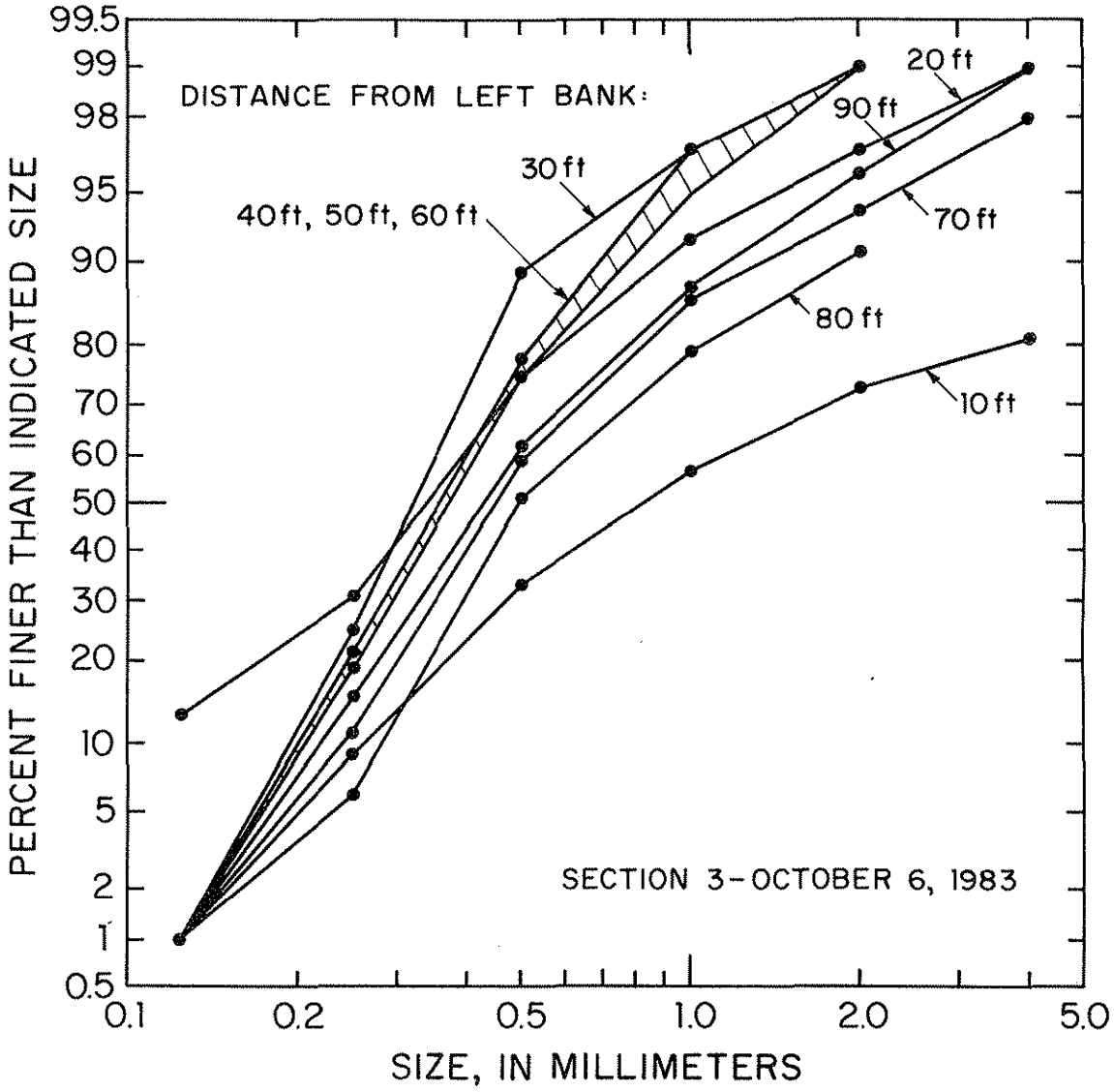
99.5
99
98
95
90
80
70
60
50
40
30
20
10
5
2
1
0.5
PERCENT FINER THAN INDICATED SIZE
DISTANCE FROM LEFT BANK:
20 ft
90 ft
30 ft
40 ft, 50 ft, 60 ft
70 ft
80 ft
10 ft
SECTION 3-OCTOBER 6, 1983
0.1
0.2
0.5
1.0
2.0
5.0
SIZE, IN MILLIMETERS

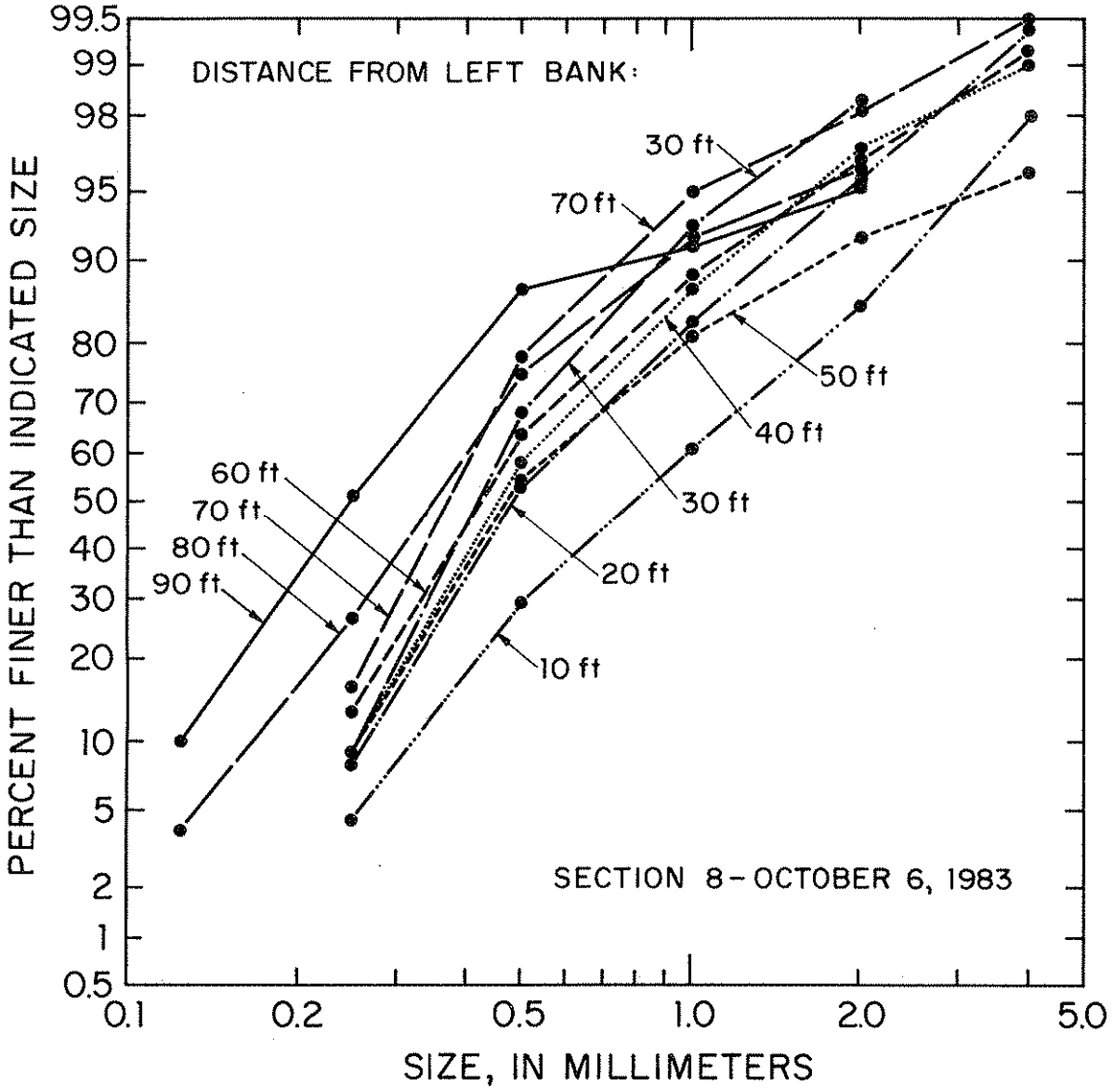
DISTANCE FROM LEFT BANK:
30 ft
70 ft
50 ft
40 ft
30 ft
20 ft
10 ft
60 ft
70 ft
80 ft
90 ft
SECTION 8 - OCTOBER 6, 1983
PERCENT FINER THAN INDICATED SIZE
99.5
99
98
95
90
80
70
60
50
40
30
20
10
5
2
1
0.5
0.1
0.2
0.5
1.0
2.0
5.0
SIZE, IN MILLIMETERS

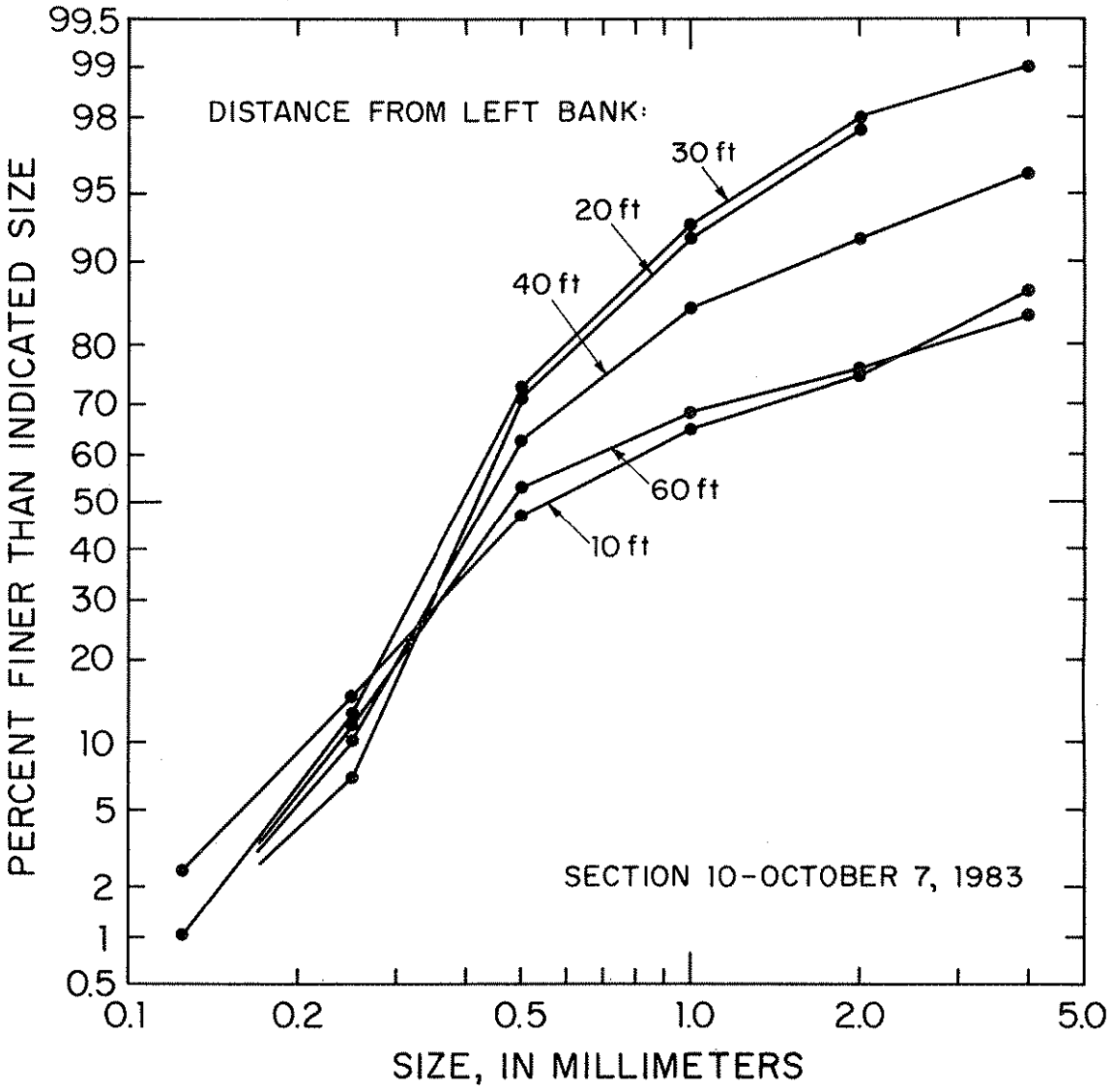
99.5
99
98
95
90
80
70
60
50
40
30
20
10
5
2
1
0.5
PERCENT FINER THAN INDICATED SIZE
DISTANCE FROM LEFT BANK:
30 ft
20 ft
40 ft
60 ft
10 ft
SECTION 10-OCTOBER 7, 1983
0.1
0.2
0.5
1.0
2.0
5.0
SIZE, IN MILLIMETERS

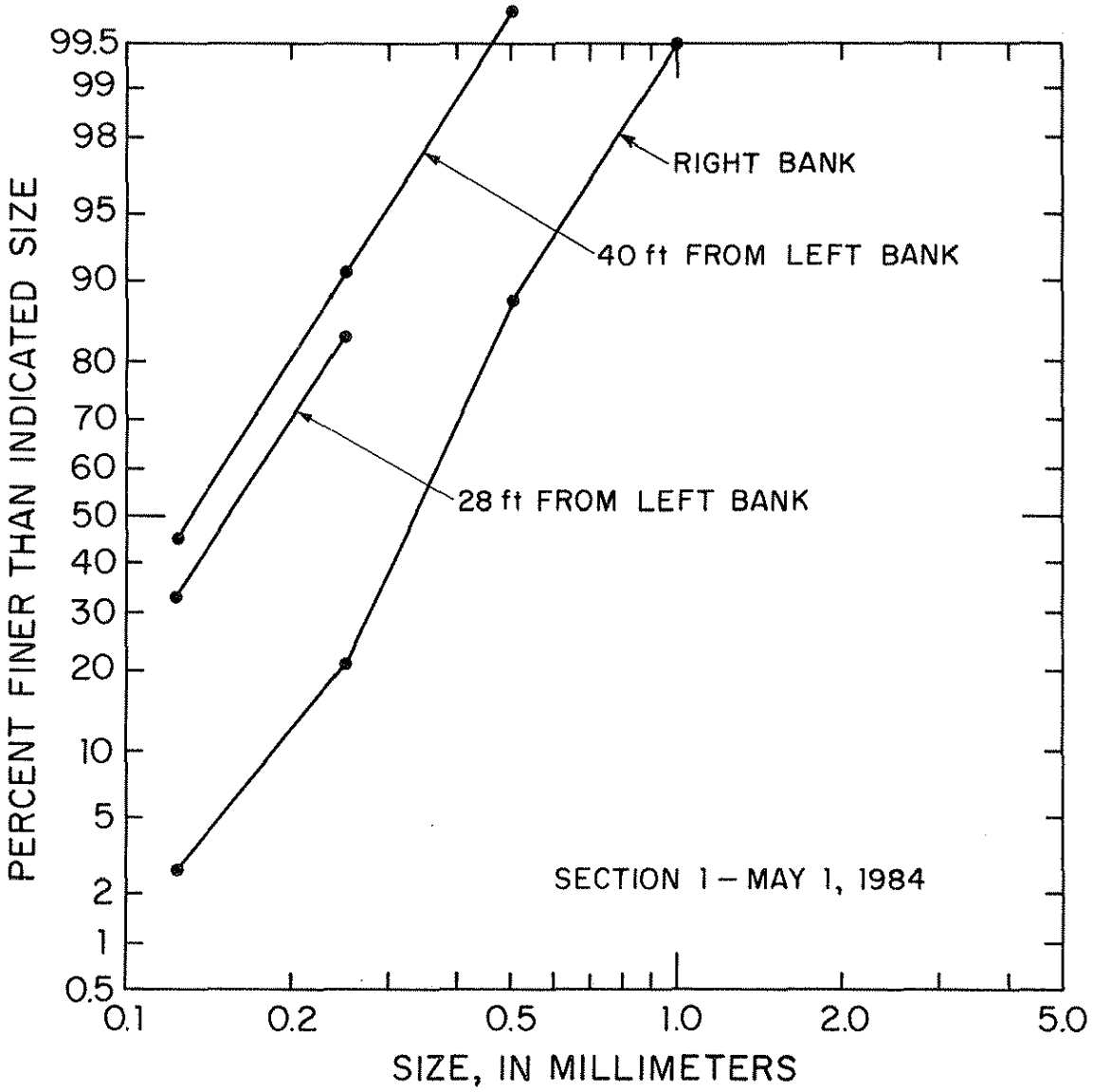
99.5
99
98
95
90
80
70
60
50
40
30
20
10
5
2
1
0.5
PERCENT FINER THAN INDICATED SIZE
0.1
0.2
0.5
1.0
2.0
5.0
SIZE, IN MILLIMETERS
RIGHT BANK
40 ft FROM LEFT BANK
28 ft FROM LEFT BANK
SECTION 1 – MAY 1, 1984

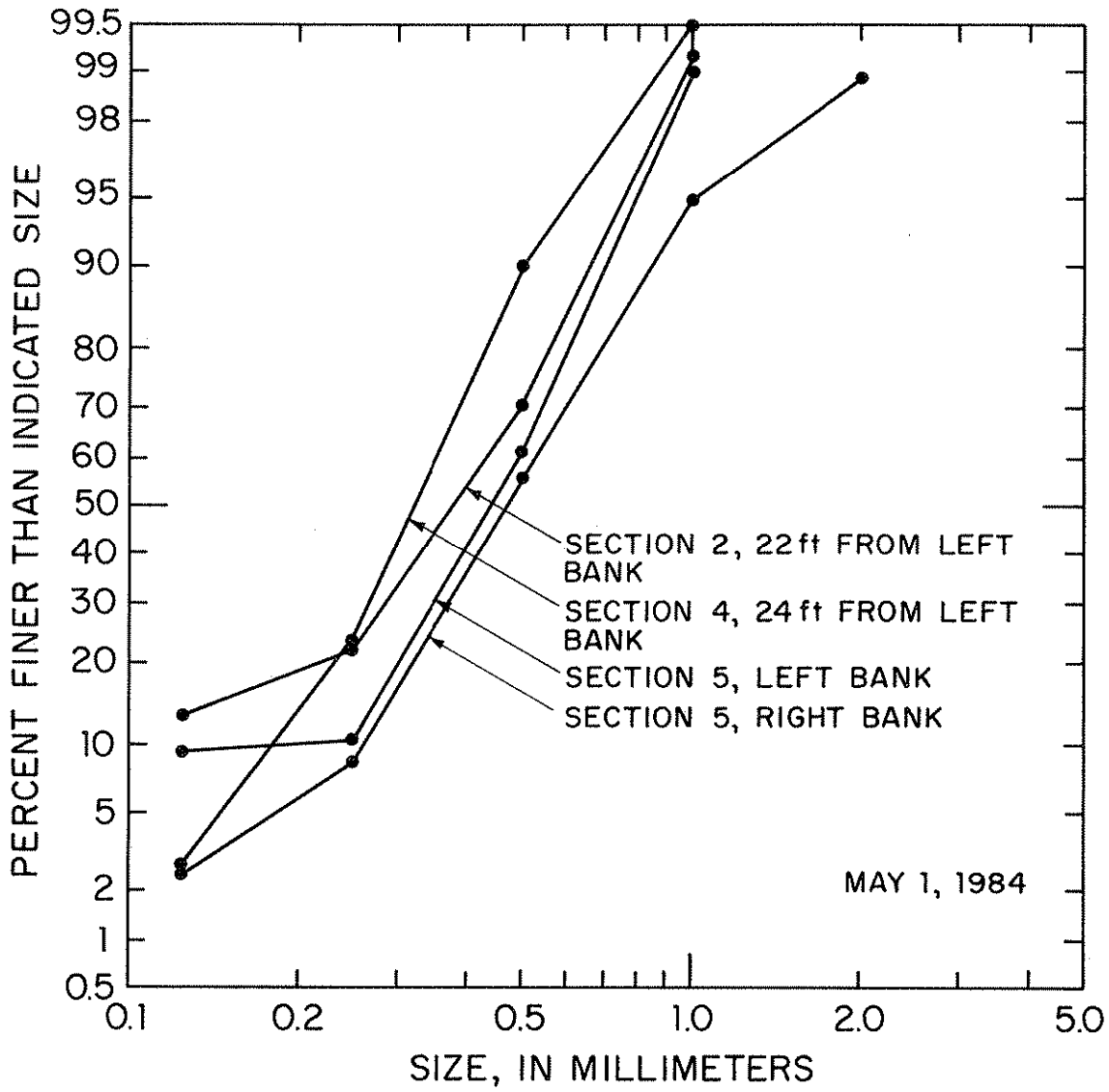
PERCENT FINER THAN INDICATED SIZE
99.5
99
98
95
90
80
70
60
50
40
30
20
10
5
2
1
0.5
0.1
0.2
0.5
1.0
2.0
5.0
SIZE, IN MILLIMETERS
SECTION 2, 22 ft FROM LEFT BANK
SECTION 4, 24 ft FROM LEFT BANK
SECTION 5, LEFT BANK
SECTION 5, RIGHT BANK
MAY 1, 1984

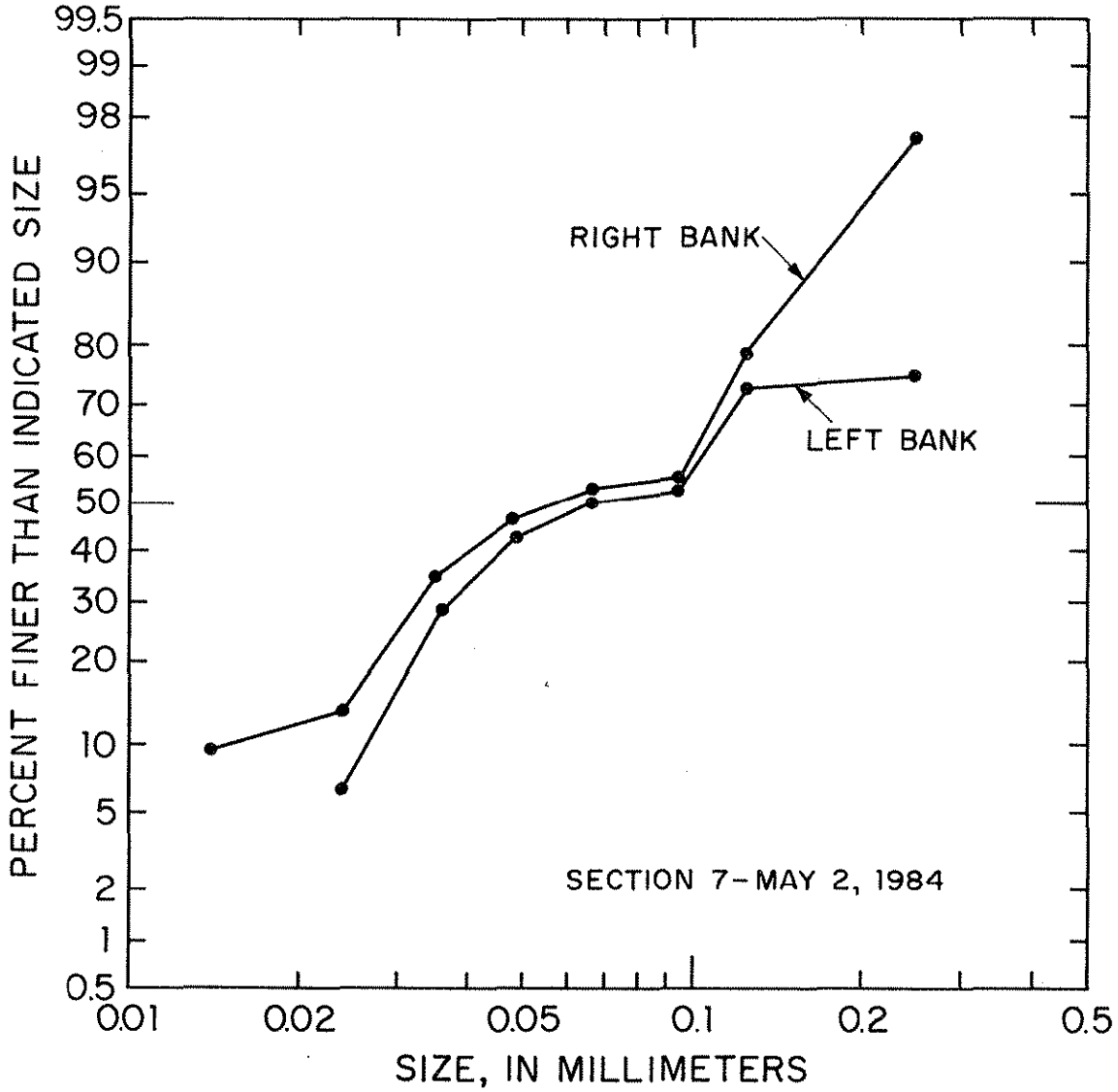
99.5
99
98
95
90
80
70
60
50
40
30
20
10
5
2
1
0.5
PERCENT FINER THAN INDICATED SIZE
0.01
0.02
0.05
0.1
0.2
0.5
SIZE, IN MILLIMETERS
RIGHT BANK
LEFT BANK
SECTION 7-MAY 2, 1984

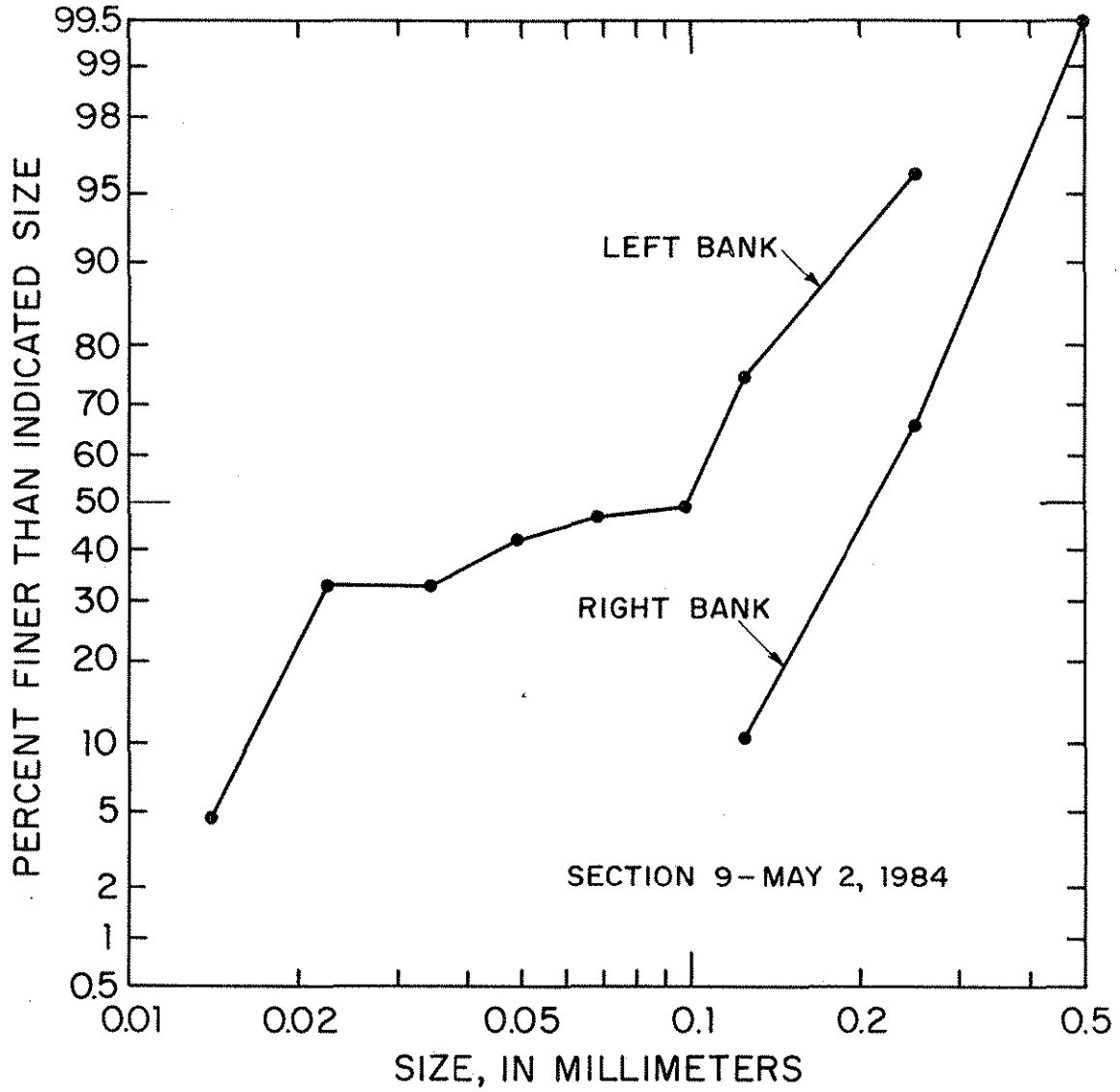
99.5
99
98
95
90
80
70
60
50
40
30
20
10
5
2
1
0.5
PERCENT FINER THAN INDICATED SIZE
LEFT BANK
RIGHT BANK
SECTION 9 – MAY 2, 1984
0.01
0.02
0.05
0.1
0.2
0.5
SIZE, IN MILLIMETERS

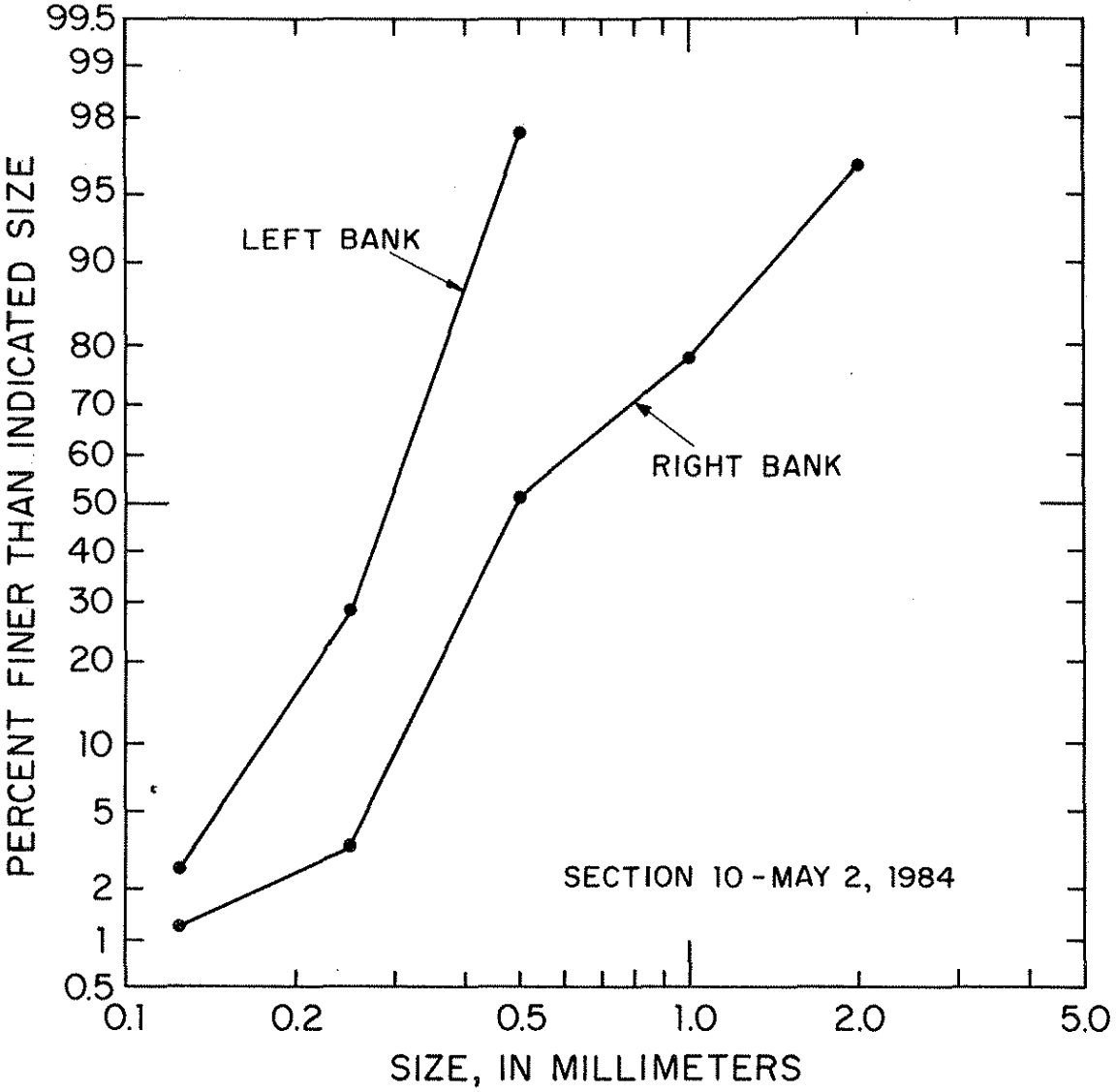
99.5
99
98
95
90
80
70
60
50
40
30
20
10
5
2
1
0.5
PERCENT FINER THAN INDICATED SIZE
LEFT BANK
RIGHT BANK
SECTION 10 - MAY 2, 1984
0.1
0.2
0.5
1.0
2.0
5.0
SIZE, IN MILLIMETERS